San Bernardino County Museum Association

Quarterly

Volume 38 Number 2, Summer 1991

The Mojave River Formation, Manix Basin, California:

Stratigraphy, Correlation, Magnetostratigraphy, and Rotation

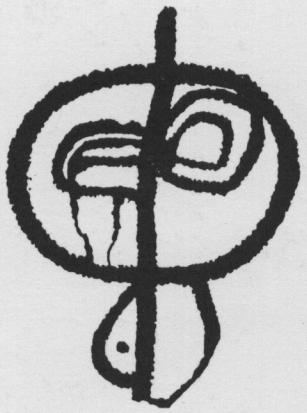

Abstracts of Proceedings and Evening Lecture 5th Annual Mojave Desert Quaternary Research Symposium

San Bernardino County Museum
May 17 - 18, 1991

Stratigraphy and Intra-basin Correlation of the Mojave River Formation, Central Mojave Desert, California

Elizabeth A. Nagy and Bruce C. Murray

Magnetostratigraphy and Clockwise Rotation of the Plio-Pleistocene Mojave River Formation, Central Mojave Desert, California.

Christopher J. Pluhar, Joseph L. Kirschvink, and Robert W. Adams

Abstracts of Proceedings from the 5th Annual Mojave Desert Quaternary Research Symposium

Jennifer Reynolds, compiler

Ancient Astronomy of the Black Canyon Indians: The 1991 Mojave Desert Quaternary Research Symposium Evening Lecture

Wilson G. Turner

San Bernardino County Museum Association
2024 Orange Tree Lane
Redlands, California 92374

Quarterly, Volume 38 Number 2
Summer, 1991

Front cover:
Petroglyph TMT-31D, Black Canyon complex,
San Bernardino County, California.
Wilson G. Turner rendering.

Table of Contents

Stratigraphy and Intra-basin Correlation of the Mojave River Formation, Central Mojave Desert, California
Elizabeth A. Nagy and Bruce C. Murray 5

Magnetostratigraphy and Clockwise Rotation of the Plio-Pleistocene Mojave River Formation, Central Mojave Desert, California.
Christopher J. Pluhar, Joseph L. Kirschvink, and Robert W. Adams 31

Abstracts of Proceedings from the 5th Annual Mojave Desert Quaternary Research Symposium
Jennifer Reynolds, compiler 43

Ancient Astronomy of the Black Canyon Indians: The 1991 Mojave Desert Quaternary Research Symposium Evening Lecture
Wilson G. Turner 57

Stratigraphy and Intra-basin Correlation of the Mojave River Formation, Central Mojave Desert, California

Elizabeth A. Nagy and **Bruce C. Murray**, Division of Geological and Planetary Sciences, California Institute of Technology, MS 170-25, Pasadena, CA 91125

ABSTRACT

Detailed stratigraphic description of a previously undefined sequence of deposits, in transitional contact with the overlying Pleistocene Manix Formation, has resulted in the definition of an 80+ meter thick section referred to here as the Mojave River Formation. The stratotype is located at the intersection of Manix Wash with the Mojave River. Intra-basin lithologic correlation between three geographically separate exposures of the deposits within the Manix Basin of the Mojave Desert are independently supported by volcanic ash chemistry and geomagnetic reversals.

The deposits of the Mojave River Formation predominantly represent accumulation within a closed basin of a desert depositional system. They record a fairly complete history of changing Plio-Pleistocene depositional environments prior to the formation of Pleistocene Lake Manix. Age assignment based upon stratigraphic relationships, tephrochronology, and magnetic polarity reversals indicate that the Mojave River Formation at the type locality represents about 1.5 Ma of time, spanning from 0.92 Ma to 2.48 Ma.

The deposits yield information concerning the timing and nature of motion along the adjacent Manix Fault, which shows evidence for both left lateral and reverse motion in the type area. Regional implications of the Mojave River strata include the timing of uplift of the Transverse Ranges and change in the flow direction of the "ancestral" Mojave River system from westward to eastward. Both of these developments appear to be post 0.97 Ma.

INTRODUCTION

A sequence of previously undefined sedimentary deposits underlie the well-studied Manix Formation (Jefferson et al., 1982; Jefferson, 1985) within the basin of ancient Lake Manix (Buwalda, 1914) in the central Mojave Desert (Figure 1). This paper presents detailed descriptions of the exposures in the vicinity of the intersection of Manix Wash with the Mojave River. Local correlation between three exposures of the deposits permits us to describe an 80+ meter thick section referred to here informally as the Mojave River Formation (MRF). This section records information about Plio-Pleistocene climatic, hydrologic, and tectonic conditions

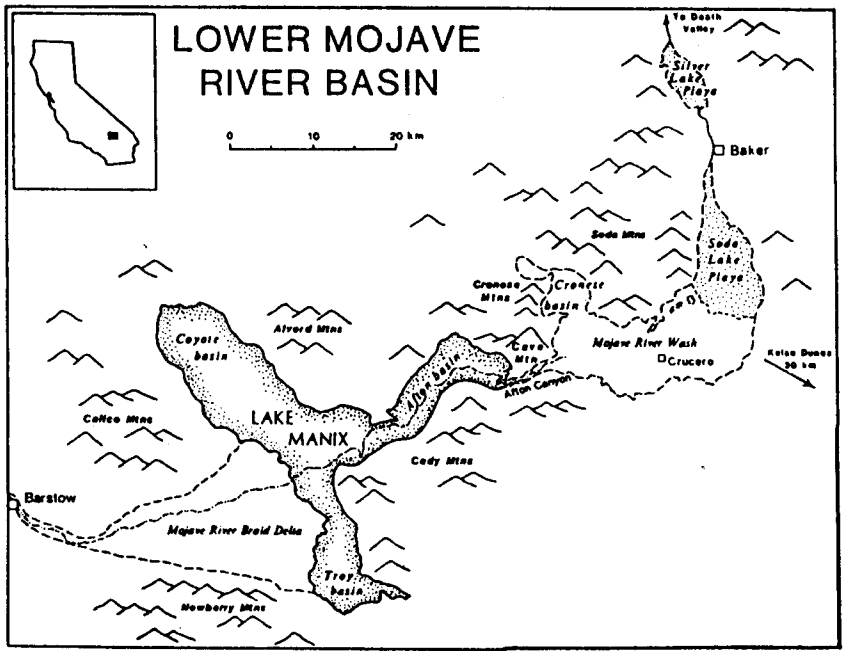

Figure 1. Location map showing approximate shoreline of Pleistocene Lake Manix (after Meek, 1989).

immediately prior to the development of Pleistocene Lake Manix. This history is relevant to the Plio-Pleistocene tectonic history of the Mojave block. The purpose of this paper is to provide data upon which regional interpretations can be based. This paper does not formally define the Mojave River Formation according to the North American Stratigraphic Code. Instead, we provide descriptions of these beds adequate to permit others to verify the lithologies and stratigraphic relationships upon which our preliminary interpretations are based. We envision later a more formal and comprehensive publication.

Plate 1 is a map showing the locations and important contact relations of MRF exposures. Note that the "Big Bend" of the Mojave River in our field area (Plate 1) is located in Figure 1 just below the "X" in the words "Lake Manix". Three geographically separate exposures of the MRF (study areas outlined with black line) occur along the Mojave River east of the Manix Wash tributary and are shown as Q_R. The MRF is in apparent transitional contact with the lowest Member of the overlying Pleistocene Manix Formation (Q_{Ma}) at the western end of the southern cliff site (SCS) on the south side of the Mojave River (Murray et al., 1990). Paleomagnetic sampling sites at BBW and BBE (Big Bend West and East) are in close proximity to the zone of transition (Pluhar et al., 1991, this volume). MRF is in disconformable to unconformable contact with Manix beds (Q_{Mbcd}) on the north side of the river. Splays of the Manix fault traverse both formations on the north side of the river. The Manix Formation, first carefully described by Jefferson (1968, 1985), was mapped in detail by McGill et al., (1988) in the area surrounding Manix Wash. Additional geologic units shown on Plate 1 include an older fanglomerate unit (T_{of}) underlying Buwalda Ridge which predates MRF, and Tertiary intrusive andesitic rocks (T_u) as mapped by Dibblee and Bassett (1966).

Fossils throughout the middle and upper Manix Formation at the type locality have provided uranium/thorium and carbon-14 dates ranging from at least 350 to 19.3 Kyr BP (Jefferson, 1985). Also, an ash layer provides a stratigraphically consistent tephrochronologic date of 184 Kyr BP. Preliminary field investigations indicate additional exposures of the MRF continue to the south and east of the map area, possibly as far east as Afton Canyon.

Detailed stratigraphic columns from each of the three MRF sites have been constructed from bed-by-bed examinations and descriptions (Figure 2). Inferred intra-basin correlations between these three sections, shown in Figure 3, are based independently upon lithologic features and volcanic ash chemistry of several ash beds within the formation. Magnetostratigraphic evidence from Pluhar et al., (1991, this volume) provides a third independent correlation

Figure 2. Mojave River Formation (MRF). Stratigraphic columns showing sorting, grain size distribution, color (restricted to tan, green, and red for simplicity), primary structures (see Legend for explanation of symbols), location of volcanic ash beds, and thickness of beds. The column also illustrates the relative field appearance of units, i.e., the more indurated, ledge forming beds versus the softer, slope forming beds. The column on the far right shows our division of each section into coarse (C), fine (F), and gypsiferous (G) units.

LEGEND

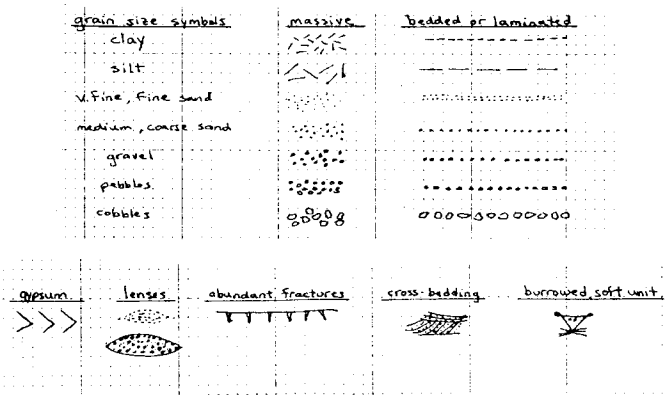

SYMBOLS FOR COLOR OF UNIT

- primarily reddish-tan
- primarily grey-green
- ranges from light tan to brown

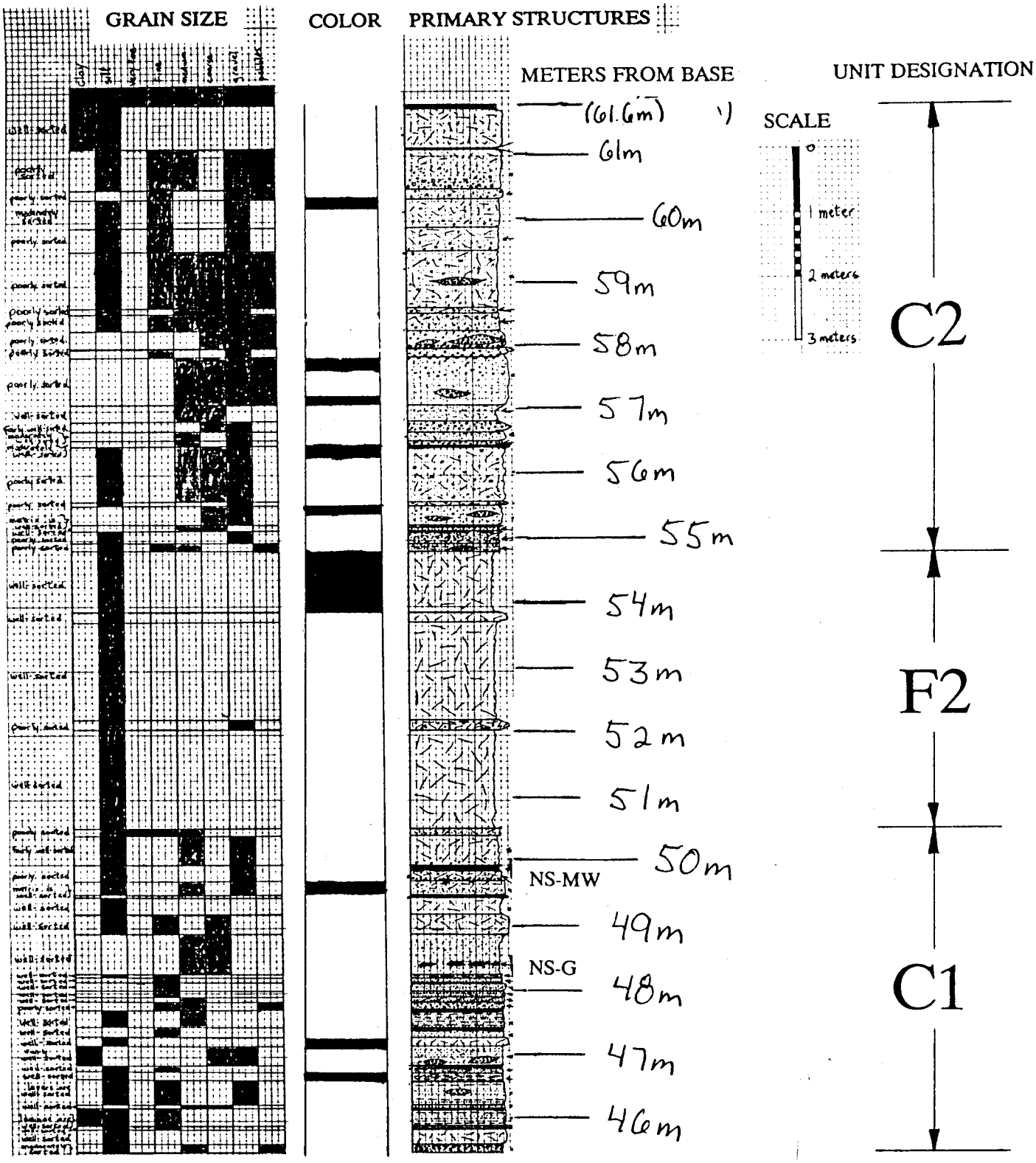

Figure 2a. NS - northern site

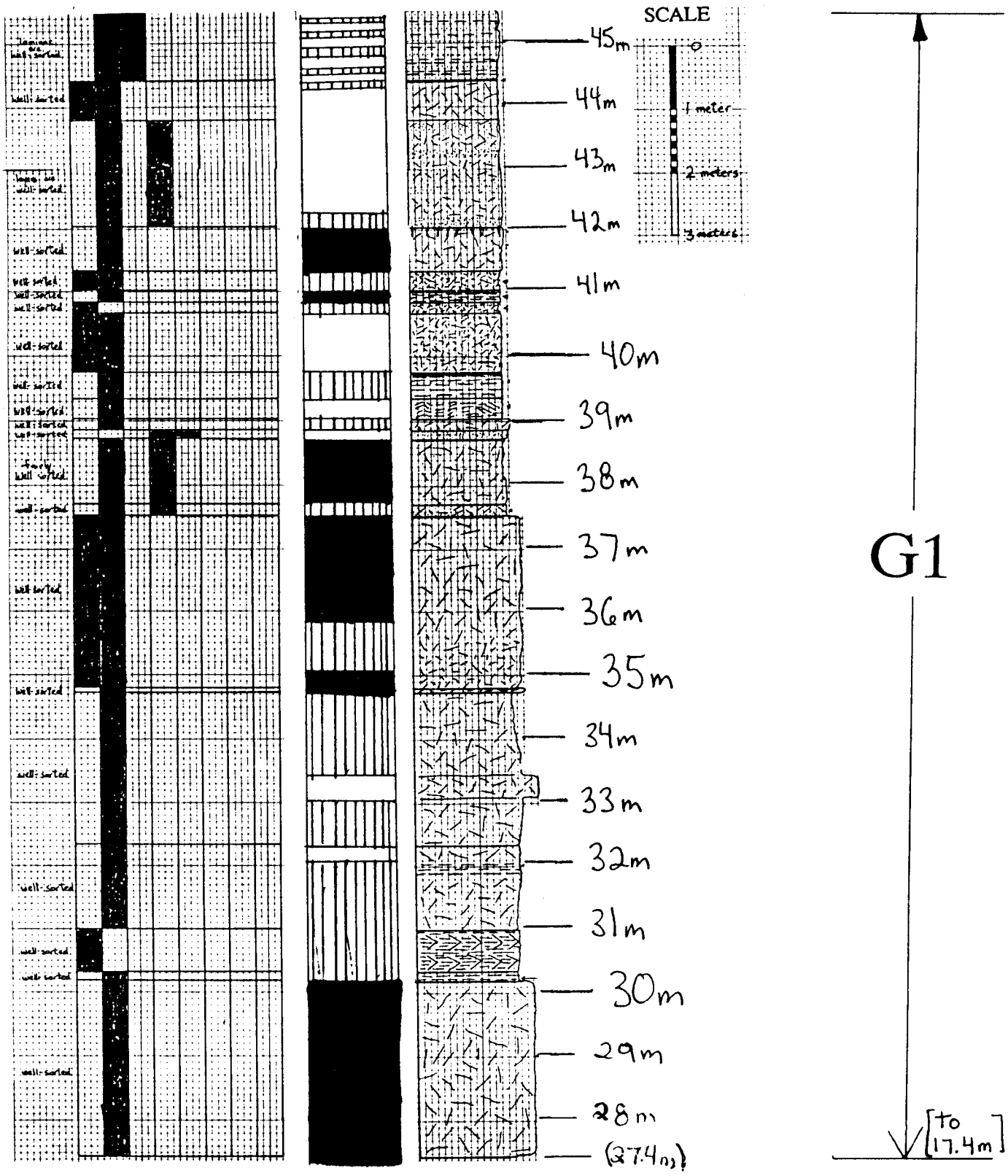

Figure 2a. (cont.) NOTE: Unit F1 extends from the base of the section to 17.4 m. Unit G1 begins at 17.4 m.

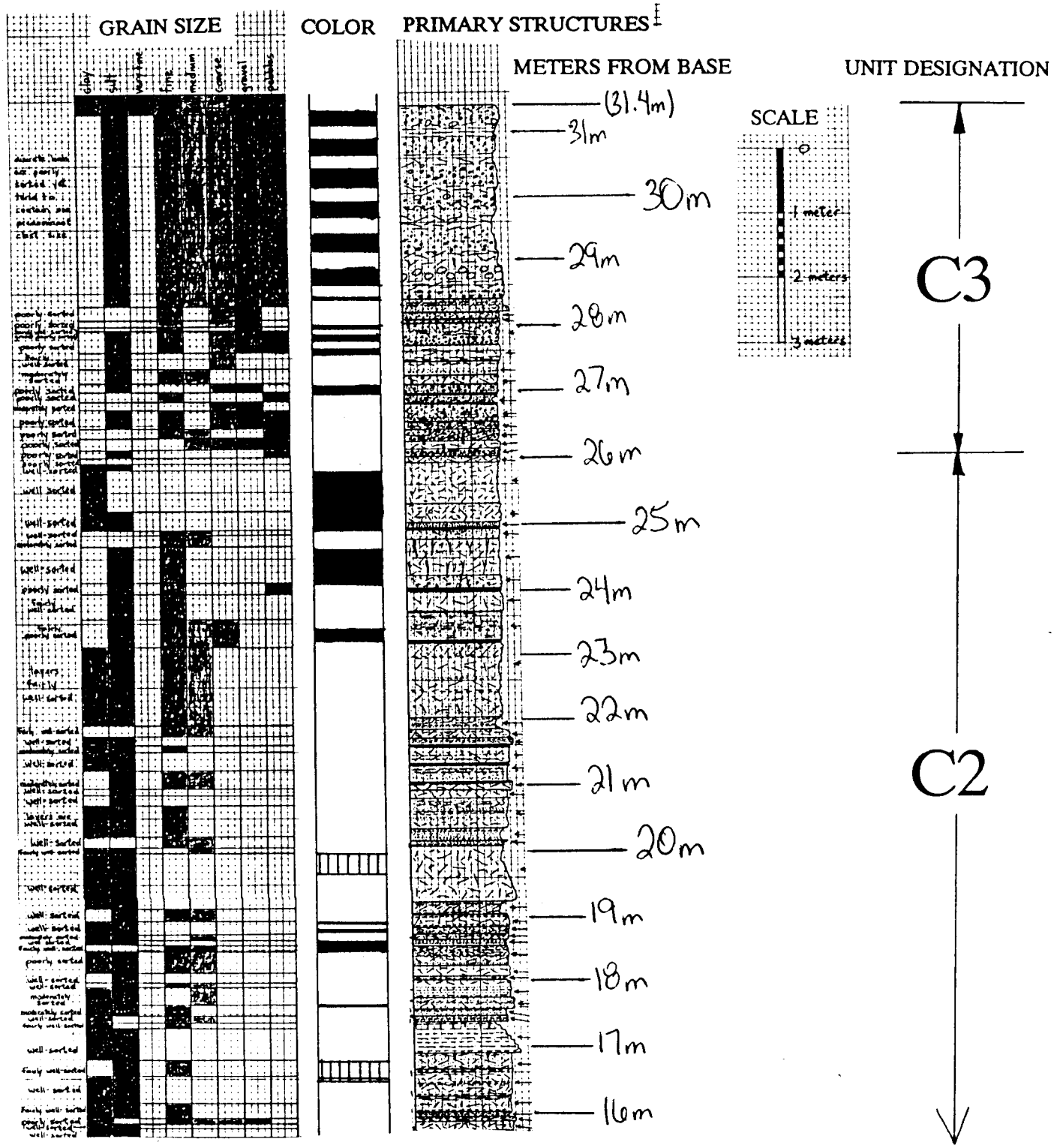

Figure 2b. SCS - southern cliff site

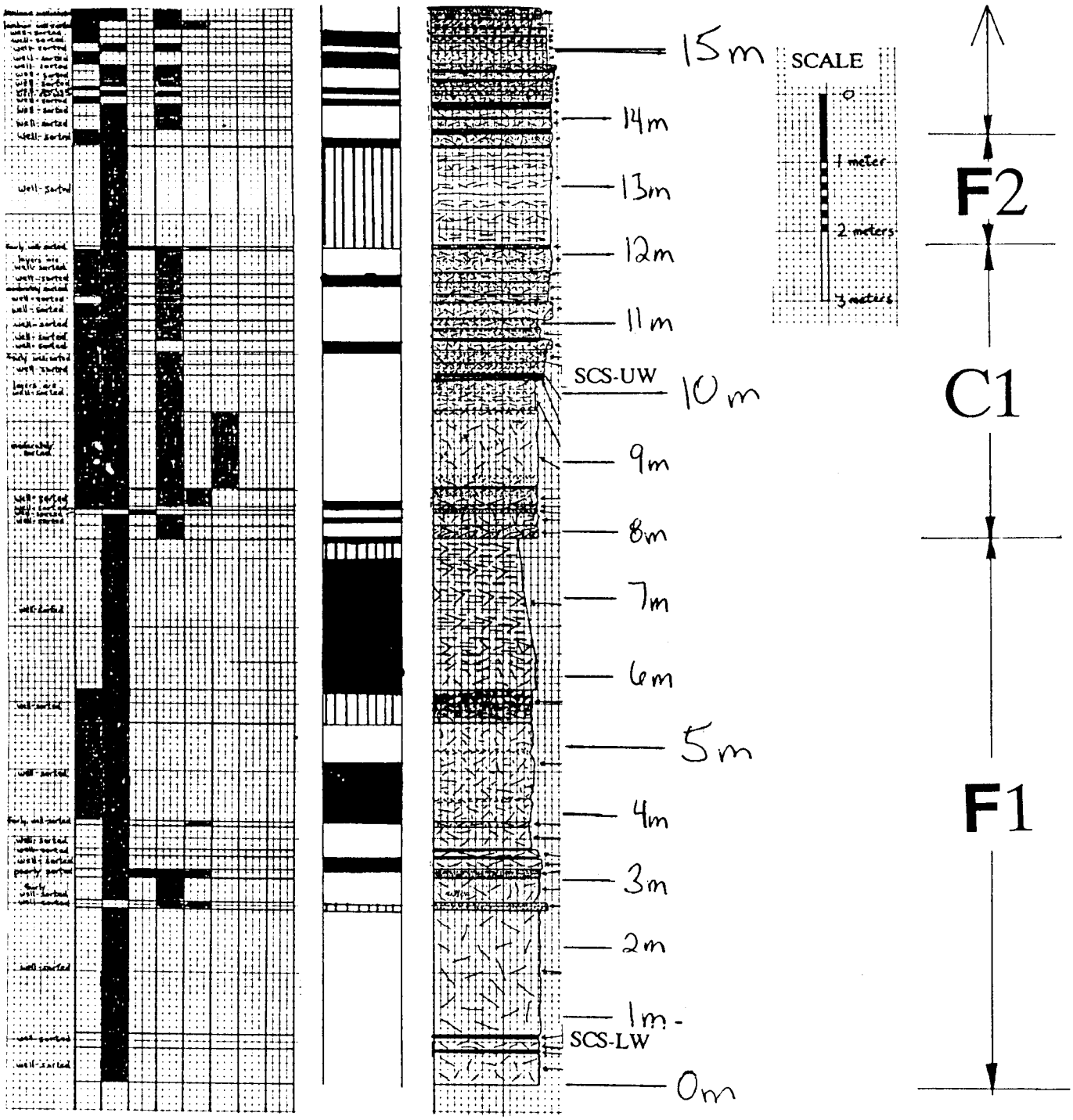

Figure 2b. (cont.)

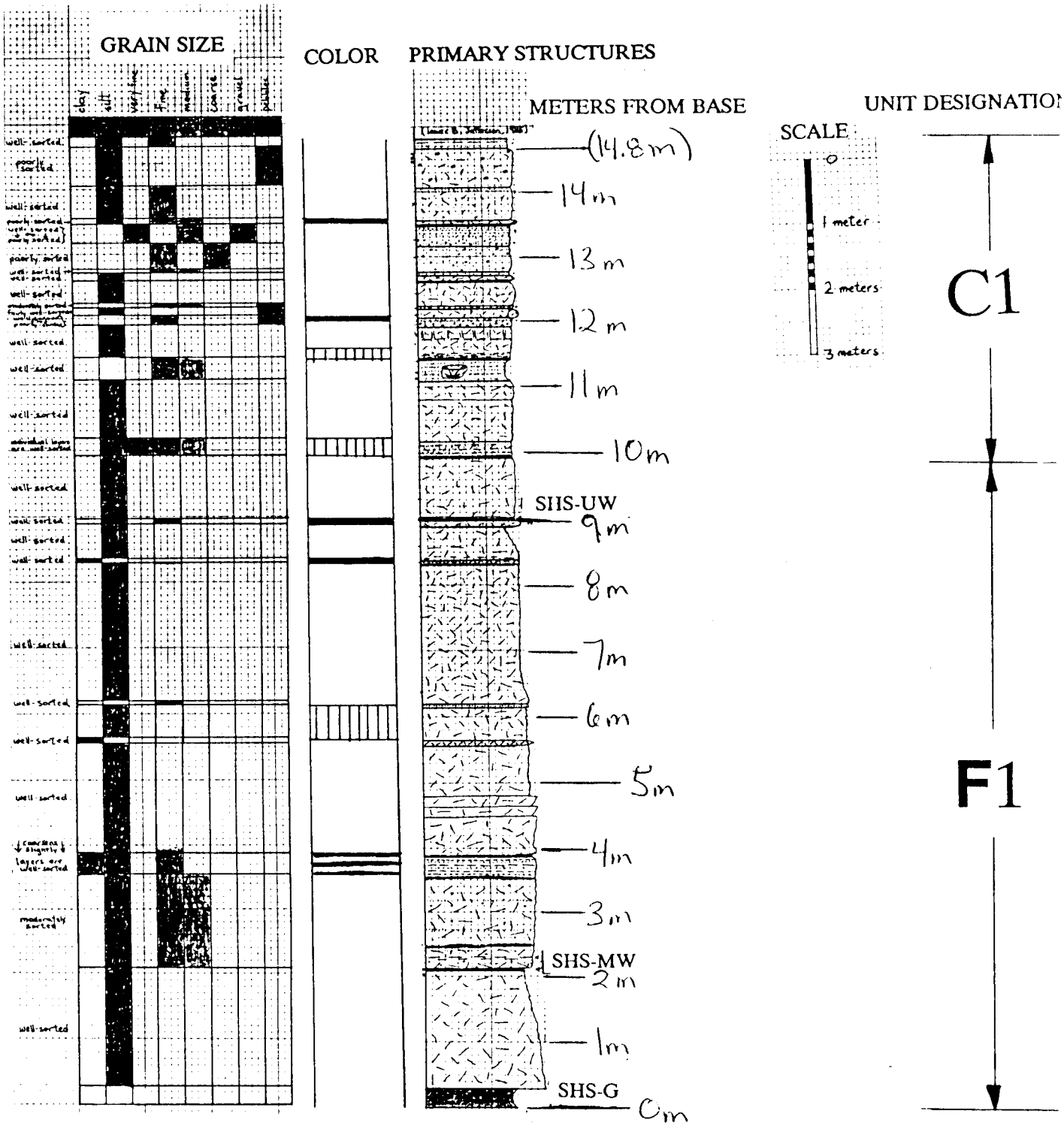

Figure 2c. SHS - southern hill site

technique which we believe supports our proposed stratigraphic correlations, and also provides an absolute time reference.

METHODS

Geologic mapping was carried out on an enlarged USGS topographic map (Manix Quadrangle; Provisional Edition, 1982; 1:24000 scale). The map of McGill et al., (1988) has been transferred, but neglecting (for simplicity) their subdivision of the Manix Formation into Jefferson's (1985) four members. Aerial photographs and a USGS geologic map (Newberry Quadrangle; Dibblee and Bassett, 1966; 1:62500 scale) provided auxiliary information for some of the mapping. Stratigraphic thicknesses were carefully determined with a tape measure. Each bed, in most cases defined by sharp upper and lower contacts and between 5 and 50 cm in thickness, was examined and described. Special attention was given to mineralogy, color, grain size and shape, sorting, primary sedimentary structures, cementation, and the occurrence of evaporites. Extensive slope wash, as well as local changes in bedding thicknesses and tilts, complicate measurements enough to result in slight discrepancies in thickness values reported by different workers. The three exposures studied in detail are designated the northern site (NS), adjacent to the north side of the Mojave River, the southern cliff site (SCS), located at a bend on the south side of the river and across from Manix Wash, and the southern hill site (SHS), located southeast of SCS and set back from the river. This terminology has also been adopted in companion paper on the magnetostratigraphy (Pluhar et al., 1991, this volume).

One grey and several white volcanic ash beds occur in the MRF. It should be mentioned here that there are occasional beds of very fine silt, and in some cases caliche, which appear remarkably similar to the ash beds until examined with a hand lens or binocular microscope. Twenty-one volcanic ash samples, over 300 grams each, were methodically collected during one field session by one of the authors (Nagy) and Laszlo Keszthelyi. Care was taken to avoid contamination from overlying beds. The ash samples were sieved by the same workers at facilities located at the Chevron Oil Field Research Company in La Habra, California, and sent directly to X-Ray Assay Laboratories in Toronto, Canada for chemical analysis. The analysis included X-Ray fluorescence, neutron activation analysis, and inductively coupled plasma mass spectrometry. The results are discussed in Section V.

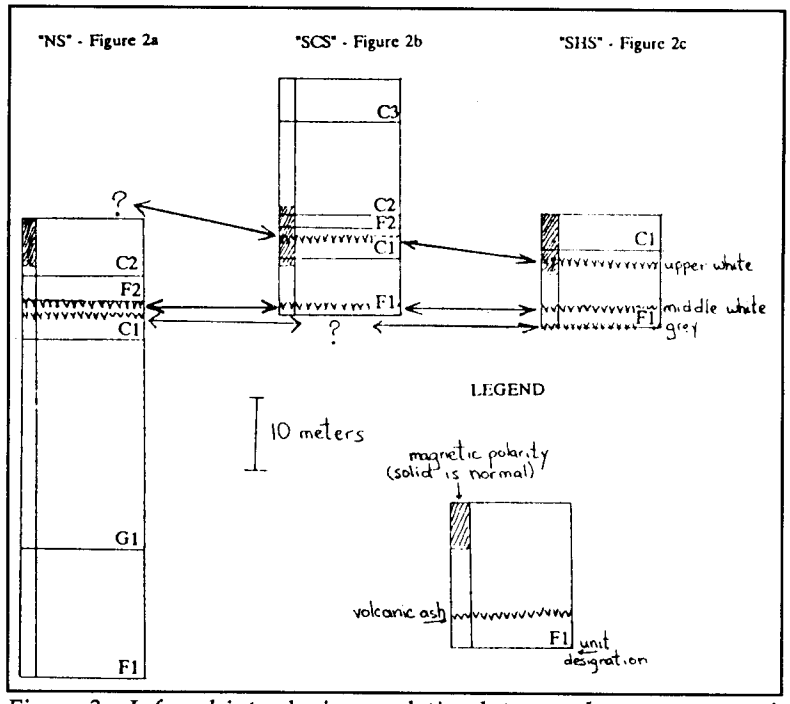

Figure 3. Inferred intra-basin correlation between three exposures of the Mojave River Formation (MRF). Magnetic polarity scale as determined by Pluhar et al., (1991, this volume).

GEOLOGY OF MANIX BASIN

Pleistocene Lake Manix was a tri-lobed lake which extended north to Coyote dry lake basin, south to Troy dry lake basin, and east along the Mojave River valley to Afton Canyon (Jefferson, 1985). One of the best studied geologic units within the associated basin has been the Pleistocene Manix Formation. In his description of the Manix Formation, Jefferson (1985) describes underlying "Plio-Pleistocene lacustrine sediments" which are equivalent to the MRF

GEOLOGIC MAP OF STRATOTYPE REGION FOR MOJAVE RIVER FORMATION

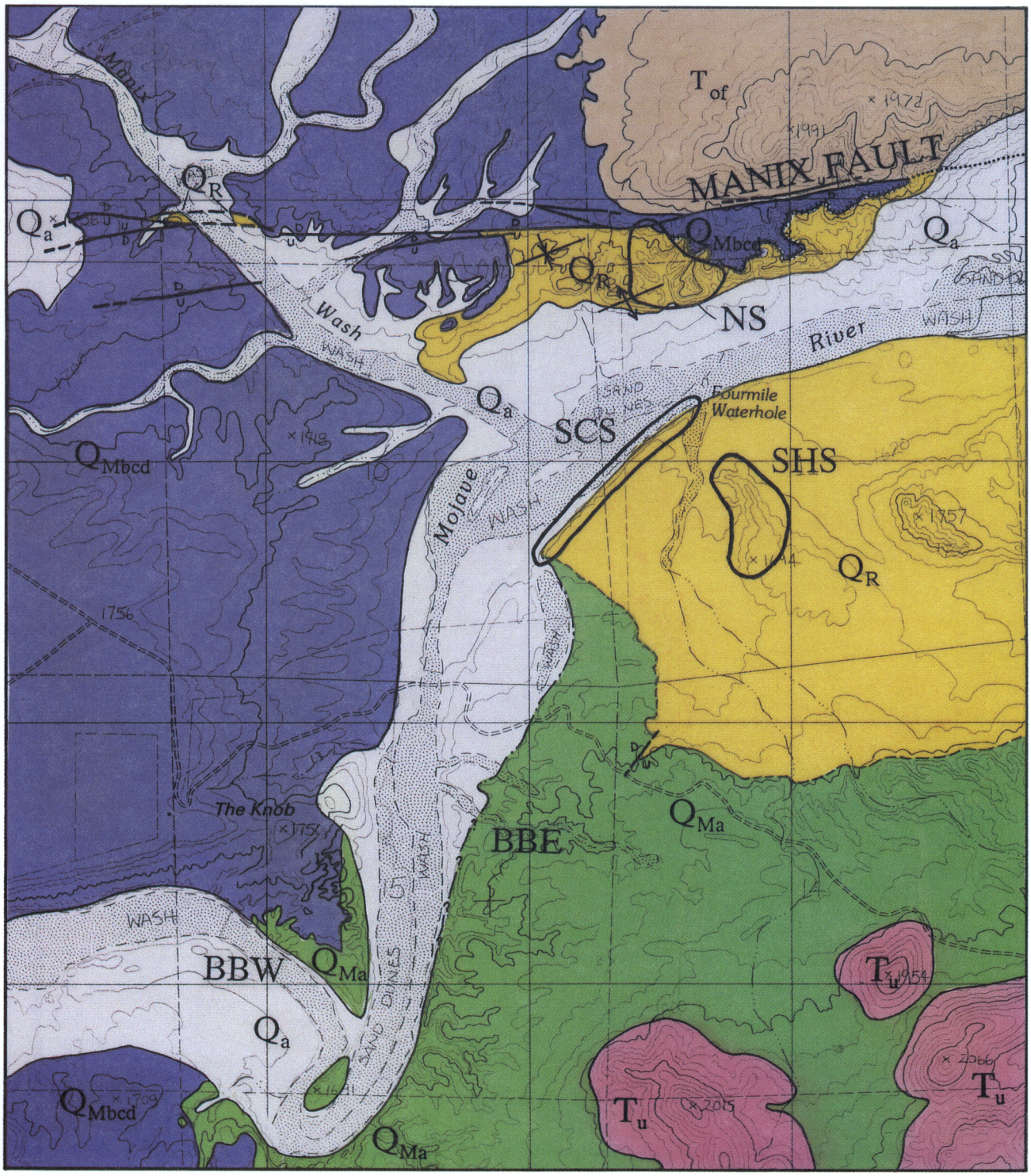

Plate 1. Areas outlined in heavy lines indicate sites of stratigraphic columns: "NS" is the northern site, "SCS" is the southern cliff site, and "SHS" is the southern hill site. Other sites discussed here and in Pluhar et al., (1991, this volume) are "BBW" (big bend west) and "BBE" (big bend east).

EGEND

Q_a Quaternary alluvium

Q_{Mbcd} Members B, C, D
Q_{Ma} Member A
} Manix Formation

various contacts (see below)

Q_R Mojave River Formation

unconformity

T_{of} older fanglomerate unit

unconformity

T_u Tertiary volcanics

SCALE 1:24 000

0 .5 1 KILOMETER

CONTOUR INTERVAL 20 FEET

ntacts

conformable

angular unconformable

transitional

inferred

possibly transitional/
definitely conformable

D
U
fault

her structures

anticline

syncline

(Jefferson, pers. comm., 1990). At the western edge of the northern exposure of MRF the Manix formation is in concordant contact with the underlying MRF while the northern and eastern contacts at the same locality are discordant. The extensive exposures of both formations in this region are a consequence of downcutting by the present Mojave River.

In addition to exposure by denudation from the Mojave River, the Manix fault has uplifted and deformed both the Mojave River and Manix Formations (McGill et al., 1988). Many kinematic models for late Cenozoic evolution of Mojave Block tectonics classify the 38-kilometer-long Manix fault as one in a series of east-west trending, left-lateral strike-slip faults (for example Dokka and Travis, 1990). However, unambiguous field evidence for that interpretation is not evident from the area of our map. Minor faults within the MRF, present at all three of the studied localities, are mostly vertical, strike approximately northeast, and generally show a down-to-the-northwest sense of motion (Figure 4). A magnitude 6.2 earthquake along the Manix fault in 1947 (Buwalda and Richter, 1948) demonstrates present day activity. However the aftershock pattern was oblique to the fault indicating that primary movement may actually have occurred on an unidentified sub-surface fault (McGill et al., 1988). The section of MRF north of the river along Buwalda Ridge (lat: 34 48′ N, long: 116 35′ W) immediately adjacent to the Manix fault, is not only topographically higher than the two sections south of the river but is also stratigraphically the lowest portion of the reference section. This indicates that fault-related uplift has occurred. The angular unconformity between the MRF and the relatively flat-lying Manix Formation, well displayed along the southern margin of Buwalda Ridge, places activity on the Manix fault back to at least early Manix Formation time. The lowest unit of the Manix Formation, Jefferson's Member A (1985), is a wedge-shaped, coarse conglomerate emanating from the Cady Mountains to the southeast (Figure 1 and Plate 1). While several workers have reported that these sediments are separated from underlying strata by an unconformity (Sarna-Wojcicki et al., 1984; Jefferson, 1985), we believe that on the south side of the river Member A of the Manix Formation is in transitional contact with the uppermost exposures of the MRF (Murray et al, 1990; see Figure 5). This interpretation has important implications for the age of the top of the MRF and for the hydrologic and tectonic regime recorded.

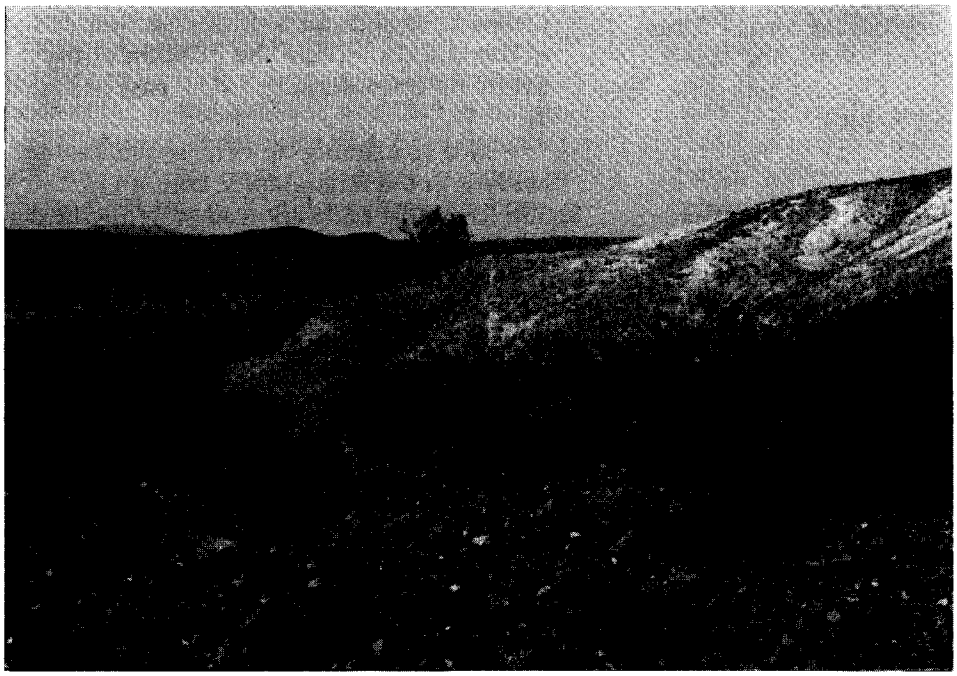

Figure 4. Looking northeast at the Mojave River Formation (on right) faulted against Member A of the Manix Formation (on left). The fault is shown on Plate 1 south of SHS and east of BBE.

The MRF contains at least three traceable volcanic ash layers which are important for both intra- and inter-basin correlation. The Long Valley-Glass Mountain center in California and the Yellowstone center in Wyoming were the primary sources of volcanic ash for this part of the

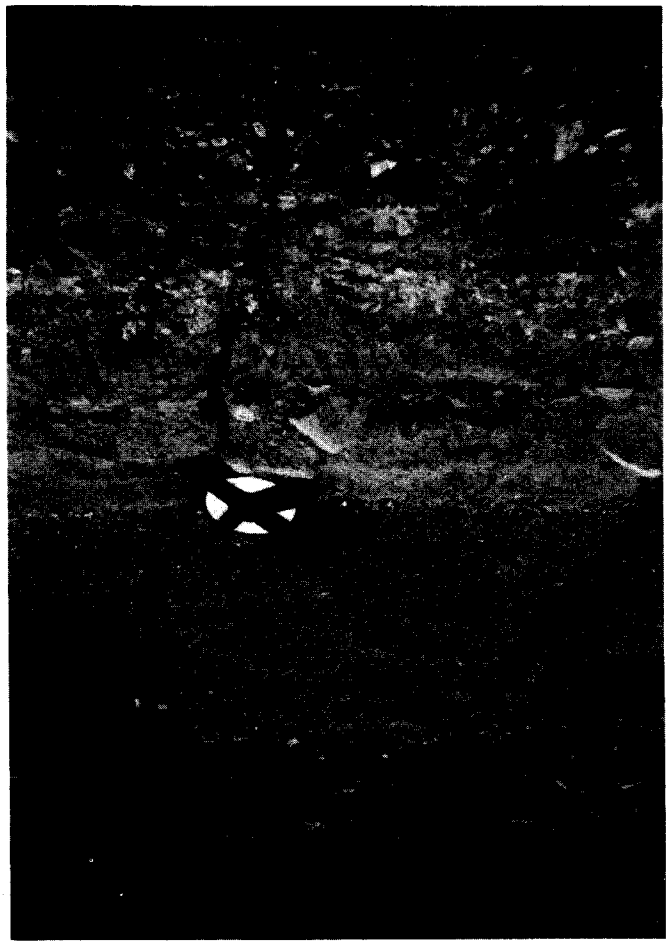

Figure 5. Transitional zone between the Mojave River Formation and the overlying Member A of the Manix Formation. The tape measure is 12 inches in length. This photo was taken in the channel at BBE.

country during Plio-Pleistocene time. Samples of some of the MRF volcanic ashes have been analyzed previously in an effort to ascertain volcanic sources and make tephrochronologic correlations with documented tuffs of the western U.S. (Izett et al., 1970; Sarna-Wojcicki et al., 1980; Sarna-Wojcicki et al., 1984; Izett et al., 1988). Correlation is possible if distinct chemical and petrographic properties from the two presumed volcanic sources are retained in the preserved ashes (Izett et al., 1970).

STRATIGRAPHY OF THE MOJAVE RIVER FORMATION

Overall the MRF represents a desert depositional system which accumulated in a closed basin. Inferred depositional environments represented in these beds generally progress from an older playa/sabkha facies into a younger alluvial plain facies. This interpretation is discussed in Section VII. Figure 2 (a,b,c) shows stratigraphic columns constructed from detailed examinations measured bed-by-bed.

NS - the northern site - (Figure 2a)

Exposed along the northern side of the Mojave River, adjacent to the Manix fault and in disconformable (to the west) to unconformable (to the east) contact with the overlying Manix Formation, is a two-kilometer-long exposure of MRF. These beds have been folded into a series of anticlines and synclines with axes that vary greatly in direction, but most frequently they trend approximately northwest or northeast. Measured dips range from horizontal to 25 degrees. Overall the entire MRF unit forms a broad anticline. The core of the broad anticline, exposed at the eastern limit of NS (Plate 1), represents the stratigraphically lowest exposures at this site. From this point it is possible to trace the continuous section by walking either east or west. We have chosen to describe the section going to the west from these lowest beds because a thicker section exists in this direction (note the position of the overlying unconformity to the east in Plate 1).

Two coarsening-upward sequences are evident in the stratigraphic column of Figure 2a. Most beds are well-sorted with the distinct exception of the uppermost coarse beds (designated Unit C2). On this basis, and the occurrence of a thick gypsiferous sequence, we have separated the 61.6 m of section at this location into five units: two fine-grained units (F1, F2), two coarse-grained units (C1, C2), and one gypsiferous unit (G1). It should be noted here that an additional 27.4 m of section is exposed below the lowest units shown in Figure 2a. The uppermost 10 m of this additional portion is included in unit G1. Although we include a general description of these lowermost beds, extensive slope wash and time-constraints prevented the same degree of detailed, bed-by-bed investigations applied to other sedimentary layers in this study.

F1 (0 to 17.4 meters)

The lowest exposures at NS, not shown in Figure 2a, consist of alternating layers of tan, well-sorted siltstones and fine sandstones made up primarily of cemented quartz grains. A few of the beds near the top of this unit are a distinct olive green. Abrupt contacts within F1 were not discernible. Most of the unit is massive, although faint cross-bedding (of an indeterminate direction) can be seen in some parts. Gypsum crystals were not found within this unit although they are quite common in higher beds. Stratigraphic resolution is poor in comparison to other units, as explained above. We interpret F1 to have been deposited in a playa environment.

G1 (17.4 to 45.5 meters)

The 27.6 meters of section denoted G1 are comprised primarily of 1-2 m thick beds of massive siltstone. The entire unit is well-sorted and siliciclastic. Most beds in G1 are either green or red and quite distinct from the much more common shades of tan found elsewhere throughout the section. In some places the red and green color alternation occurs every 3-15 cm. The beds return to various shades of tan above the 42 m point. The frequency of laminations, as well as the occurrence of fine sands and clays, increases toward the top of this unit (Figure 2a). Contacts between beds are usually gradational. Well indurated, ledge-forming beds occur at the 33, 34.7, and 38.9 m points.

Gypsum, in the form of 1-2 cm crystals and mm-sized-clumps of needles, is abundant throughout this unit and has been the basis for this unit's distinction. A 66 cm-thick green, gypsiferous claystone, whose upper contact is at 31 m, has an anomalously high concentration of gypsum needles. It is a key bed for southward correlation across the Mojave River. Calcium carbonate layers, interpreted to be primary caliche nodules based upon appearance and morphology, occur at irregular intervals in five different beds. The frequency of secondary gypsum (i.e., crystals filling crevasses as opposed to bedded within the silts) and caliche increase towards the top of the unit. The stratigraphically highest bed containing gypsum tops at 44.3 m. The high gypsum content of this unit suggests deposition in a sabkha environment.

C1 (45.5 to 50.5 meters)

Above G1 is the first of two coarse units within the section, unit C1. Individual beds average 10-20 cm in thickness, are tan siltstones and fine sandstones, are fairly well-sorted or at least preserve well-sorted laminae, and are composed primarily of quartz grains. Coarser material occurs in a few granule gravel lenses (at 46.4 and 46.9 m of Figure 2a) and some pebble layers (at 45.5 and 47.7 m of Figure 2a). The contacts between beds are usually sharp. The coarse clasts are principally sub-angular, intrusive igneous rock fragments. Bedding is both massive and laminated. East-dipping cross-bedding occurs in a unit just below 48-m and overlies a layer of pebbles which exhibit a slight, eastward imbrication. Caliche nodules are abundant at 46.6 and 49.6 m. Distinct ledge-forming beds occur at 45.8, 47.2, 49, and 49.5 m. Evidently this coarse unit was deposited in an alluvial plain environment with intermittent fluvial conditions separated by periods of extended subaerial, oxidizing conditions.

Two volcanic ash layers occur in unit C1. The lower one (NS-G) is a discontinuous, laminated, grey ash which was found at only two localities at NS. Thickness varies greatly, pinching out from 2.5 cm in a matter of tens of centimeters. Both the upper and lower contacts of NS-G are sharp and it is located between 48 and 49 m (Figure 2a). The upper ash layer, NS-MW, located just below 50 m, can be traced throughout the entire NS outcrop at this stratigraphic position. This white ash averages 2.5 to 5 cm-thick, has a sharp upper contact and a sharp but wavy lower contact, and appears to have been reworked with silt in some areas. There are also infrequent silt-filled, vertical root casts which penetrate the entire layer.

F2 (50.5 to 54.8 meters)

Poor exposures due to thick slope wash prevented detailed observations for parts of F2. Unit F2 consists of well-sorted, massive siltstone. The 4.3-meter thick, tan siliciclastic unit consists of three very thick beds separated by two thinner, well-indurated beds at 52 and 53.8 m. The contacts are fairly sharp. This unit appears to be rather featureless in comparison to the coarse units above and below it which contain abundant stratification. No caliche nodules were found

in this unit.

One of the two thinner beds (20 cm thick at 52 m) weathers to a lighter tan color than neighboring beds. It forms a gravelly bench which can be consistently found approximately 2 meters above the white ash (NS-MW) of unit C1. This coarse, resistant unit contains sub-angular to sub-rounded clasts which are primarily quartz, but includes some feldspar and igneous rock fragments. The clast to matrix ratio in this bed is approximately 1:2. Unit F2 appears to have accumulated in a playa environment, similar to F1.

C2 (54.8 to 61.6 meters)

The uppermost unit, C2, is a poorly-sorted, caliche-rich group of beds with frequent coarse-grained lenses (at 54.8, 55.3, 57.2, 58.1, and 59 m) and many occurrences of graded bedding (at 58.3, 60, and 60.5 m for examples). Clasts are dominantly quartz, feldspar, and angular granitic rock fragments. In general, the unit is various shades of tan; however a few beds are a distinct reddish-tan. The contacts between beds are usually quite abrupt and bed thicknesses vary greatly. Several of the thinner beds are more indurated ledge-forming beds. The bed whose lower contact begins at 58 m has a westward imbrication of coarse clasts at its base. A very thin (2 cm) bed just above 61 m exhibits southwest dipping cross-bedding.

While only 6.8 meters are described here, further east C2 extends a few meters higher. This is very important because a third volcanic ash as well as an additional geomagnetic reversal (Pluhar et al., 1991, this volume), not shown in Figure 2a, have been located in these thicker, and stratigraphically higher, exposures. Samples of this ash were not included in the chemical analysis; however, as discussed below, we have excellent reason to believe that this third ash correlates with one found at both of the other sites. Unit C2, like C1, represents a return to a time of increased relief, occasional but sometimes heavy runoff, and extensive physical weathering under arid conditions. (It should be noted that the opposite generalization about relief has been advocated by Blair and Bilodeau (1988) who believe that fine-grained sedimentation above coarse-grained deposits is indicative of renewed tectonic activity. If this is the case the underlying fine-grained unit, F2, would indicate the renewal of tectonic activity.) No major changes in the source rocks for the coarse clastics are evident.

SCS - the southern cliff site - (Figure 2b)

The southern cliff site, SCS, located opposite Manix Wash at a bend on the south side of the Mojave River, is a continuous section of MRF (Plate 1). Here, the beds dip gently to the southwest (at approximately 5 degrees) along an 800 m, 4-to-5 m high, cliff. The eastern edge of the cliff, where the lowest beds are exposed, terminates at Fourmile Waterhole (Plate 1). The western edge of the cliff provides good exposures of the transitional contact with the overlying alluvial deposit, Member A of the Manix Formation. These beds can be traced westward along strike all the way to the "Big Bend" of the Mojave River, Jefferson's type section for his Member A. Individual dipping MRF beds can be followed from the ground surface to their disappearance at the eroded cliff top. Few, if any, lateral variations in thickness, mineralogy, and structure occur within the units.

Figure 2b shows a stratigraphic column constructed in the same manner as that described for NS, although the absence of slope wash and the excellent stream-cut exposures made a detailed description much easier to obtain. Again, on the basis of a coarsening-upward trend throughout the section, we have divided the 31.4+ m section of MRF at SCS into two fine-grained units (F1, F2) and three coarse-grained units (C1, C2, C3). Note that our chosen unit labels, such as C1 or F1, merely indicate course- and fine-grained units at each site and are not to be interpreted as correlative with identical unit labels at NS or SHS.

F1 (0 to 7.9 meters)

The lowest exposures at SCS include 7.9 m of massive, well-sorted silts with intermittent clay and fine-grained sand layers. An increase in grain size, up to medium-sized sand, occurs between 2.5 and 3.9 m. The contacts between beds are usually sharp and bed thicknesses vary greatly. The mineralogy of the sand fraction is almost entirely siliciclastic, but some feldspar and mafic rock fragments occur in a well-laminated bed at 3

m. A distinct color change, from tan to red, occurs at the base of this well-laminated bed. The beds above this point alternate between red and tan and then remain red above 5.8 m with the exception of a distinct 48 cm-thick olive green bed which lies just above 5.3 m. This bed is referred to as the "olive marker bed" in the correlations discussed below. Secondary gypsum fills cracks throughout unit F1 and is especially abundant in the uppermost 2 m-thick bed.

A 2.5-3.5 cm-thick white volcanic ash (SCS-LW) occurs 0.7 m above the base of the section. The ash is continuously exposed laterally for 5.9 meters from the present channel to the top of the cliff . Its lower contact is abrupt and the upper contact has thin laminae of clay or silt indicative of reworking.

C1 (7.9 to 12.1 meters)

The lowest relatively coarse-grained unit, C1, is 4.2 m thick and consists primarily of 10-cm thick, fairly well-sorted, tan beds of clay, silt, and fine sand. A 1.1 m-thick bed occurs near 8.6 m which includes a layer of coarse sand near its base. Both normal and reverse grading occurs within this unit. Beds are massive, laminated, and in two cases cross-bedded with dips to the southwest. All beds are siliciclastic. Caliche nodules and secondary gypsum are also common. Contacts are generally sharp, and thin cusp-shaped clay layers (mudcracks) occur at the upper contact of nearly every bed. Many of the beds contain pervasive fractures which are most likely the remnants of deep mudcracks. Unit C1 is primarily tan with a few redder beds. Evidently this unit was deposited in an alluvial plain environment like units C1 and C2 from NS, and was apparently derived from the same source area.

A second white volcanic ash (SCS-UW) occurs in Unit C1 at 10.2 m. Its thickness varies from 2.2 to 3.2 centimeters and is overlain by a 1 cm-thick, light tan, clay layer. The upper and lower contacts are sharp.

F2 (12.1 to 13.8 meters)

The second fine-grained unit, F2, at SCS consists of one well-sorted, greenish tan, siliciclastic, laminated siltstone bed. There are no clay layers or caliche nodules within this siliciclastic unit although these features are very abundant above and below F2. Upper and lower contacts are sharp as are the contacts between layers at every 1 to 8 centimeters. The bed is highly fractured, suggestive of mudcracks, and weathers to a purplish red. The unit's distinct color, as exposed in outcrop, and grain size warrant its distinction. This unit implies a return to playa conditions.

C2 (13.8 to 26 meters)

Unit C2 consists of 12.2 meters of a gradual transition from well-sorted, thin and fine-grained lower beds to moderately sorted, relatively thicker and coarser-grained overlying deposits. Bedding is massive, laminated, and in some places graded. Clast mineralogy is primarily quartz but also sub-rounded to sub-angular feldspar and volcanic rock fragments in some of the coarser units. Thicknesses of individual layers vary from 10 cm to 20+ cm. Grain sizes range from clay to medium sand. The two beds near the top of unit C2, at 23.2 and 24 m, contain coarse sand-sized grains and pebbles, respectively. The beds are predominantly tan although both greenish-tan and reddish-tan beds are common.

Cross-bedding dips northeast in a bed at the 15.4-meter mark while those in beds at 19.1 and 23 m exhibit dips to the southwest. Several beds have deep vertical fractures (mudcracks?) penetrating down from their upper contact at systematic intervals (see fracture symbols at 15.3, 16.8, 17.3, and 18.7 m). Larger fractures, 25 cm in length and spaced 23 cm apart from one another, permeate the bed beginning just above 25 m. Clay layers (mudcracks) occur at nearly every contact in the lower half of the unit and diminish in frequency upward starting at 19.2 m. The same stratigraphic horizon marks the disappearance of frequent caliche nodules with one exception at 24.1 m. Layers of gypsum crystals fill fractures at 21 and 21.4 m. Like the coarse units at NS this unit appears to have accumulated in an alluvial plain environment. However, Cady Mountain volcaniclastic and metavolcaniclastic sources to the south are evident in the coarse clastics of this unit.

C3 (26 to 31.4+ meters)

The base of unit C3 marks the beginning

of a broad zone of alternating beds. Two sequences are common: 1) beds with a similar lithology and structure to those of unit C2 and 2) much coarser beds of gravel, pebble, and cobble conglomerates. The change in lithology is quite visible from a distance between the light-colored silts and the overlying dark-colored conglomerates. We consider the conglomerates, indistinguishable in lithology from those of Jefferson's Member A of the Pleistocene Manix Formation (1985), to be continuous with the beds of Member A described to the southwest by Jefferson. Thus unit C3 of SCS is a transitional unit between MRF and Member A of the Manix Formation. Implications of this interpretation are discussed below. In the upper-most portion of unit C3 contacts are both sharp and gradational between the two distinct lithologies and have been depicted in Figure 2b as one transitional unit. Caliche is restricted to the conglomerates.

The silt beds in C3, for example at 29 and 31 m, are relatively thin, interfingering beds indistinguishable from beds within the MRF. These beds are tan, siliciclastic, and infrequently laminated. They tend to be approximately 30 cm thick, massive, and fairly well-sorted.

The distinctive purplish-red, poorly sorted, coarse conglomerates are composed of a tan, silty, siliceous matrix, constituting between 30 and 70% of each bed, supporting distinct sub-angular clasts of purple and green, tufa(?)- and caliche-covered, volcanic and metavolcanic rock fragments. These conglomerate layers are, on the average, thicker than the interfingering silt beds and thicken up-section. Although the conglomerate beds tend to be poorly sorted, clasts are well-sorted in some laminated horizons in the uppermost bed. In addition, most of the conglomerate beds are graded. The conglomerate beds represent the distal portions of alluvial fans originating from the south.

Although our measured stratigraphic column ends only 5 meters above the base of the zone of interfingering silt and volcaniclastic layers, we have traced the transition another kilometer south, which is probably stratigraphically higher due to the very gentle southwesterly dip of the southern cliff section, along the eastern edge of the Mojave River. Although exposures are discontinuous, one stream channel (BBE - Big Bend East - on Plate 1) yields an excellent exposure of both the MRF silt and Manix Formation Member A conglomerate lithologies (see Figure 5). Green lacustrine deposits of Manix Formation (Member C) conformably overlie the outcrop within 5 meters of a location where MRF lithology interfingers with Manix Formation Member A lithology. Distinct tufa zones occur in the Member A conglomerates throughout this area, perhaps suggesting an encroachment of early Lake Manix over distal alluvial fan deposits.

SHS - the southern hill site - (Figure 2c)

A small but interesting exposure of the MRF crops out in low hills set back from the river to the southeast of SCS (see Plate 1 and Figure 2c). Quaternary alluvium surrounds the hills. The beds at SHS are weathered in a manner similar to those at NS, covered in many places with thick slope wash. They strike N30W with a slight dip (< 5 degrees) to the southwest.

Based on a coarsening-upward trend like that seen at NS and SCS the 14.8 meter section is divided into two units: a fine-grained lower unit (F1) and a coarse-grained upper unit (C1).

F1 (0 to 9.9 meters)

The bottom half of SHS consists of massive, thickly bedded (average is about 70 cm) siltstone. Fine- and medium-sized sand occurs between 2.1 and 3.9 m. All contacts are fairly sharp. The siliciclastic beds are generally well-sorted and tan in color, although the thinnest beds are often red. One bed, which lies at the 5.6-meter mark, is a very distinct olive green. This bed is probably correlative with the "olive marker bed" that was described above in Unit F1 for SCS. Caliche nodules first appear in the thin, well-indurated bed just below the "green marker bed". Another well-indurated bed appears at 9 m. As with the other "F" units at NS and SCS, we ascribe these deposits to a playa environment.

Three volcanic ashes are present in unit F1. The lowest (SHS-G) marks the base of the SHS section and is at least 30 cm thick in some places. It is a well-laminated, silvery-grey ash which has been reworked with mm-

thick laminae of tan silt. The upper contact is abrupt while the lower contact is not exposed. A white ash (SHS-MW), which occurs at 2.1 m, is also reworked with silt laminae. It is about 2.5 cm thick, varying +/- 1 cm laterally. The lower contact is abrupt while the upper contact is gradational with the overlying silt bed. A second white ash (SHS-UW) occurs at 9 m. It averages 3 cm thick, although it pinches out and reappears laterally. Upper and lower contacts of SHS-UW are sharp and a continuous clay layer overlies the ash.

C1 (9.9 to 14.8 meters)

The top 4.9 meters of the SHS section have been designated unit C1. Although this unit does become coarser in its uppermost beds it does not contain as high a percentage of coarse-grained clasts as the coarse units at NS and SCS. The dominant grain mineralogy is quartz while the coarser clasts include sub-angular igneous rock fragments. The grain size ranges from silt to pebbles. The beds, which are mostly massive, range from well-sorted near the base to poorly sorted near the top. Relatively thin, laminated beds (at 10 and 11.1 m) tend to be less indurated than the massive, thicker beds. Highly indurated beds occur at 12.1 and 13.5 m. The beds are mostly tan but some green and red beds occur. The entire unit is rich in caliche and has many thin, cuspate clay layers (mudcracks?) at contacts. Very large fractures which look like mudcracks occur at the top of the bed beginning at 11.4 m. The contacts are predominantly sharp.

The upper contact of MRF at SHS is unconformably overlain by what appears to be a thin cover of Member B of Jefferson's (1985) Manix Formation.

Lithologic Correlation

Figure 3 shows our preferred stratigraphic correlation between the three exposures of the MRF based upon lithology. Also shown are the magnetic polarity intervals of Pluhar et al., (1989; 1991, this volume). The paleomagnetic work independently supports the lithologic correlations. The stratigraphically lowest MRF beds in this area are exposed at NS while the uppermost beds are in the transition zone C3 at the top of SCS. Neither site represents a complete time sequence of the MRF although we believe that the deposition of the bottom of SCS overlaps in time with the deposition of the top of NS. SHS is a section of the middle of the MRF. The base of the exposure at SHS is slightly lower stratigraphically than the base of SCS. No evidence of the SCS transition zone C3 is seen at the top of SHS.

The volcanic ash beds within the MRF support the lithologic correlation. Based upon lithology and stratigraphic position, we believe that a portion of a sequence of three ash beds is present at each site. The ash sequence consists of a grey ash bed overlain by two different white ash beds (designated middle white ash and upper white ash). Inspection with a binocular microscope distinguishes primary characteristics between the grey ash and either of the white ashes. The grey ash has a spindle-like texture and contains numerous transparent glass shards, many of which are smooth and highly reflective and give this ash a distinct sparkle in sunlight. The ash consists of less than 5% total of black-mica flakes, pale white feldspar grains, and black rock fragments. The white ashes both have a sugary texture and consist almost exclusively of opaque glass shards; they are not distinguishable from each other under the binocular microscope. The mineralogy of the white ash clasts is similar to the grey except that 5-10% are quartz.

The stratigraphic separation between these ashes varies from section to section, which is important in discerning local depositional histories. 1.5 m separate the grey and middle white ashes at NS while the separation at SHS is 2.2 m. The grey ash is not seen at SCS although we speculate that it is approximately 2 m below the surface at the eastern limit of the cliff exposure. The distance between the middle and upper white ashes is 9.4 m and 6.7 m at SCS and SHS, respectively. The upper white ash is not found at NS within the beds that have been described. However it was found further to the west during subsequent field work. At NS the alluvial nature of the sediments between 5 and 11 m above the middle white ash suggests unfavorable conditions for the preservation of fine ashy material. Detailed chemical analyses of all ashes, described below, provides strong support for the lithologic correlations of Figure 3.

Additional evidence for the proposed correlations (Figure 3) includes similar

lithologies above the middle white ash at all three sites. Both F1 units at SHS and SCS are comprised of fairly thick beds of silt. An uninterrupted occurrence of fine and medium sand-sized grains occurs in beds just above the middle white ash. Both units contain the 48 cm-thick "olive marker beds" which are overlain by a 2-m thick massive gypsiferous siltstone. Of all beds at NS, those in unit F2 are the most similar in thickness and lithology (excepting an "olive marker bed") to the F1 units correlated between SHS and SCS.

Two additional exposures of the MRF (Plate 1), known informally as Gyp Hill, are exposed west of Manix Wash between several fault strands. Preliminary investigations suggest that these particular exposures of MRF correlate with the gypsiferous unit, G1, of NS. The elevation of the gypsiferous unit at Gyp Hill is approximately 1690 feet while the elevation of G1 at NS is approximately 1640 feet. This suggests 15 meters of relative vertical displacement since deposition.

CHEMICAL ANALYSES OF ASHES

In total seven volcanic ash exposures occur among the three localities of MRF. Three ash beds are located at SHS and two ash beds occur at NS and SCS. While macroscopic properties (described above) are useful as a tool for lithologic correlation, the use of chemical analyses provide an important quantitative enhancement.

All ash samples collected for the analysis were collected during one field excursion by two workers. For each of the seven ash exposures three 300-gram samples were acquired as far apart as possible along strike after making certain we could trace the ash bed continuously between the three sampling places. Analysis of each of the 21 samples consisted of 78 chemical determinations including REE (Rare Earth Elements) using X-Ray fluorescence, neutron activation analysis, and inductively coupled plasma mass spectrometry.

Data from the complete analyses are given in Table 1. Zero values should be read as "below detection limit". Several graphs of major oxides, trace elements, and REE (Figure 6 a,b,c) illustrate both consistency among the three samples taken from each ash bed at each locality, and well-defined variations between ashes. The ash samples are graphed in three groups corresponding to the sequence discussed above (grey below middle white below upper white). All graphs support the stratigraphic correlation by clearly distinguishing each of these groups of ashes.

Samples from the grey ash show 3 to 4 times as much Fe_2O_3 and about twice as much TiO_2 as samples from either of the white ashes (Figure 6a). Weight percent MnO clearly differentiates the middle white ash from the grey and upper white ashes. Samples from the grey ash show larger amounts of Zr and Rb than samples from either of the white ashes (Figure 6b). Samples from the middle white ash have a larger amount of Rb than those from other beds and samples from the upper white ash have an anomalously low amount of Nb. REE abundances were determined by inductively coupled plasma mass spectrometry and show the clearest evidence for within-bed sample consistency (Figure 6c).

Previous Analyses of Volcanic Ashes

Sarna-Wojcicki et al., (1980) analyzed a total of seven ash samples from the MRF. From their descriptions of ash localities we believe the ashes sampled were from the following sites: two samples from the upper white ash and two samples from the middle white ash at SCS, and two samples of the middle white ash and one sample of the grey ash at NS. The upper and middle white ashes were designated "Manix-3" and "Manix-2", respectively, by Izett (1981). Detailed stratigraphic control was not reported in these earlier studies so it is difficult to make comparisons between them and the chemical analyses conducted for our study. Additionally, most of these earlier studies were performed exclusively on the glass shards while our study examined the chemistry of the undifferentiated, whole, ash beds. Because a heavy liquid separation was not performed on our ashes, comparisons between MRF ash data and results from these earlier studies are not appropriate. Consequently our data have been primarily used to test intra-basin correlations. However it is worth noting that plots of REE of the Huckleberry Ridge ash and the white "Manix-2" and "Manix-3" ashes (Izett 1981) are very similar to our REE plots for our grey ash and

Table 1. Chemical analyses of volcanic ash beds found within the Mojave River Formation (MRF), central Mojave Desert, California.

	'SiO2	'Al2O3	TiO2	Fe2O3T	MnO	CaC	MgO	Na2O	K2O	P2O5	SUM	S	LOI	Sn	Au	Pd	Pt	Cr	Rb	Sr	Y
NS-G-1	70.1	11.6	0.15	1.58	0.05	1.15	0.17	5.81	3.13	0.06	100.49	2750	6.54	9	0	0	0	25	175	121	105
NS-G-2	69.2	11.6	0.16	1.7	0.05	0.88	0.19	6.69	2.99	0.06	100.02	1200	6.39	9	0	0	0	25	169	63	95
NS-G-3	68	11.3	0.15	1.61	0.05	1.57	0.15	6.6	2.76	0.06	99.99	2870	7.62	0	6	0	0	20	168	127	81
SHS-G-1	68.2	11.7	0.18	1.84	0.05	3.41	0.32	4.39	3.3	0.03	100.3	157	6.77	0	0	0	10	20	175	63	76
SHS-G-2	69.5	12.2	0.19	2.16	0.05	1.86	0.51	4	3.55	0.04	100.11	0	5.93	0	0	0	0	44	182	94	86
SHS-G-3	69.5	12.3	0.2	1.88	0.05	1.99	0.5	4.11	3.4	0.04	100.12	0	6	0	3	1	0	23	177	152	99
NS-MW-1	70.7	12.1	0.08	0.52	0.1	0.65	0.12	5.95	3.07	0.05	99.07	1020	5.7	0	0	0	0	20	281	0	41
NS-MW-2	70.8	12.1	0.09	0.64	0.11	0.61	0.13	6.47	3.07	0.05	99.51	0	5.39	8	0	1	10	24	288	81	53
NS-MW-3	71.3	12.2	0.09	0.59	0.12	0.65	0.11	6.68	3.08	0.04	100.44	4310	5.54	0	0	0	0	24	279	79	45
SHS-MW-1	70.1	12.1	0.09	0.8	0.1	1.86	0.21	5.28	3.46	0.02	100.45	2630	6.39	0	0	0	0	22	270	97	37
SHS-MW-2	73.1	12.6	0.09	0.44	0.11	0.76	0.15	4.86	3.35	0.02	100.38	193	4.85	0	1	2	10	25	288	46	49
SHS-MW-3	72.9	12.6	0.09	0.77	0.11	0.59	0.17	4.89	3.45	0.02	100.26	167	4.62	0	0	0	0	51	289	41	46
SCS-LW-1	72.2	12.8	0.1	0.65	0.1	0.68	0.32	5.09	3.23	0.06	100.28	684	5	0	2	3	10	23	288	113	32
SCS-LW-2	73.4	12.7	0.09	0.48	0.1	0.58	0.2	5.06	3.08	0.04	100.62	129	4.85	0	0	1	0	30	294	0	56
SCS-LW-3	72.8	12.7	0.09	0.69	0.1	0.54	0.25	5.09	3.18	0.02	100.27	164	4.77	0	0	2	0	22	286	22	52
SCS-UW-1	72.7	12.3	0.08	0.47	0.06	0.42	0.08	4.94	3.18	0.02	99.13	0	4.85	0	0	0	0	23	190	0	15
SCS-UW-2	72.9	12.3	0.08	0.53	0.06	1.03	0.17	4.79	3.28	0.05	100.62	3080	5.39	0	0	0	0	24	184	121	25
SCS-UW-3	73.6	12.4	0.08	0.63	0.06	0.42	0.1	4.79	3.26	0.02	100.39	0	5	0	0	0	10	28	188	18	37
SHS-UW-1	73.8	12.5	0.09	0.55	0.06	0.54	0.14	4.75	3.61	0.06	100.52	0	4.39	0	0	1	0	20	191	0	32
SHS-UW-2	75.3	12.7	0.08	0.41	0.06	0.51	0.07	4.75	3.26	0.02	101.34	0	4.16	0	0	0	0	21	183	0	0
SHS-UW-3	72.9	12.3	0.09	0.56	0.06	0.55	0.11	4.81	3.48	0.02	99.68	76	4.77	0	0	1	10	20	190	0	52

	Zr	Nb	Ba	LA	CE	PR	ND	SM	EU	GD	TB	DY	HO	ER	TM	YB	LU
NS-G-1	259	67	783	304.4	203	194	124.1	74.5	12.3	44.8	38.8	34.8	31.4	31	31.3	26.8	24.8
NS-G-2	246	65	503	290.2	196.8	197	124	72.4	12.2	45.6	38.8	33.5	29.6	29.6	31.3	26.8	24.1
NS-G-3	240	65	482	294.9	200.5	196	120.4	70.8	11.5	41.3	36.7	30.8	28.2	27.7	28.1	24.9	22.9
SHS-G-1	234	60	510	293.7	193.1	188	119.8	70.8	12.7	44.4	38.8	33.5	29.7	29.1	28.1	24.4	22.3
SHS-G-2	249	64	474	287.6	196.8	186	122.3	70.3	13.2	42.9	38.8	32.9	29.9	29.6	31.3	25.4	22.9
SHS-G-3	237	65	731	267.3	185.7	183	115.1	72.4	13.6	43.2	38.8	33.2	30	29.6	28.1	24.9	23.5
NS-MW-1	96	68	138	56.8	56.2	60	37.5	33.3	2.8	22.4	22.4	19.4	17.8	17.4	18.8	17.2	18.9
NS-MW-2	101	72	148	52.4	52.4	58	35.8	31.8	2.8	22	20.4	17.8	16	15.5	15.6	16.3	16.4
NS-MW-3	94	66	126	52.1	50.9	58	37	32.8	2.5	22.8	20.4	18.8	16.5	16	15.6	16.7	17.3
SHS-MW-1	99	66	114	56.5	52.8	59	37.4	32.3	3.5	21.2	20.4	18.5	17.2	17.8	18.8	17.2	18.9
SHS-MW-2	103	74	146	58.7	54.5	61	39	32.8	1.4	19.7	18.4	16.3	14.4	14.6	15.6	14.4	12.1
SHS-MW-3	99	67	181	56.2	53.6	58	38.5	32.8	1.5	20.5	18.4	16	14.4	14.6	15.6	13.9	12.4
SCS-LW-1	111	80	154	53.7	50.2	58	38.9	31.8	1.2	20.1	18.4	16.9	14.3	14.1	15.6	14.8	12.4
SCS-LW-2	97	70	112	55.2	53	60	38.4	33.3	2.4	23.6	20.4	19.7	17.8	17.8	18.8	17.2	18.9
SCS-LW-3	103	68	138	53.7	52.4	56	36.2	31.2	3	21.2	20.4	18.5	17.4	16.9	18.8	17.2	18.6
SCS-UW-1	96	42	132	65.7	55.8	55	35.2	25.5	0.3	13.9	12.2	9.8	8.3	8.9	9.4	8.6	6.5
SCS-UW-2	90	34	111	59	52.2	57	34.3	26	2.1	14.7	14.3	10.5	10.4	10.8	12.5	10	12.4
SCS-UW-3	90	39	100	56.8	51.4	58	34.2	25	2.6	15.4	14.3	11.7	10.6	10.3	12.5	11	12.7
SHS-UW-1	93	39	79	59	52.5	57	35	24	1.9	14.3	12.2	10.8	10.1	10.3	9.4	9.6	10.8
SHS-UW-2	89	43	75	59.7	54.4	56	34.5	24.5	2.5	14.3	14.3	11.7	11	10.8	12.5	11	11.8
SHS-UW-3	95	40	102	60.6	52.6	58	35.5	25	0.7	12.7	12.2	9.2	8.2	8	9.4	8.1	6.2

[Oxide concentrations given in weight percent; REE are chondrite normalized to the following values: La 0.315, Ce 0.8130, Pr 0.1000, Nd 0.5970, Sm 0.1920, Eu 0.0722, Gd 0.2590, Tb 0.0490, Dy 0.3250, Ho 0.0720, Er 0.2130, Tm 0.0320, Yb 0.2090, and Lu 0.0323; all other concentrations given in parts per million]

our upper white ash, respectively, but different from our middle white ash plots.

Neither of the white ashes have been correlated radiometrically to dated tuffs. However several workers (Sarna-Wojcicki et al., 1980, 1984; Izett, 1981; Izett et al., 1988) have concluded that the white ash chemistry is very similar to ashes generated from the Long Valley-Glass Mountain area, California. Sarna-Wojcicki et al., (1980, 1984) calculated a high similarity coefficient (0.97) between the chemistry of the grey ash and a sample of the Huckleberry Ridge ash (formerly called the Pearlette type B ash bed) from Meade County, Kansas. They also cite isotopic and stratigraphic evidence, independent of glass chemistry, in support of this correlation. The Huckleberry Ridge ash is correlative with the family of ashes from Yellowstone National Park, Wyoming, and has been dated at 2.01 Ma on the basis of several K-Ar determinations (reported by Izett, 1981).

Figure 6. Selected plots from the data in Table 1 showing a clear chemical distinction between six upper white ash samples (two localities), nine middle white ash samples (three localities), and six grey ash samples (two localities). Graphs include: a) major oxides, b) trace elements, c) REE, and d) two extreme examples taken from each of the three ash beds.

INTERPRETATION

Correlations between the three MRF exposures yield an 80 meter thick composite section that records an arid/semi-arid depositional system. The relatively finer grained deposits at SCS and SHS (both F1 units) are very similar and appear to represent a more distal facies (with respect to a topographic source associated with the active Manix fault) than the coarser deposits (C1) present at NS. Primary bedding features such as the dip direction of cross-bedding may be a more reliable indicator of flow direction at SCS and SHS than adjacent to the fault.

The depositional history of the MRF is generally dominated by (1) an upward coarsening sequence of silt and clay to fine- and medium-sized sand, (2) an upward increase in caliche and desiccation features, and (3) an upward decrease in gypsum occurrence. The strata record a period of sabkha/playa conditions when the Manix basin was probably internally drained, followed by repeated cycles of desiccation and a combination of subaerial, lacustrine, and fluvial sedimentation. The preservation of the three volcanic ashes within fine silts supports a playa or lacustrine environment rather than a surface dominated by alluvial processes. The upper portion of the MRF, preserved at both SCS and NS, exhibits a lateral facies variation between the two sites. At NS active tectonic uplift has created alluvial fan deposits which are most likely responsible for the absence of portions of the grey and upper white ash beds. This prograding fan sequence interfingers with the alluvial deposits from the south which we refer to as Member A of the Manix Formation and is preserved in unit C3 at SCS.

A more detailed chronological history can be correlated to specific MRF units. The earliest period of MRF time is represented by 48 meters of section, prior to the deposition of the (2.01 Ma?) grey ash. Massive deposits of bedded gypsiferous silts and clays accumulated (see Figure 2a - units F1, G1, and C1) during this interval. Given the magnetostratigraphy of Pluhar et al., (1991, this volume) and assuming that the grey ash is indeed the 2.01 Ma Huckleberry Ridge ash, the maximum amount of time represented by the section of MRF below the grey ash is 470 Kyr. This yields a minimum sedimentation rate of approximately 10 cm/Kyr for the period of time preceding deposition of the grey ash.

At NS are many relatively thinner, coarse beds (C1) between gypsiferous silts and the grey ash. These coarse sediments could represent a time of either increased fault-related uplift and/or basin subsidence adjacent to the Manix fault, perhaps also in conjunction with increased runoff. The only occurrence of east-dipping cross-bedding within the MRF is found at the top of section C1 at NS. Because correlative beds at SCS and SHS are buried, it is difficult to determine whether this change in direction of deposition was a local, fault related phenomenon or whether it was regional in scale. The grey ash is laminated at both NS and SHS and is reworked with overlying silts at SHS, suggesting a shallow,

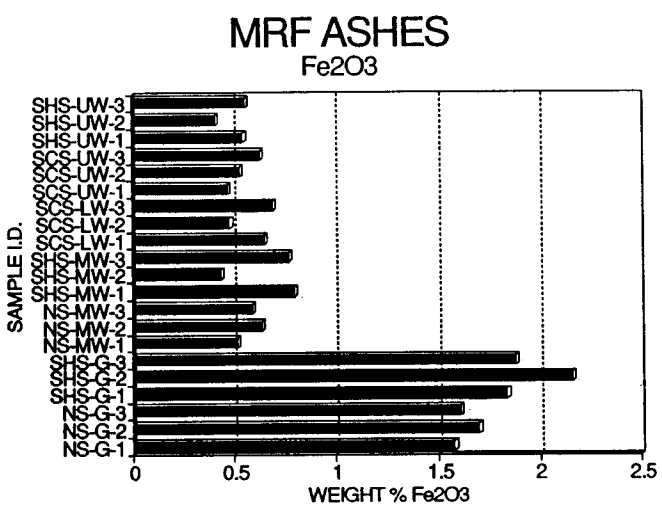

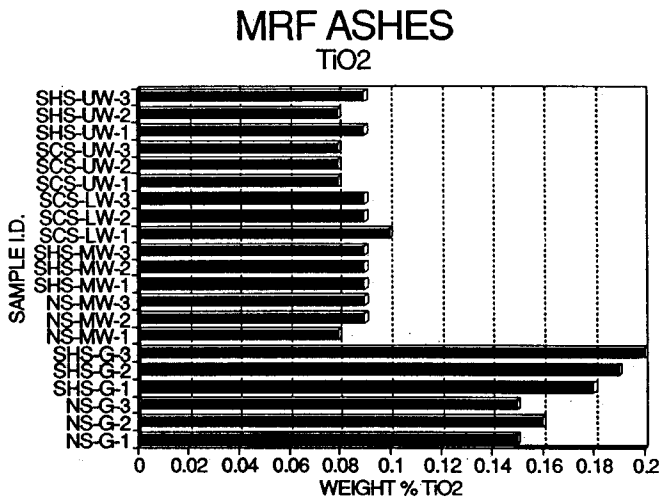

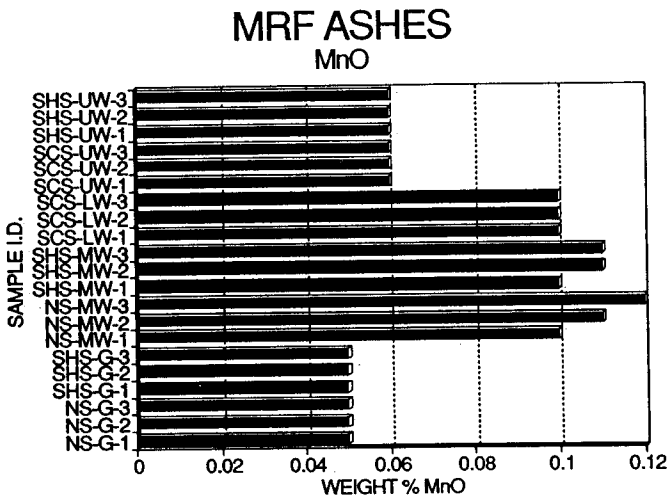

Figure 6a. Plots of Fe_2O_3, TiO_2, and MnO as determined from X-Ray fluorescence analysis of volcanic ash beds found within the Mojave River Formation, central Mojave Desert, California. Oxide concentrations are given in weight percent.

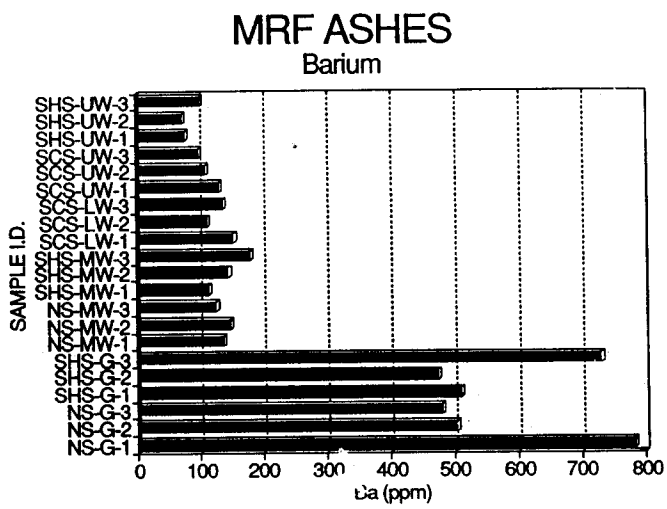

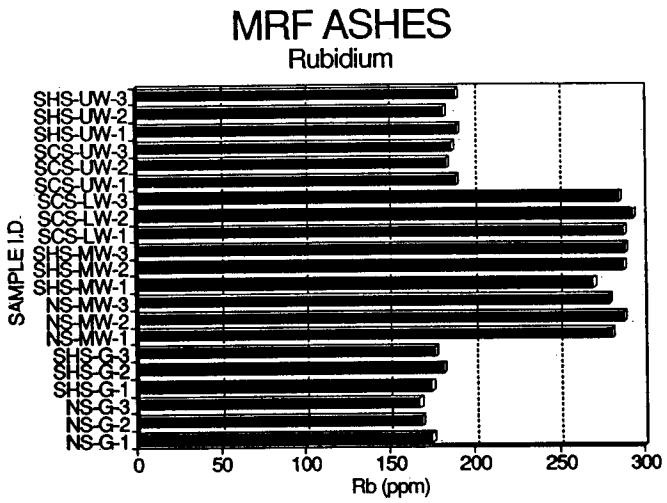

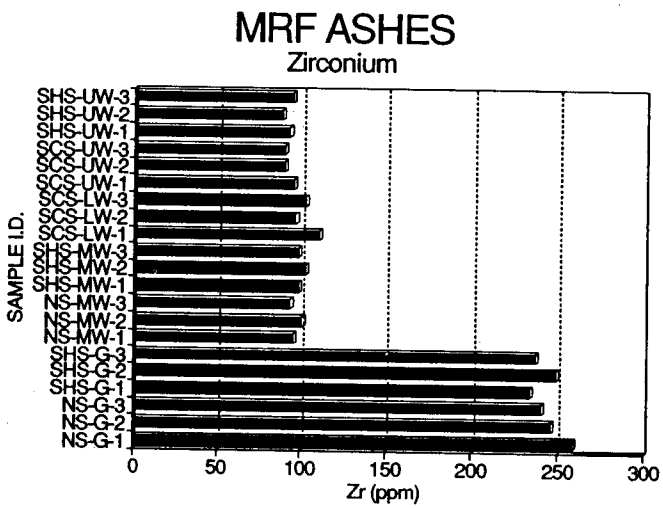

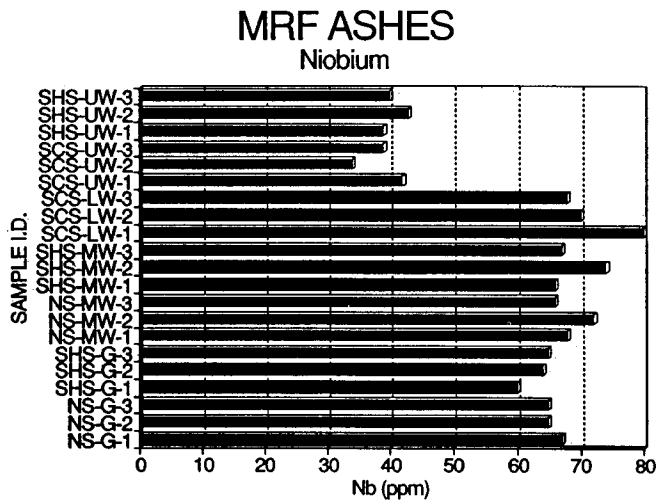

Figure 6b. Plots of Barium (Ba), Rubidium (Rb), Zirconium (Zr), and Niobium (Nb) as determined from X-Ray fluorescence analysis of volcanic ash beds found within the Mojave River Formation, central Mojave Desert, California. Concentrations are given in parts per million.

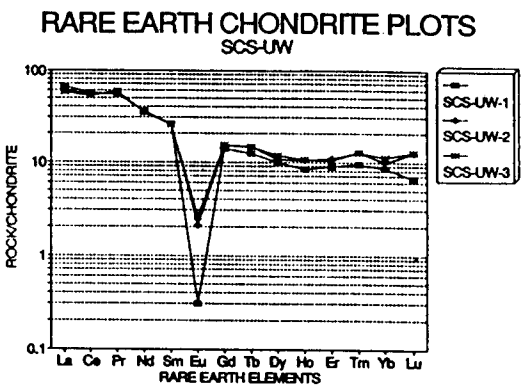

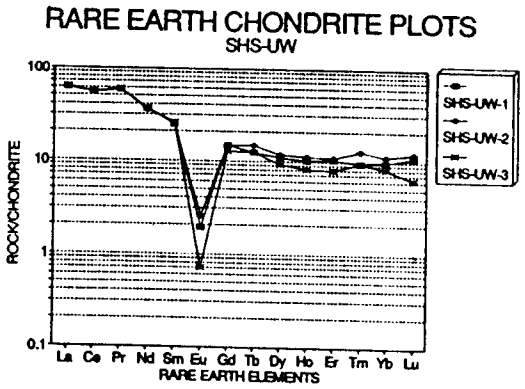

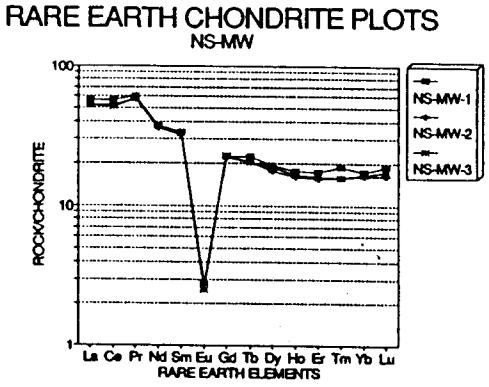

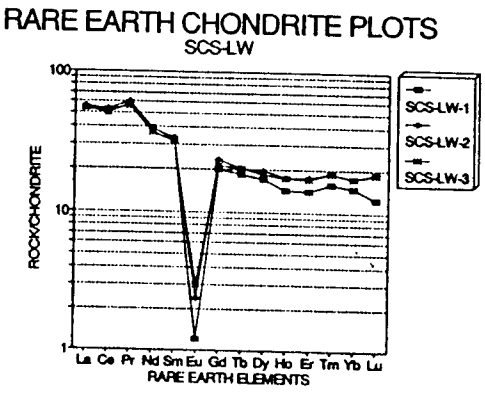

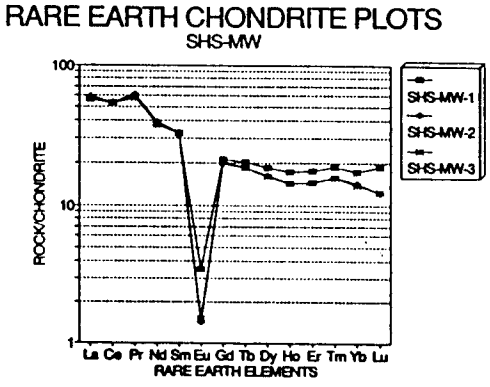

Figure 6c. REE analysis (determined by inductively coupled plasma mass spectrometry) of volcanic ash beds found within the Mojave River Formation, central Mojave Desert, California. Each graph shows sampling consistency within any given ash bed. The graphs have been placed together in accord with our lithologic correlation (i.e., the first two graphs are from the upper white ash, the next three are from the middle white ash, and the next two are from the grey ash) to emphasize the similarity between the exposures of upper white (UW), middle white (MW and LW), and grey (G) ashes .

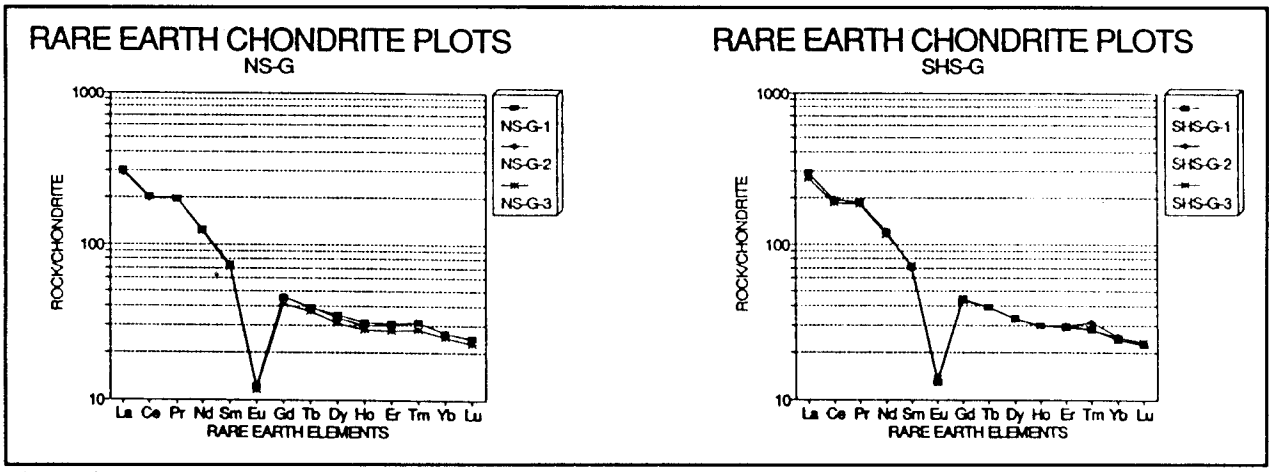

Figure 6c. (cont.)

quiet water environment.

The period of time between the deposition of the grey and upper white ashes is represented at all three sites by thickly bedded, massive silts with minor occurrences of coarser clastics (see Figure 2a - C1 and F2; Figure 2b - F1 and C1; and Figure 2c - F1). The only exception are the alluvial units at NS beginning at 54.8 m (Figure 2a) which we attribute to unique conditions at this site as a result of its proximity to the Manix fault. The lack of primary structures, the abundance of color alterations from red to green, and the presence of gypsiferous silts at SCS (see Figure 2b, 6.2 m) provide clear testimony to an internally drained system, an arid climate, and the absence of local tectonic uplift. The first southwest-dipping climbing ripples occur just above these gypsiferous silts. All ash samples show evidence supporting subaqueous deposition.

The remainder of the MRF above the upper white ash is most complete at SCS, although there are 5.8 meters of section exposed above the upper white ash at SHS. At SHS, the grain size increases upwards to pebble sized and the bedding is massive. Caliche nodules and thin cuspate clay layers (interpreted to be mudcracks) and other desiccation features, such as pervasive fractures are abundant. Primary features at SCS are similar, but the beds are generally thinner and desiccation features are much more extensive. Few coarse clasts exist. At least six beds show southwest dipping crossbedding which may reflect change from a closed internally drained basin to an open one along the course of an ancestral Mojave River system. It also suggests that the local drainage flow was in an opposite direction from today, which could be an important clue to early and middle Pleistocene paleogeography in the Mojave Block.

The transitional contact with the overlying Manix Formation is extremely important because it preserves information concerning changing environmental conditions during deposition. The deposition of the coarse alluvial fan, Member A of the Manix Formation, marks the end of

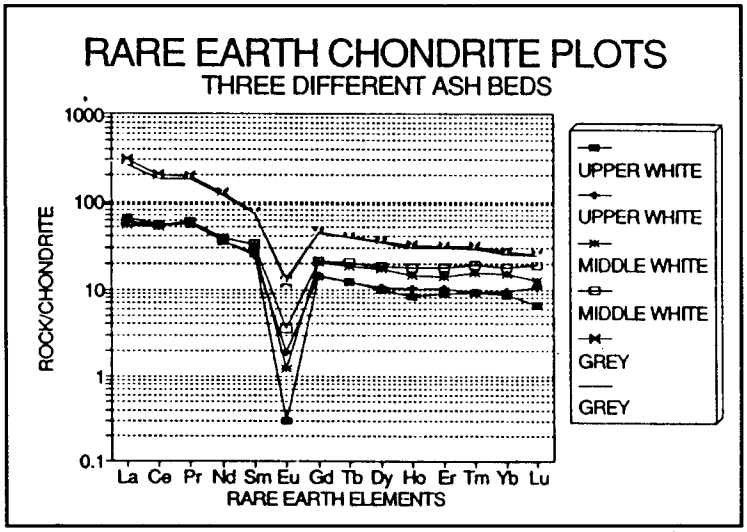

Figure 6d. REE patterns from two extreme samples taken from each of the three ash beds. The plots illustrate how each ash bed is chemically unique.

MRF depositional processes and the beginning of time when perennial Lake Manix first occupied Manix basin (Jefferson, 1985). Caliche-covered clasts, found in the lowest interfingering layers of Member A lithology within the transition zone, testify to a continued arid environment. Tufa-covered pebbles and cobbles found within the higher conglomerate beds are indicative of ancient shorelines. Manix Formation Member A lithology clearly records tectonically generated relief in what is now the Cady Mountains. The onset of lacustrine conditions implies a natural damming in Afton Canyon, perhaps related to the same episode of renewed tectonism as well as the opening (or re-opening) of drainage northward from the San Gabriel and San Bernardino Mountains.

AGE OF THE MOJAVE RIVER FORMATION

A diagrammatic summary of the most likely possibilities for the age span of the MRF and the Manix Formation (Figure 7) is based upon chemical data from the ashes and the magnetostratigraphic work by Pluhar et al. (1991, this volume). The oldest U/Th date from the Manix Formation is greater than 350 Kyr BP (Jefferson, 1985). Jefferson (1985) calculated a maximum age of 500 Kyr based upon extrapolation of oxygen isotope stages dates and a pulsed lacustrine sequence. As discussed above, the grey ash in the MRF has been correlated with the 2.01 Ma Huckleberry Ridge ash on the basis of glass chemistry and stratigraphic position. The most probable age for the normal polarity zone near this ash (Figure 3) is 1.67 to 1.87 Ma which corresponds to the Olduvai normal subchron (Harland et al., 1990). This assessment is based upon independent magnetostratigraphic evidence that another normal polarity subchron exists near the base of the transition zone at the top of SCS, just slightly above the position where our detailed description ends. This upper subchron is interpreted to be either the Jaramillo Event (0.92 to 0.97 Ma) or the Cobb Mountain Event (1.1? Ma) by Pluhar et al., (1991, this volume).

These dates yield a total age of approximately 1.5 million years for the MRF, spanning from just after the Matuyama/Gauss boundary (2.48 Ma) to the end of the Jaramillo Event (0.92 Ma). The average sedimentation rate for the entire 80 m deposit can be calculated to be approximately 5.3 cm/Kyr.

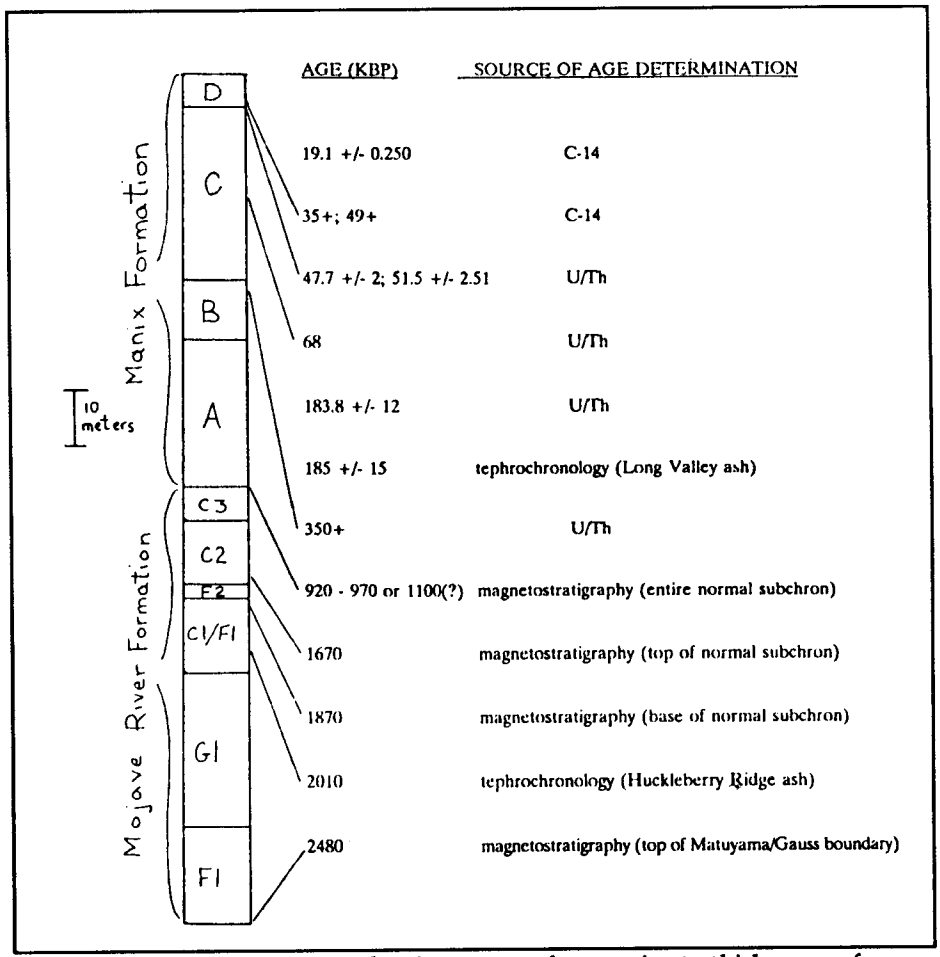

Figure 7. Composite diagram showing ages and approximate thicknesses of Manix Formation (Jefferson, 1985) and of Mojave River Formation (described in this paper).

There is good evidence of variable sedimentation rates and specifically a higher rate of sedimentation at NS.

Preliminary field studies further to the south and east of SHS suggest that the previously unrecognized transitional contact between the MRF and the Manix Formation may be traceable all the way to Afton Canyon. The Brunhes/Matuyama magnetic reversal was not detected in the coarse deposits of the transition zone south of SCS presumably due to the unsuitable character of such coarse clastic deposits. Perhaps it may be possible to locate it along one of these eastern exposures. Also, at approximately the same stratigraphic level as the Brunhes/Matuyama reversal, we would expect to find remnants of the 0.74 Ma Bishop Ash, a widespread Long Valley-Glass Mountain ash which occurs farther south than Manix Basin (Izett et al., 1988). Presumably, the coarse alluvial beds believed to contain the magnetic reversal, at the top of the MRF, would likewise be unsuitable for preserving an ash.

IMPLICATIONS FOR THE MOJAVE RIVER

The MRF provides constraints on where and when the Mojave River flowed prior to the formation of Pleistocene Lake Manix. Interpreted depositional systems and age estimates for the MRF and Manix Formation allow reconstruction of the paleoclimate/paleohydrology for much of the Mojave Block, and especially the Manix basin and the "ancestral" Mojave River system.

Prior to the uplift of the San Bernardino and San Gabriel Mountains, the Mojave Desert drainage system flowed eastward from the Sierra Nevada Mountains and from ranges in the southern Great Basin, westward across the San Andreas fault zone, through the Los Angeles basin, and into the Pacific Ocean (Meisling and Weldon, 1989). Uplift of the Transverse Ranges, which progressed northward from south of Cajon Pass to the area between Puzzle Creek and Valyermo, commenced 1.5 Ma and continues to the present (Meisling and Weldon, 1989). These constraints set the timing of tectonic-related drainage reversal to after 1.5 Ma.

Our study has shown evidence for westward flow prior to the beginning of the Jaramillo/Cobb Mountain (?) Event (at the top of SCS). If these strata actually record significant transport by the ancestral Mojave River system, the change in flow direction from west to east did not take place before 0.97 Ma. This shifts the oldest possible age of the change in the Mojave River's flow direction from 1.5 Ma to 0.97 Ma. It is possible, however, that Pliocene drainage patterns in the Manix basin record the history of only local, not regional, tectonic changes. Thus, the Mojave River may have flowed along an alternate, yet-to-be-discovered, course prior to filling Lake Manix.

CONCLUSION

The MRF preserves a fairly complete history of the changing Plio-Pleistocene depositional environments that preceded the formation of Pleistocene Lake Manix. An absolute chronologic history can be attached to the section. No evidence is found within the MRF for sustained eastward flow of the ancestral Mojave River system, or even for the ancestral river itself, before 0.97 Ma, which is considerably less than the previously determined drainage reversal age of 1.5 Ma. This constraint on the timing of eastward flow, believed to be tectonically controlled by the uplift of the Transverse Ranges, implies either (1) the Mojave River followed some other drainage system or (2) the drainage reversal, and possibly the corresponding tectonism, took place at an earlier time than previously thought.

ACKNOWLEDGMENTS

The authors wish to thank those people who participated in our field study including George Rossman, Bob Adams, Joe Kirschvink, Chris Pluhar, Fred Budinger, James Consolver, and especially Laszlo Keszthelyi, who was not only extensively involved in our field work, but who also participated in the collection and preparation of the volcanic ash samples. We also thank Manny Bass, Alden Carpenter, Janet Anwyl and all others at Chevron Oil Field Research Company in La Habra, California for their financial support for volcanic ash analyses and for enthusiastic cooperation in helping us complete this study. We thank George Jefferson and Norman Meek for reviewing this paper and providing very

helpful corrections and important clarifications. CONTRIBUTION NO. 4999 FROM THE DIVISION OF GEOLOGICAL AND PLANETARY SCIENCES OF THE CALIFORNIA INSTITUTE OF TECHNOLOGY.

REFERENCES

Blair, T. C., and Bilodeau, W. L., 1988, Development of tectonic cyclothems in rift, pull-apart, and foreland basins: Sedimentary response to episodic tectonism: *Geology, 16*, p. 517-520.

Buwalda, J. P., 1914, Pleistocene beds at Manix in the eastern Mojave Desert region: *Bull. Dept. Geology, Univ. of Calif., Berkeley, 7 (24)*, p. 443-464.

Buwalda, J. P., and Richter, C. F., 1948, Movement on the Manix (California) fault on April 10, 1947: *Geol. Soc. Amer. Bull. (abstr.), 59*, p. 1367.

Dibblee, T. W., Jr., and Bassett, A. M., 1966, Geologic map of the Newberry Quadrangle, San Bernardino County, California: *Miscellaneous Geologic Investigations Map I-461*, scale 1:62,500, U.S.G.S. Washington D. C.

Dokka, R. K., and Travis, C. J., 1990, Late Cenozoic strike-slip faulting in the Mojave Desert, California: *Tectonics, 9 (2)*, p. 311-340.

Harland, W. B., Armstrong, R. L., Cox, A. V., Craig, L. E., Smith, A. G., and Smith, D. G., 1990, A Geologic Time Scale 1989: Cambridge University Press, Cambridge, 263 p.

Jefferson, G. T., 1968, Camp Cady local fauna from Pleistocene Lake, Manix, Mojave Desert, California: *University of California, Riverside, unpublished thesis (MA)*, 130 p.

_____, 1985, Stratigraphy and geologic history of the Pleistocene Lake Manix Formation, central Mojave Desert, California: *Geologic Investigations along Interstate 15, Cajon Pass to Manix Lake, California*, R. E. Reynolds, ed., San Bernardino County Museum, p. 157-169.

Jefferson, G. T., Keaton, J. R., and Hamilton, P., 1982, Manix Lake and the Manix fault field trip guide: San Bernardino Co. Mus. Assoc. *Quarterly, 29(3-4)*, p. 1-47.

Izett, G. A., 1981, Volcanic Ash Beds: Recorders of upper Cenozoic silicic pyroclastic volcanism in the western United States: *J. Geophys. Res., 86 (B11)*, p. 10200-10222.

Izett, G. A., Obradovich, J. D., and Mehnert, H. H., 1988, The Bishop Ash bed (middle Pleistocene) and some older (Pliocene and Pleistocene) chemically and mineralogically similar ash beds in California, Nevada, and Utah: *U.S.G.S. Bulletin 1675*, 37 p.

Izett, G. A., Wilcox, R. E., Powers, H. A., and Desborough, G. A., 1970, The Bishop Ash bed, a Pleistocene marker bed in the western United States: *Quat. Res., 1*, p. 121-132.

McGill, S. F., Murray, B. C., Maher, K. A., Lieske Jr., J. H., and Rowan, L. R., 1988, Quaternary history of the Manix fault, Lake Manix basin, Mojave Desert, California: San Bernardino County Museum Assoc. *Quarterly, 35(3,4)*, Mojave Desert Quaternary Research Symposium, San Bernardino County Museum, Redlands, California, p. 3-20.

Meek, N., 1989, Geomorphic and hydrologic implications of the rapid incision of Afton Canyon, Mojave Desert, California: *Geology, 17*, p. 7-10.

Meisling, K. E., and Weldon, R. J., 1989, Late Cenozoic tectonics of the northwestern San Bernardino mountains, southern California: *Geol. Soc. Amer. Bull., 101*, p. 106-128.

Murray, B., and Nagy, E., 1990, The relationship of the Manix Formation to the underlying "Mojave River Formation": San Bernardino County Museum Assoc. *Quarterly, 37(2)*, Abstracts of Proceedings, 1990 Mojave Desert Quaternary Research Symposium, San Bernardino County Museum, Redlands, California, p. 32.

Pluhar, C. J., and Kirschvink, J. L., 1989, Preliminary magnetostratigraphy of Plio-Pleistocene lake sediments near Manix Wash, Central Mojave Desert: San Bernardino County Museum Assoc. *Quarterly, 36(2)*, Abstracts of Proceedings, 1989 Mojave Desert Quaternary Research Symposium, San Bernardino County Museum, Redlands, California, p. 63.

Pluhar, C. J., Kirschvink, J. L., and Adams, R. W., 1991, Magnetostratigraphy and clockwise rotation of the Plio-Pleistocene Mojave River Formation, central Mojave

Desert, California: San Bernardino County Museum Assoc. *Quarterly, 38(2),* Mojave Desert Quaternary Research Symposium, San Bernardino County Museum, Redlands, California, this volume.

Sarna-Wojcicki, A. M., Bowman, H. R., Meyer, C. E., Russell, P. C., Asaro, F., Michael, H., Rowe, J. J., Baedecker, P. A., and McCoy, G., 1980, Chemical analysis, correlations, and ages of late Cenozoic tephra units of east-central and southern California: *U.S.G.S. Open File Report 80-231,* 52 p.

Sarna-Wojcicki, A. M., Bowman, H. R., Meyer, C. E., Russell, P. C., Woodward, M. J., McCoy, G., Rowe, J. J., Jr., Baedecker, P. A., Asaro, F., and Michael, H., 1984, Chemical analysis, correlations, and ages of upper Pliocene and Pleistocene ash layers of east-central and southern California: *U.S.G.S. Professional Paper 1293,* 40 p.

Magnetostratigraphy and Clockwise Rotation of the Plio-Pleistocene Mojave River Formation, Central Mojave Desert, California.

Christopher J. Pluhar and **Joseph L. Kirschvink**, Division of Geological & Planetary Sciences, The California Institute of Technology, Pasadena, CA 91125, and **Robert W. Adams**, 7400 Tampa Ave., Reseda, CA 91335

ABSTRACT

Oriented samples collected for paleomagnetic analysis from sediments of the newly-named Mojave River Formation (Nagy & Murray, 1991, this volume) possess stable characteristic components of Natural Remanent Magnetization (NRM). Progressive demagnetization reveals characteristic components of both normal and reversed polarity which are stratigraphically distinct. The oldest sediments exposed within the field area are reversely magnetized and were probably deposited during the early portion of the Matuyama reversed Chron. Stratigraphically higher units contain what appears to be the Olduvai normal Subchron, as well as a shorter normal zone which probably is either the Cobb Mountain or Jaramillo Event. The location of the Brunhes/Matuyama boundary at one site is within an alluvial fanglomerate which grades upward conformably into the lowest unit of the overlying Manix Formation, possibly accounting for the absence of the Bishop ash in the section.

Demagnetization data from 143 samples yielding acceptable least-squares lines suggest a net clockwise rotation of 8 ± 2.7° over the past two million years, perhaps with some of the rotation during deposition. This rate of rotation could account easily for larger rotations reported elsewhere in the Mojave Desert on units of Miocene age.

INTRODUCTION

Perhaps the best sedimentary records of latest Pliocene and Pleistocene age are found in the relict lake and playa beds of the intermontane basins of the southwest United States. However, a complete tectonic and climatic history of this period remains to be unearthed. Detailed stratigraphic and paleomagnetic studies are necessary to correlate the nature and timing of depositional and deformational events; ongoing investigations in southern Death Valley and Manix Basin are designed to provide detailed information about such events in these locations.

Death Valley is the sink for internal drainage of a vast region from the east slope of the Sierra Nevada, the Transverse Ranges and the southwestern Nevada desert. Topographic basins along major drainage systems; Owens Valley, Searles Valley, Manix Basin and Tecopa Basin all contain Pleistocene lacustrine and playa sediments dated at more than 1,000,000 years B.P.. These drainages are now evidenced by dry playas and by the eroded remnants of bedded deposits from wetter periods.

Beds of volcanic ash from two source areas are evident in many of these lake beds and are potentially useful in stratigraphic correlations. Sequential eruptions in the Long Valley resurgent caldera region north of Bishop, California produced white ashes containing biotite. Gray ash, lacking biotite, was airborne into California from the Yellowstone Caldera. Of these ashes, only three are consistently identified with any degree of confidence in Southern California: the 0.73 Ma Bishop ash, the 0.6 Ma Lava Creek B, and the 2.0 Ma Huckleberry Ridge ash from Yellowstone (Sarna-Wojcicki, et al., 1984). The general similarity in chemistry within each of these suites of ashes inhibits accurate correlations of individual beds; however they are helpful in determining relative positions in a stratigraphic column.

A 400 square kilometer area in the central Mojave Desert east of Barstow was once the site of a Pleistocene lake known as Lake Manix (Buwalda, 1914; Blackwelder and

Ellsworth, 1936). Primarily supplied by the Mojave River, late Pleistocene Lake Manix persisted for more than 350,000 years (Jefferson, 1985) as an intermittent freshwater body until its permanent drainage after 14,230 ± 1325 years B.P. through Afton Canyon (Meek, 1989), possibly as a result of renewed motion along the left-lateral Manix fault. The stratigraphy and paleontology of the late Pleistocene Lake Manix deposits have been studied intensively by Jefferson (1985, 1987). Subsequent work by a California Institute of Technology group (McGill, et al., 1988; Murray, Nagy and Adams, 1990) has focused on field mapping of the older deposits that underlie the Manix Formation, referred to here and in the Nagy and Murray (1991, this volume) paper as the Mojave River Formation. Nagy and Murray provide the stratigraphic background for the present magnetostratigraphic study.

Paleomagnetic work in the Manix area has been concentrated on several separate exposures of the Plio-Pleistocene beds whose stratigraphic correlations are not always clear. Previous workers have sampled ten ash beds in these exposures and have identified them as four ashes known from other regions. Of these four ash layers, the "uppermost white ash" is in the younger series of lake beds, the Manix Formation, and has been correlated with the Long Canyon tephra in the southern Sierra Nevada at 0.185 Ma (Bacon and Duffield, 1981). Sarna-Wojcicki, et al., (1984) correlated the "lowermost gray ash" with the 2.0 Ma Huckleberry Ridge tephra from the Yellowstone caldera, whereas a "middle white ash" bed was equated with Waucoba Road bed W3A (=Taylor Canyon C @ 2.3 Ma). In one Mojave River Formation section, the "middle white ash" is stratigraphically 3 meters above the gray ash and therefore younger. (This inconsistency illustrates the general problem of attempting correlation solely by means of chemical "fingerprinting".) An "upper white ash" appears in two localities, paired with a white ash at one site and in sequence above a white ash and a gray ash at another site. Magnetostratigraphic work within the field areas were directed at providing additional tests of these stratigraphic correlations.

Site localities and abbreviations used here and in Nagy and Murray (1991, this volume) are defined relative to the dry Mojave River bed shown on their Plate 1. These include the Northern Site (NS), the Southern Cliff Site (SCS), the Southern Hill Site (SHS), the Big Bend East and West (BBE and BBW) sites, and the Southern Road Site (SRS).

METHODS

The Mojave River Formation varies in composition from well indurated claystones to friable sandstones (Nagy and Murray, 1991, this volume). These beds are difficult or impossible to sample with typical paleomagnetic techniques which employ water cooled diamond-tipped drill bits. Unlithified sandstones fall apart when drilled and the claystones turn to mud. For these reasons we used a combination of soft-sediment sampling techniques with quartz-glass cups for the sandy sediments (Weldon, 1984) and simply drilled the claystones using compressed air instead of water as the coolant for the bit. In the conglomeratic facies, we found that it was occasionally possible to obtain an oriented sample of silty standstone which had washed into gaps between adjacent cobble-sized clasts. In the fine-grained sediments we were able to collect between ten and twenty samples per hour using these techniques. Samples were collected in stratigraphic succession (one sample per horizon) from a total of seven localities on both the north and south sides of the Mojave River.

Unconsolidated samples were stabilized in the laboratory using a 10% sodium silicate solution and ceramic cement where necessary. All measurements were performed on a computer-controlled cryogenic SQUID (superconducting quantum interference device) magnetometer with a backgroud noise level of $5 \times 10^{-12} Am^2$. Progressive demagnetization experiments involved an initial alternating field (AF) demagnetization in several steps up to 15 militesla (mT) to remove any magnetically soft components which may have been the result of large, multi-domain magnetites or have been induced by the drilling process. This was then followed by progressive thermal demagnetization experiments stepping from 150° to 500°C at 50° intervals; a procedure which is usually effective for removing magnetic overprints held by maghemite, goethite, or fine-grained

hematite produced by Recent weathering. Characteristic components of the Natural Remanent Magnetization (NRM) vectors were then found using the least-squares method of principal component analysis (Kirschvink, 1980).

Small amounts (approximately 0.1 g) of material were removed from representative fine-grained samples and subjected to a battery of rock-magnetic analyses, in an attempt to place constraints on the mineralogy and magnetic granulometry of the material which preserves the magnetic remanence. These sub-samples were first gently disaggregated by crushing, placed in a 1 ml plastic epindorph tube, and loaded into the fully computer-controlled SQUID magnetometer system housed in the California Institute of Technology biomagnetics clean laboratory (e.g., Kirschvink, 1983). Rock-magnetic experiments include: (1) an acquisition of Anhysteretic Remanent Magnetizaiton (ARM) in a standard 100 mT alternating field, with progressively stronger background biasing fields between 0 and 2 mT as done by Cisowski (1981), (2) the progressive AF demagnetization of the ARM after the 2 mT ARM step, (3) the progressive AF demagnetization of a 100 mT Isothermal Remanent Magnetization (IRM), and (4) an IRM acquisition experiment in fields of up to 800 mT.

RESULTS

Demagnetization Analysis

Figure 1 shows demagnetization results typical of normal, reversed, and unstably magnetized samples from the Mojave River Formation. The intensity of the NRM was fairly uniform, at about $5x10^{-4}$ Am^2/kg, which is reasonably strong for sediments, and probably reflects a significant component of detrital magnetite eroded from crystalline rocks within the drainage basin of the Mojave River. Virtually all of the samples collected contain a magnetic component aligned roughly along the present magnetic field direction which usually could be removed by low-intensity alternating fields (< 15 mT) or by thermal treatment below 250°C. This is presumably held by large crystals of multi-domain magnetite, which are magnetically viscous, or by the magnetic fine-grained ferric oxide pigments (goethite, maghemite, or hematite) produced by Recent subaerial weathering. The magnitude of this component is far less pronounced at SCS, which has excellent bed-by-bed exposures produced by Recent downcutting of the Mojave River. Recognition of this normal-polarity magnetic overprint is relatively easy in the reversely magnetized samples, as it shows up as a major junction between adjacent linear segments on the orthogonal projections, such as in Figure 1A. Due to a minimal amount of tectonic deformation, these components are sometimes difficult to recognize in the normally-magnetized samples. They often stand out as slight breaks in the demagnetization paths, yielding distinct directions with principal component analyses. As it is sometimes difficult, however, to determine precisely the point at which the overprint overlaps with the characteristic (or primary) direction, overall directions from the normal polarity samples probably have a small amount of residual contamination from these overprints.

Rock Magnetic Analysis.

Figure 2 shows typical results from the rock magnetic experiments. Information on the distribution of particle coercivities is provided by the acquisition of an IRM curve labeled on Figure 2A, indicating that most of the magnetization is gained in the interval between 10 and 100 mT. This suggests that fine-grained magnetite is the principal magnetic mineral. A slight tendency to gain magnetic remanence after exposure to peak fields above 100 mT suggests the presence of ferric iron oxide pigments. Also shown on Figure 2A are results of a modified Lowrie-Fuller ARM test (e.g., Johnson et al. 1975), which compares the resistance to alternating-field demagnetization of both the IRM produced in a 100 mT peak field and the ARM gained in a 100 mT oscillating field. The fact that the ARM demagnetizes at higher peak fields than does the IRM indicates that the magnetic remanence is dominated by fine-grained (< 10 um) particles of magnetite of single-domain or pseudo-single domain size.

Figure 2B shows the results of ARM acquisition experiments from several of the fine-grained samples from the Mojave River Formation. This procedure tests mainly for

Table 1. Summary of stable paleomagnetic directions from all sites sampled within the Mojave River Formation. Directions are based on principal component analyses of the progressive demagnetization data as described in the text, and were from specimens which yielded maximum angular deviation (MAD) values for best-fit lines of 10^{o} or less, using the method of Kirschvink (1980). Results enclosed in parentheses have been corrected for the tilt of the bedding. The parametric test of coincident mean directions (Fisher et al. 1987, p. 211) shows that, although close, the normal and reversely magnetized direction groups are not truly antiparallel (Chi^2 = 10.96 with 2 d.f., $p < .005$ for rejection of the hypothesis of antiparallelism). Errors for the rotation values quoted in the text are modified from the a_{95} by the method of Demarest (1983). Bingham statistics follow the methods of Onstott (1980). The sites are located in the Mojave Desert near 35^{o}North latitude, 243.5^{o}east longitude. Equal-area projections for the directional data corresponding to letters A thourgh F on this table are shown on Figure 3.

	Grouping	N	Decl.	Incl.	Fisher Stats.			Bingham Statistics				
					K	a_{95}	R	K1	K2	a_{min}	a_{max}	ov.
A.	All	50	6.9	52.8	19.1	4.7	47.43	-14.0	-9.0	4.0	5.1	22
	Normals		(5.1	48.8	20.4	4.6	47.60	-14.3	-9.5	4.0	4.9	82)
B.	All	93	193.0	-49.2	11.8	4.5	85.22	-8.6	-6.5	4.0	4.6	99
	Reversed		(189.0	-40.8	12.2	4.4	85.46	-8.8	-6.6	3.9	4.6	114)
C.	Pre-Olduvai	73	193.0	-50.9	10.9	5.3	66.38	-8.8	-5.8	4.5	5.6	98
	Reversed		(190.0	-42.3	11.4	5.1	66.67	-9.0	-5.9	4.4	5.5	114)
D.	Olduvai & younger											
	Directions	70	8.9	50.3	18.0	4.1	66.18	-13.1	-8.8	3.5	4.4	13
			(5.1	45.1	18.0	4.1	66.17	-13.7	-8.5	3.4	4.5	3)
E.	Post-Olduvai											
	Reversed	20	193.1	-43.6	18.2	7.9	18.96	-13.0	-9.2	6.6	8.0	10
			(185.0	-35.6	17.5	8.0	18.92	-12.3	-9.2	6.8	7.8	5)
F.	All directions	143	11.1	50.6	13.6	3.3	132.52	-8.8	-7.5	3.1	3.4	86
	Combined		(8.0	43.8	13.8	3.3	132.74	-9.1	-7.5	3.1	3.4	133)

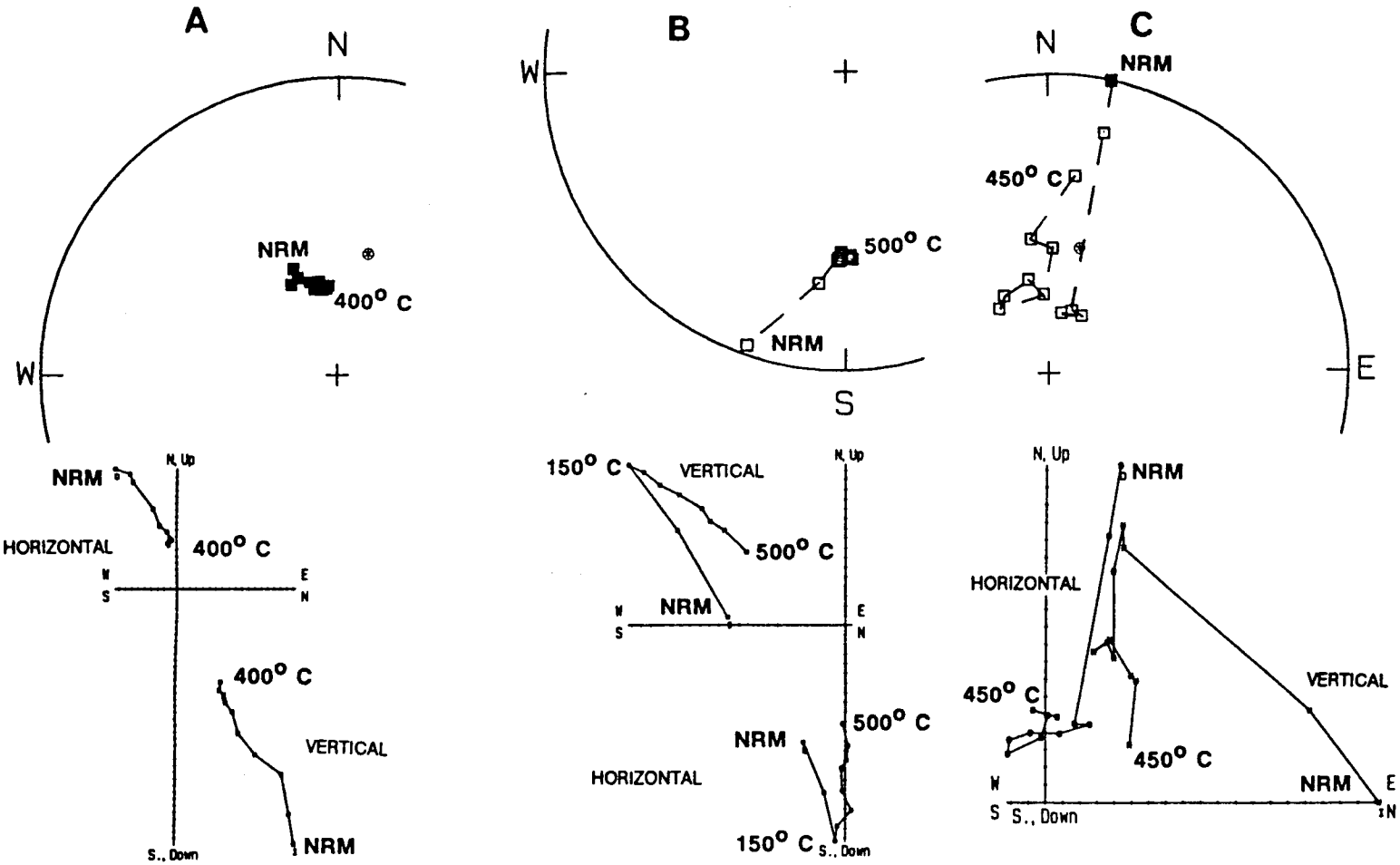

Figure 1. Progressive demagnetization of typical normal (A) and reversed (B) samples as well as an unstable sample (C). Top figures are equal area projections with open squares being the upper hemisphere and solid squares the lower. The bottom figures are orthogonal projections on the horizontal and vertical north-south planes.

the microscopic packing geometry of the fine-grained magnetite in the sediments. A sample in which the magnetic particles are separated from each other enough that they are out of range of the magnetic fields of other magnetic particles will plot above the top curve on figure 2B (labeled magnetotactic bacterium). On the other hand, samples in which the magnetic particles are clumped densely together, or which are dominated by large, multi-domain grains of magnetite, will plot on or below the lowest reference curve on figure 2B (labeled chiton tooth). Results from samples of the Mojave River Formation fall in intermediate positions, suggesting mixtures of both types of packing geometries. Hence, a considerable fraction of the magnetic particles are present as isolated grains in the clay matrix of the silty mudstones. These particles are most likely to align spontaneously with the earth's magnetic field during deposition, and therefore the natural remanent magnetization preserved by them is probably detrital or early post-depositional in origin.

Magnetic Directions

Figure 3 and Table 1 show results from the stable, characteristic magnetic components determined from the principal component analyses of the progressive demagnetization data, pooled from all sites in the field area. As the strata are mostly flat-lying, it is not possible to conduct a fold test on the sediments. When analyzed separately, the distributions for the normal and reversely magnetized samples are not quite antiparallel (Table 1), with the normal group displaying slightly less net rotation than the reversed group. This slight antiparallel offset could either be related to the presence of a small component of the recent field which is not completely removed by the demagnetation treatment, or it may be due to a progressive rotation during the deposition of the sediments, as the majority of reversed directions are from before the Olduvai normal Subchron. Grouping the data into two sets, one pre-Olduvai and the other Olduvai and younger (Table 1) shows that the older sediments (~2.4 - 1.87 Ma) have been rotated clockwise an average of 10 ± 4°, whereas the younger group (~1.87 - .7 Ma) is only rotated clockwise 5.1 ± 3.3° from the expected north-south direction (rotational-only errors have been calculated according to the analysis of Demarest, 1983). Hence, rotations were probably happening *during* deposition of the lake sediments, and this is the most probable cause for slight mis-alignment of the total normal and reversed groups.

It is intriguing to note that the youngest group of samples (post-Olduvai reversed in Table 1) have the shallowest average inclination. These samples at SCS of the Mojave River Formation, however, include the gradual transition up into the conglomeratic beds of the overlying basal Manix Formation. This decrease in dip may be due either to the effects of depositional inclination error, which ought to be more pronounced with an increase in grain size, or to a loss of proper quiet-water bedding planes necessary to correct for tectonic tilt.

Magnetostratigraphy

Figure 4 shows the Virtual Geomagnetic Pole (VGP) latitude from all samples yielding least-squares directions which were judged to be reliable enough to use for magnetic polarity interpretations (MAD values generally < 15°), plotted with respect to stratigraphic position within the sequence. Locations of the three ash units as well as the lithologic groups of Nagy and Murray (1991, this volume) are also shown for comparison.

It is clear from these data that the normally and reversely magnetized samples occur in stratigraphically concordant groups. The presence of these layer-bound, correlative units is the strongest field evidence that the primary magnetic directions were acquired at or soon after deposition of the beds. The thickest continuous stratigraphic section is the NS locality. This section is a composite of three, which overlap stratigraphically, but are offset laterally from each along the "middle and upper white ashes", respectively. The 75-meter-thick composite NS section is reversely magnetized except for a 12-meter-thick normal magnetozone which contains the "upper white ash". The lower reversed zone has the "middle white ash" within it as well as a discontinuous exposure of the "gray ash", identified as the 2.0 Ma Huckleberry Ridge by Sarna-Wojcicki, et al., (1984), an interpretation supported by Nagy and Murray (1991, this volume). Hence, the normal magnetozone overlying the "gray ash" can be identified

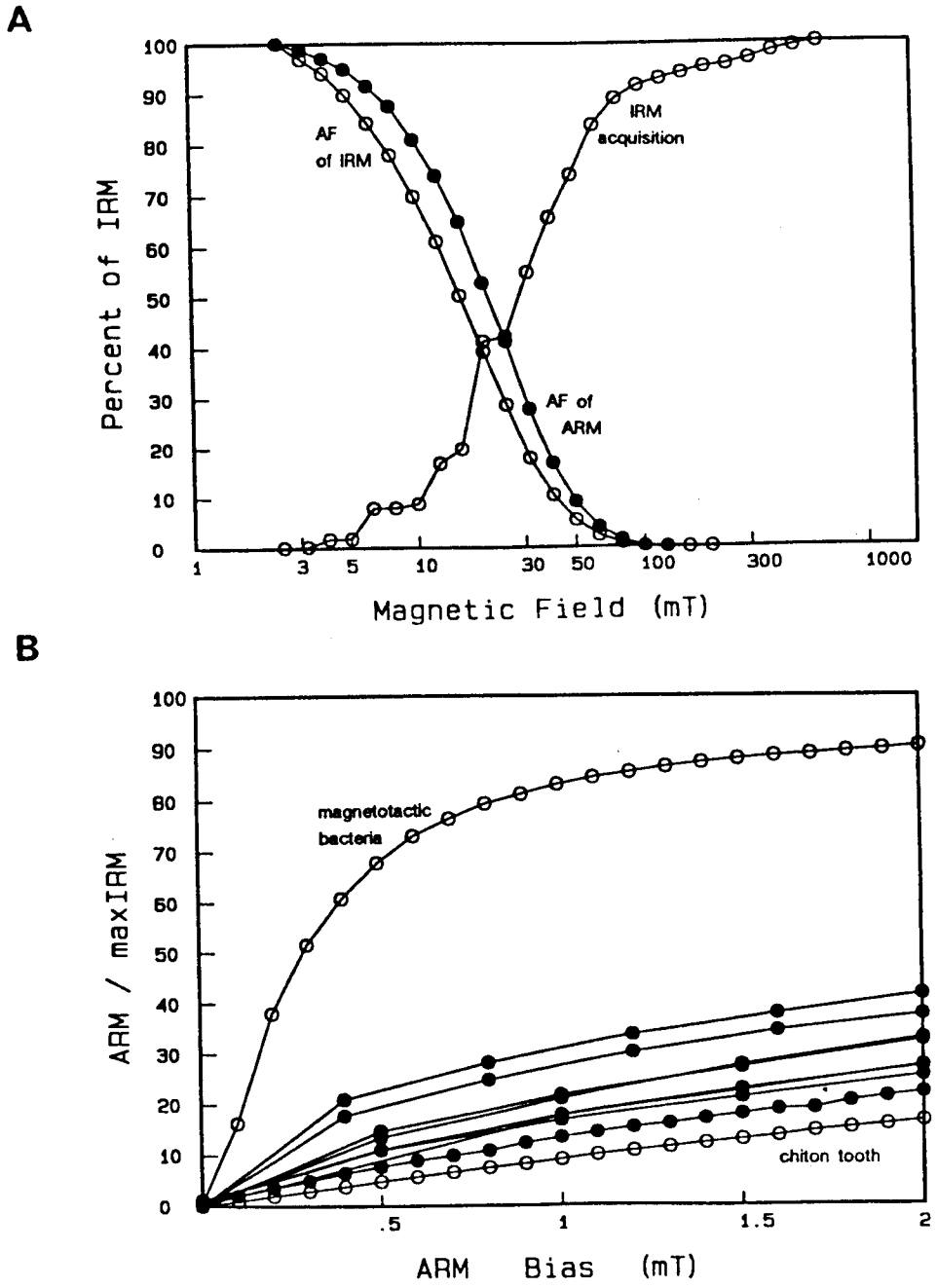

Figure 2. Rock Magnetic Properties; (A) Isothermal Remanent Magnetization (IRM) acquisition and demagnetization (open circles) and Anhysteretic Remanent Magnetization (ARM) demagnetization (solid dots) of a typical sample. These studies indicate that magnetite minerals in this rock are dominated by pseudo-single and single domain magnetite with some ferric iron minerals. (B) ARM acquisition for several samples indicating that a substantial fraction of the magnetic particles are in magnetic isolation.

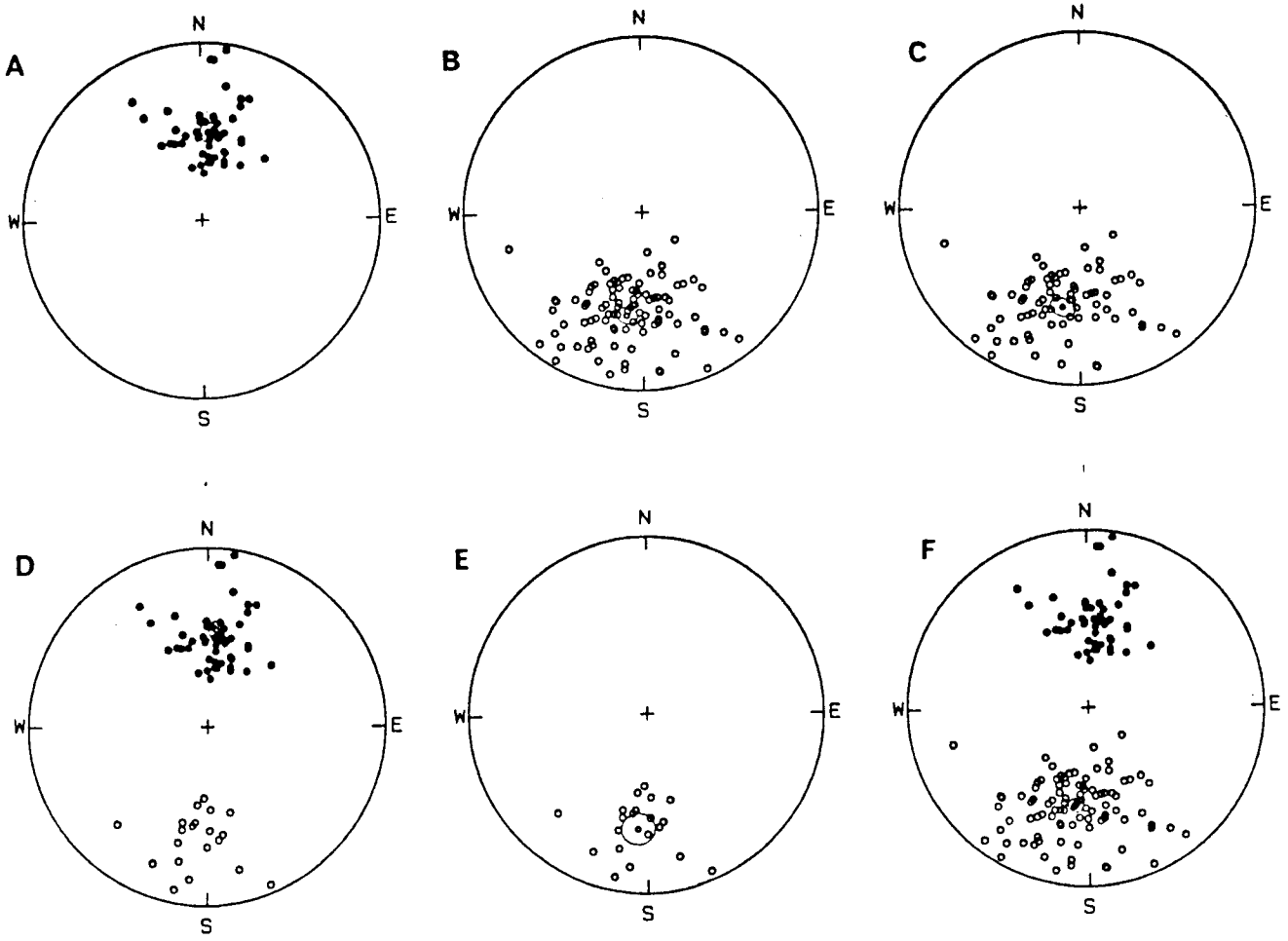

Figure 3. Equal area projections of the groupings of samples from Table 1. Mean directions are indicated by the larger open circles. (A) all normal samples, (B) all reversed samples, and (F) all samples grouped together. (C) all samples older than 1.87 Ma and (D) samples younger than 1.87 Ma. (E) all reversed samples younger than 1.67 Ma.

confidently as the Olduvai normal Subchron which ranges from 1.67-1.87 Ma (Harland et al., 1990).

No clear evidence exists in this section for the presence of the Reunion events. Two of the pre-Olduvai samples at the NS locality (one each at the 37 and 50 meter levels) may have an underlying normal component. However, these samples did not yield reliable directions during the progressive demagnetization experiments (figure 4, indicated by triangular symbols).

Both the normal zone and the two white ashes from NS correlate uniquely across to the SCS and SHS exposures on the southern side of the Mojave River, as discussed in detail by Nagy and Murray (1991, this volume). In particular, the SCS section contains both white ashes and the Olduvai normal Subcron, and extends stratigraphically higher in the sequence. The upper portion of this section includes a very thin normal zone which was initially discovered as a single sample, and then confirmed by resampling. Its stratigraphic position suggests that it is either the Jaramillo Event (0.91-0.97 Ma) or the Cobb Mountain Event (1.1 Ma), although its rather short stratigraphic thickness in comparison with that of the Olduvai suggests that it is the Cobb Mountain Event.

Southwest of the SCS site, stratigraphically higher lake sediments and interfingering conglomerates are exposed. Two of the 'Big Bend' sites (BBE and BBW) gave consistently normal directions. In addition, the section at BBW is within the basal units of the Manix Formation, which based on U/Th analyses and vertebrate faunal correlation is believed to be late Pleistocene in age (Jefferson, 1985, 1987). These sites are within the Brunhes normal Chron, and the Brunhes/Matuyama boundary presumably lies in a conglomeratic section between the SCS and BBE sections. Hence, the absence of the Bishop ash, which slightly post-dates this reversal boundary, may be due to its local deposition in an environment unfavorable for its preservation.

Two other sections corroborate data from the NS and SCS sites. SHS duplicates the stratigraphy of the "grey ash" below the "middle white ash", with an intervening reverse-to-normal transition (Figure 4). The section at SRS also contains the "lower grey ash" within a reversed polarity zone.

Stratigraphic thicknesses and age constraints of the reversals and the "lower grey ash" are used to calculate deposition rates within the Mojave River Formation. For these calculations the "lower gray ash" is taken as the Huckleberry Ridge ash (@ 2.0 Ma), the normal zone above it as the Olduvai normal Subchron (1.87-1.67 Ma) and the thin normal event above that, found only in section SCS, as the Cobb Mountain event. The reversed section under the "gray ash" must have had a deposition rate of greater than 9.7 cm per thousand years since the top of the Gauss normal Chron was not found there. The section between the "gray ash" and the bottom of the Olduvai normal Subchron had a deposition rate of 5.5 $\pm$ 0.3 cm/kyr at site NS, and 4.7 $\pm$ 0.6 cm/kyr at SHS. During the Olduvai Subchron the deposition rate was 5.3 $\pm$ 0.5 cm/kyr at NS and only 3.9 $\pm$ 0.3 cm/kyr at SCS. If the short normal zone in the upper part of the SCS section is the Cobb Mountain Event, then the deposition rate between it and the top of the Olduvai Subchron would be 2.8 $\pm$ 0.2 cm/kyr. Extrapolating this rate to strata higher in that section implies that the Jaramillo Event is not present there. If, on the other hand, the short normal is indeed the Jaramillo Event, then the deposition rate between it and the Olduvai Subchron would be 2.2 $\pm$ 0.2 cm/kyr, and less than 0.6 cm/kyr within the Jaramillo Event itself. In this scenario the overlying section the deposition rate at SCS could not be less than 1.3 cm/kyr since the Brunhes-Matuyama reversal was not found within the section.

DISCUSSION

Combined data from magnetostratigraphy and tephrochronology indicate that deposition of the Mojave River Formation began substantially earlier than the eruption of the 2.0 Ma Huckleberry Ridge ash and continued until after the Jaramillo Event at rates which fluctuated by nearly an order of magnitude. From these inferred deposition rates, the two white volcanic ashes analyzed by Nagy and Murray, the "middle white" and "upper white", (1991, this volume) may be assigned extrapolated ages of 1.8 and 1.95 Ma respectively. The distinctive "gray ash" found in the reversed magnetozone of the Mojave

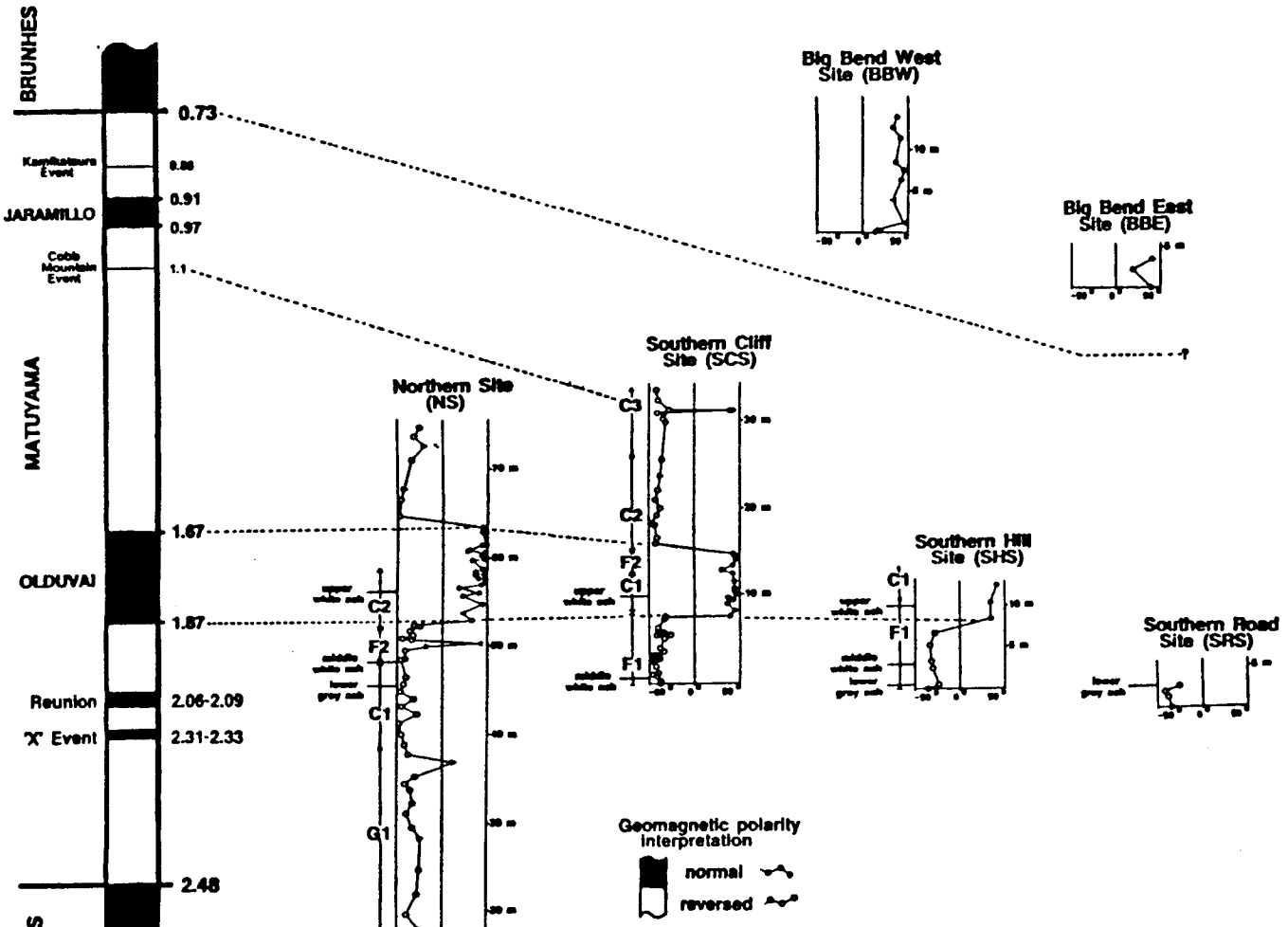

Figure 4. Magnetostratigraphy of all Mojave River formation sections sampled. These sections have been tied to the MRF units of Nagy and Murray (1991) and the locations of volcanic ashes are shown to the right of each section. Dashed lines show magnetic reversal correlations. Part of the magnetostratigraphic timescale is shown at right for reference, adapted from Harland et al. (1990).

River Formation is most probably the Huckleberry Ridge tephra since the other Yellowsone gray ashes may be eliminated from consideration: the 0.6 Ma Lava Creek tephras are within the Brunhes normal Chron and the Mesa Falls ash has not been found west of Nebraska. Additional trace element analyses reported by Nagy and Murray (1991, this volume) confirm this identification. Thus the reverse-normal transition above the gray ash can be identified with the lower boundary of the Olduvai normal sub-chron @ 1.87 Ma. This relationship is consistent with strata in the Confidence Hills of southern Death Valley where the gray Huckleberry Ridge ash beds and the entire Olduvai normal Subchron are reliably placed in a 110m section of similar sediments.

A stratigraphically higher normal magnetozone entirely within a reversed section may be either the Cobb Mountain Event (@ 1.1 Ma) or perhaps the Jaramillo Event (0.92-0.97 M). The "upper white ash" in the normal magnetozone may belong to the Glass Mountain series from the Bishop region. Stratigraphic description of the Mojave River Formation (Nagy and Murray, 1991, this volume) can aid in the interpretation of the ages and depositional sequences of this tectonically complicated area and result in a better correlation of the ash "marker" beds in the region.

Our observation that the oldest sediments are rotated tectonically more than the younger suggests that the area has been moving clockwise at an average rate of approximately 5° per million years for at least the past 2 Ma. This is the first detection of rotation in beds as young as 2 Ma in the Mojave Desert. Several authors (Ross et al., 1989; Golombeck and Brown 1988) have suggested substantial (up to 50°) clockwise rotation of Miocene volcanic rocks in the Mojave Desert from a number of localities. Wells and Hillhouse (1989), however, find no evidence for such consistent rotation of large regions in their paleomagnetic studies of the widespread Peach Springs Tuff (dated at 19 Ma); their 11.6° and 13.1° clockwise rotations in the Cady Mountains and near Barstow, respectively, may be attributed to drag effects from nearby strike-slip faults. The Manix Basin may likewise be affected by the immediately adjacent, left-lateral Manix Fault, which has been active for at least the past 1 Ma (McGill et al., 1988). Hence, it seems reasonable to suggest that the larger rotations in the Miocene volcanics are due simply to similar tectonic rotation processes acting over longer intervals of time.

ACKNOWLEDGMENTS

Supported partially by NSF grant EAR-8351470 and matching funds from the Chevron Oil Field Research Company, the ARCO Foundation, and the California Institute of Technology Summer Undergraudate Research Fellowship (SURF) program. CONTRIBUTION NO. 4998 FROM THE DIVISION OF GEOLOGICAL AND PLANETARY SCIENCES OF THE CALIFORNIA INSITUTE OF TECHNOLOGY.

REFERENCES

Bacon, C.R. and W.A. Duffield, 1981, Late Cenozoic rhyolites from the Kern Plateau, southern Sierra Nevada, California: American Journal of Science, vol. 281, p. 1-34

Blackwelder, E., and E.W. Ellsworth, 1936. Pleistocene lakes of the Afton Basin, California. *American Jour. Sci., 4th Ser., 31*: 453-463.

Buwalda, J.P., 1914. Pleistocene beds at Manix in the eastern Mojave Desert region. *Bull. Dept. of Geology,* Univ. Calif., Berkeley 7(24): 443-464.

Cisowski, S., 1981. Interacting vs. non-interacting single- domain behavior in natural and synthetic samples. *Phys. Earth Planet. Inter. 26*:56-62.

Demarest, H.H., 1983. Error analysis for the determination of tectonic rotation from paleomagnetic data. *J. Geophys. Res. 88*: 4321-4328.

Fisher, N.I., Lewis, T., and B.J.J. Embleton, 1987. *Statistical Analysis of Spherical Data.* Cambridge University Press, Cambridge U.K., 329 pp.

Golombeck, M.P. and L. L. Brown, 1988. Clockwise rotation of the western Mojave Desert. *Geology 16:* 126-130.

Harland, W.B., Armstrong R.L., Cox A.V., Craig L.E., Smith A.G., and D.G. Smith, 1990, *A Geologic Time Scale.* Cambridge: Cambridge University Press, 263 pp.

Jefferson, George T., 1985, Stratigraphy and geologic history of the Pleistocene Manix formation, central Mojave Desert, California. in Reynolds, Robert E. ed., Geological investigations along Interstate 15, Cajon Pass to Manix Lake, p. 157-169

_____, 1987, Camp Cady Local Fauna: Paleo-environment of Lake Manix Basin San Bernardino County Museum Association Quarterly, 34(3&4), pp. 3-35

Johnson, H.P., Lowrie, W. and Kent, D.V., 1975. Stability of anhysteretic remanent magnetization in fine and coarse magnetite and maghemite particles. *Geophys. J. R. Astron. Soc., 41*: 1-10.

Kirschvink, J. L., 1980. The least-squares line and plane and the analysis of paleomagnetic data: examples from Siberia and Morocco, Geoph. J. Royal Astr. Soc. 62, 699-718.

_____, 1983. Biogenic ferrimagnetism: a new biomagnetism. in Biomagnetism: An Interdisciplinary Approach ed. S. Williamson, Plenum Press, pp. 472- 492.

McGill S.F., Murray B.C., Maher K.A., Lieske J.H., Rowan L.R., and F. Budinger, 1988. Quaternary history of the Manix Fault, Lake Manix basin, Mojave Desert, California. Quaterly J. San Bernardino County Museum Association 35(3&4), P. 3-20, map.

Meek, N., 1989. Geomorphic and hydrologic implications of the rapid incision of Afton Canyon, Mojave Desert, California. *Geology 17:* 7-10.

Murray, B. C., E. Nagy, R. Adams, 1990, The Relationship of the Manix formation to the underlying "Mojave River Formation", Abstract for MDQRC Symposium, May 18, 19, 1990

Nagy E.A. and B.C. Murray, 1991. Stratigraphy and intra-basin correlation of the Mojave River Formation, central Mojave Desert, California. MDQRC Symposium Quaterly, May 1991, San Bernardino County Museum (in press).

Onstott, T.C., 1980. Application of the Bingham distribution function on paleomagnetic studies. *J. Geophys. Res. 85:* 1500-1510.

Ross, T. M., Luyendyk B.P., and R.B. Hanson, 1989. Paleomagnetic evidence for Neogene clockwise tectonic rotations in the central Mojave Desert, California. *Geology 17:* 470-473.

Sarna-Wojcicki, A. M., H. R. Bowman, C. E. Meyer, P. C. Russell, M. J. Woodward, Gail McCoy, J. J. Rowe, Jr., P. A. Baedecker, Frank Asaro and Helen Michael, 1984, Chemical analyses, correlations and ages of upper Pliocene and Pleistocene ash layers of east-central and southern California: U. S. Geological Survey Professional Paper 1293, 40 p.

Weldon, Ray J. II, 1985. "The Late Cenozoic Geology of Cajon Pass; Implications for tectonics and sedimentation along the San Andreas Fault", Caltech PhD Thesis, 381pp.

Wells, R.E. and J.W. Hillhouse, 1989. Paleomagnetism and tectonic rotation of the lower Miocene Peach Springs Tuff: Colorado Plateau, Arizona, to Barstow, California. *Geol. Soc. Amer. Bull. 101:* 846-863.

Abstracts of Proceedings from the 5th Annual Mojave Desert Quaternary Research Symposium, May 17 - 18, 1991

Jennifer Reynolds, compiler, Mojave Desert Quaternary Research Center, San Bernardino County Museum, Redlands CA 92374

Absolute North American Plate Motion: An Alternative to Wrench Tectonics in Analysis of Structures related to Strike-slip Faults in Central and Southern California

R.W. Adams, 7400 Tampa Ave., Reseda, CA 91335

The present structural configuration of central and southern California is generally conceded to be the result of collisions between Pacific oceanic plates and the North American plate. Reconstructions of past plate motions have considered plate convergence based on rates and directions of plate motions, but models of the present tectonic regime have favored wrench tectonics theory to explain compressive structures related to strike-slip faults of the San Andreas fault system rather than the effects of independent southwestward movement of the North American plate over the oceanic margin. Constructs based on the present rates and directions of absolute motions of the North American and Pacific plates in convergence are consistent with observed geological structures, seismic data from COCORP profiles, and earthquake focal mechanisms.

Mid-Miocene Landform Development in the Whipple Mountains, Southeastern California

Kathi K. Beratan, MS 230-225, Jet Propulsion Laboratory, Calif. Inst. of Technology, Pasadena CA 91109

The area along both sides of the Colorado River between Lake Havasu City and Parker, Arizona is beautiful, displaying dramatic landforms and strong color contrasts between different rock types. Studies of sedimentary strata in this region indicate that the present-day topography developed as a result of early to middle Miocene detachment faulting, and has experienced little change since its formation. The landform history is particularly well exposed in the Whipple Mountains on the California side of the river. The Whipple Mountains are a classic example of Cordilleran metamorphic core complexes. Cordilleran metamorphic core complexes are Tertiary extensional terranes irregularly exposed in a belt from southern British Columbia to northern Mexico. More than 20 geographically separate "core complexes" have been recognized in this belt (Coney, 1981) in areas that experienced large amounts of Cenozoic crustal extension. Core complexes are characterized by: (1) domal or antiformal mountain ranges; (2) flanking low-angle normal faults (detachment faults) of sub-regional to regional extent; (3) lower-plate ("core") assemblages of crystalline rocks, commonly including mylinitic gneisses that formed at a depth of approximately 12-15 km; and (4) upper-plate rocks that are highly distended by closely-spaced normal faults (Davis, 1988).

The landforms seen today in the Whipple Mountains resulted from the Miocene extensional event. The topography can be divided into five dominant landscape elements.

(1) The bulk of the range consists of a domiform topographic high, primarily composed of mylonitic gneisses in the lower plate. Synextension sedimentation patterns indicate that the topographic expression of the range core developed between approximately 18.5 and 13 Ma. This uplift is thought to have resulted from localized isostatic uplift due to non-uniform tectonic denudation (Spencer, 1982).

(2) Prominent northwest-trending ridges flank the range, held up by resistant Early to Middle Miocene andesite flows and strongly cemented sandstones and conglomerates. The strata commonly are tilted to about 30 degrees to the southwest, and the southwest flanks of the ridges generally form dip slopes. Cliffs commonly occur on the northeast flanks of the ridges. Tilting along northwest-trending high-angle normal faults to form half-graben basins occurred three times during the detachment even;t the ridges observed today resulted from the final tilting episode at about 14 Ma (Nielson and Beratan, 1991; Beratan, in press).

(3) The area between the ridges consists of low, irregular hills separated by poorly interconnected washes. These rubbly hills formed on the highly fractured upper-plate granites and gneisses.

(4) A plateau capped by nearly horizontal late Tertiary basalt flows covers the tilted ridges along the east side of the Colorado River. This plateau forms the bulk of the Buckskin Mountains. The basaltic volcanism probably represents the gradual shut-off of detachment faulting (Buising and Beratan, in press).

(5) The Whipple Mountains are flanked by a broad alluvial apron deposited after the final tilting event, and low-lying regions between the other landscape elements contain nearly flat-lying fluvial deposits. These deposits range in age from late Miocene to present. Also included in this landscape elements are the Bouse Formation (Buising, this volume) and younger Colorado River gravels.

Facies analysis of synextension sedimentary strata and contact relations with younger units suggests that relatively little landscape modification has occurred since the end of detachment faulting. Although broken up and distended by the last phase of extensional faulting, most of the Middle Miocene depositional basin was preserved, including the margins and the depocenter. Erosion has reduced the size of most exposures; however, large blocks of Tertiary strata do not appear to be missing. Abundant silica cement in these rocks may account for this preservation. The only major landscape modification observed is some incisement of drainages in response to the introduction of the Colorado River to its present course (Buising, this volume).

References cited

Beratan, K.K., in press, Miocene synextension sedimentation patterns, Whipple Mountains, southeastern California: Implications for the geometry of the Whipple detachment system: Jour. Geophys. Res.

Buising, A.V. and K.K. Beratan, in press, Progress report: Stratigraphic re-evaluation of upper Tertiary units, Osborne Wash area, La Paz County, Arizona, in Sherrod, D.R. and Nielson, J.E. (eds), Tertiary stratigraphy of the highly extended terranes, California, Arizona, and Nevada: U.S. Geol. Survey Bull.

Coney, P.J., 1980, Cordilleran metamorphic core complexes: An overview: Geol. Soc. America Memoir 153:7-13.

Davis, G.A., 1988, Rapid upward transport of mid-crustal mylonitic gneisses in the footwall of a Miocene detachment fault, Whipple Mountains, southeastern California: Geologische Rundschau, 77:191-209.

Nielson, J.E. and K.K. Beratan, 1991, Tertiary basin development and tectonic implications, Whipple detachment system, Colorado River extensional corridor, California and Arizona: Jour. Geophys. Res.

Spencer, J.E., 1982, Origin of folds of Tertiary low-angle fault surfaces, southeastern California and southwestern Arizona, in Frost, E.G. and D.L. Martin (eds), Mesozoic-Cenozoic tectonic evolution of the Colorado River region, California, Arizona, and Nevada; Cordilleran Publishers, San Diego, California:123-143.

Targeting Early Man Sites in the Western United States

Fred E. Budinger, Jr., Tetra Tech, Inc., 348 West Hospitality Lane, Ste 300, San Bernardino CA 92408

Pluvial lake basins have the potential of yielding evidence of a pre-12,000 BP occupation of the New World. Especially promising are low slope basins which held moderate size lakes fed by allogenic streams, stabilized by spillway outlets, and kept potable through hydrologic export of salts. Where marsh habitats were persistent, an archaeologically visible record may have been generated. Access to such a record today is largely a function of recent erosional history.

The Manix basin in the central Mojave Desert appears to be one of very few closed basins in the western U.S. where middle and late Pleistocene lacustrine and fluviatile sediments are readily accessible for study. This paper assesses the geoarchaeological

potential of this important stratigraphic record.

Stratigraphic Evidence for Five States in the Evolution of the Lower Colorado River region (SE CA—W AZ) between ~18 and ~4 MA

Anna V. Buising, Department of Geological Sciences, California State University at Hayward, Hayward CA 94542

Strata of the Mio-Pliocene Bouse Formation. together with under- and overlying alluvial, volcanic, and fluvial units, record five stages in the evolution of what is now the lower Colorado River region of southeastern California-western Arizona: (1) the latter phases of detachment faulting (post-18.5 Ma); (2) shut-off of detachment faulting followed by development of the modern topograhic/top of basement surface; (3) regional downwarping and transgression by waters of the proto-Gulf of California; development of a stable marine-estuarine carbonate environment in the northern end of the proto-Gulf (8-5Ma); (4) southward progradation of the ancestral Colorado River delta into the northern end of the proto-Gulf (prior to ~4.3 Ma); and (5) arrival of the throughgoing Colorado fluvial channel (~4-3 Ma). Gently tilted polylithologic conglomerate and sandstone and conformably overlying basalt flows at Black Peak, near Parker, AZ, record the waning stages of detachment faulting in this area (see Beratan, this volume). These units were deposited on fault-controlled topography significantly different from the modern landscape in the region. They are overlain in a buttressing, unconformable contact by nearly flat-lying monolithologic conglomerate and sandstone composed primarily of locally derived basaltic detritus. This unit was deposited on essentially modern topography. It is capped by a dilute-flow sandstone interpreted as recording initial transgression by waters of the proto-Gulf of California. The transgressive sandstone unit is overlain by, and interfingers with, shallow marine-estuarine carbonate making up the lower part of the Bouse Formation basin fill. The upper portion of the Bouse basin fill consists of upward-coarsening fine-grained terrigenous clastic material reflecting southward progradation of the ancestral Colorado River into the proto-Gulf embayment. The Bouse Formation also includes shoreline and nearshore strata: a locally biogenic shoreline tufa, as well as carbonate, coarse terrigenous-clastic, and mixed carbonate-siliciclastic deposits. The Bouse Formation is overlain by, and interfingers with, trough cross-bedded cobble conglomerates (locally including sand, silt and mud interbeds), referred to informally as the Colorado River gravels; these far-traveled deposits document arrival of the throughgoing Colorado fluvial channel in approximately its modern geographic position, although not yet at its modern gradient.

Distribution of Color in Tourmaline from the Stewart Mine

Eric W. Cochrane, 4822 West McFadden, #64, Santa Ana, CA 92704.

The Stewart mine, San Diego County, California, is known for its gem crystals of tourmaline. Samples of tourmaline were separated from loose, fragmented material collected from the floor of the mine and categorized by color. While this does not represent a good statistical sample, it is used to obtain an estimate of the relative proportions of the different colored tourmaline. Because the sample consisted of crystal fragments, bi-colored fragments are not used in calculating percentages. The proportion of colors by weight is: pink—59%, black—25%, green—12%, colorless—2%, and blue—1%. Bi-colored fragments represented 13% of the total weight.

The configuration of color zones in the bi-colored fragments seems to indicate that Fe2+ rich tourmaline crystallized early in the core of the pegmatite, and that later crystallization was predominately Li and Mn2+ rich.

Report on a New Hemphillian (Miocene) Fauna from the El Toro area of Orange County, California, and a Comparison of it with Hemphillian Faunas from the Mojave Desert

Steven W. Conkling, Ralph B. Clark Interpretive Center, 8800 Rosecrans, Buena Park, CA 90621

A large collection (>1000 specimens) of Hemphillian vertebrates from the El Toro Materials site (Orange County, California) contains marine and terrestrial elements. Presence of *Osteoborus* sp. fixes the minimum age at Hemphillian and is also the first record of this genus from coastal California. The high abundance of *Pliohippus* sp. in the sample may indicate an early Hemphillian age, since *Pliohippus* sp. is only marginally known from this age. The mixed marine, terrestrial nature of the assemblage enables correlation of the Oso Sand Member of the Capistrano Formation with both the Hemphillian Land Mammal Age and the Delmontian Pacific Marine Stage. Harland and others (1989) places the Delmontian at 5.4 to 2.2 m.y.b.p., while Savage and Russell (1983) place the Hemphillian Land Mammal Age at between 8.3 and 4.3 m.y.b.p. This indicates that the El Toro Materials collection from the Oso Sand Member of the Capistrano Formation is between 4.3 and 5.4 million years old. A comparison of this material to collections from the Mojave Desert region indicate significant faunal variations which may be attributable to climatic factors.

Population Dynamics of the Palm, *Washingtonia filifera,* and Global Warming

James W. Cornett, Palm Springs Desert Museum, P.O. Box 2288, Palm Springs CA 92263

The desert fan palm, *Washingtonia filifera,* presently occurs at approximately 150 springs and streams in both the Colorado and Mojave Deserts of California, Arizona, Nevada, and Baja California Norte (Cornett, 1989a). The available evidence indicates that it has never been more abundant or widespread than it is today (Cornett, 1989b; McClenaghan and Beauchamp, 1986). This paper presents three lines of evidence suggesting that both the expansion in range and the increase in numbers of this species is a result of a regional warming trend.

(1) The first line of evidence involves the evolutionary associations of the desert fan palm. *Washingtonia filifera* is a member of the palm family, Arecaceae, in which approximately 2,800 species of plants have been grouped (Blombery and Rodd, 1982). The family has a worldwide distribution throughout the tropics and subtropics. Only the desert fan palm and a few other family members have entered temperate latitudes. As is true of all palm species, the desert fan palm is limited in its tolerance to subfreezing temperatures and is restricted, either directly or indirectly, in its distribution by low winter temperatures (Cornett, 1987). The expansion of a palm's range into a temperate environment should first be assumed to be the result of a rise in winter temperatures.

(2) New palm oases have arisen primarily to the north of the historic range of the species. Of the twelve newly-described palm occurrences, ten have been at least 50 km to the north of Mopah Spring, at one time the northern-most palm oasis (Munz, 1959). New, northern oases include four in Death Valley national Monument. One of these, Grapevine Spring, is located 286 km north of Mopah Spring (Cornett, 1988a). There are also four in southern Nevada (Cornett, 1988b), a group of palms along the Virgin River near Littlefield, Arizona (Cornett, unpublished data), and one at Sacramento Spring (Cornett, 1989c). The range expansion to the north suggests that either the climate has warmed sufficiently to allow this species to invade the region or that the palms have recently adapted to colder environments. Since only first and second generation palms occur at most of these northern localities, it is unlikely that *Washingtonia filifera* has suddenly adapted to colder climates.

(3) The increase in palm numbers in this century has occurred over the entire geographic range of the species. Palm oases are concentrated along the San Andreas Fault

in the Coachella Valley, Riverside County, California and the eastern base of the Peninsular Ranges in California and Baja California Norte. Most other palm oases exist in relative isolation. Palm numbers have increased in most oases found along the eastern base of the Peninsular Ranges. In Andreas Canyon, located in the northern Peninsular Ranges, the palms have increased from 322 in 1935 (Henderson, unpublished field notes) to 1,076 in 1984 (Cornett, 1986). The situation is similar in the Sierra Juarez portion of the Peninsular Ranges in Baja California Norte. In 1946, Henderson counted 198 palms at Cantu Palms but by 1984 this number had increased to 245 (Cornett, unpublished data).

Palm increases have also been noted in the second area of concentration of this species—along the San Andreas Fault. Pushawalla Palms consisted of 261 palms in 1945 (Henderson, unpublished notes) but the number had grown to 438 in 1983 (Cornett, 1986). Even remote oases, far removed from main concentrations of palms, have shown increases. The Oasis of Mara at Twentynine Palms, San Bernardino County, California, had 25 palms in 1969 (McHargue, 1969). By 1983 the number had grown to 33 individuals (Cornett, unpublished data).

In summary, palms numbers have increased generally over the entire geographic range of the species. Any explanation for this increase would need to have a regional, rather than local, basis. Increased precipitation might be one possible explanation, but the increase in palm numbers occurred between 1946 to 1976—a time when a severe drought prevailed throughout the region (National Climatic Center, 1980).

Within this century, other organisms with tropical affinities have expanded their ranges northward at the same time that a global warming trend, apparently caused by increased concentrations of carbon dioxide in the atmosphere, has been noted. The cardinal, opossum, and armadillo have all extended their ranges northward (Owen, 1980), as has the cabbage palm, *Sabal palmetto* (Brown, 1987). It seems reasonable to assume that the desert fan palm is another example of a species with tropical affinities that has extended its range northward during this period of global warming.

Literature Cited

Blombery, A. and T. Rodd, 1982. Palms. London, Angus & Robertson Publishers.

Brown, K.E., 1987. *Sabal palmetto* distribution update. Principes 31(1):42-43.

Cornett, J.W., 1986. The largest desert fan palm oases. Principes 30(2):82-84

_____, 1987. Cold tolerance in the desert fan palm, *Washingtonia filifera* (Arecaceae). Madrono 34(1):57-62.

_____, 1988a. Naturalized populations of the desert fan palm, *Washingtonia filifera,* in Death Valley National Monument, in Plant Biology of eastern California. C.A. Hall Jr. and V. Doyle-Jones, eds. University of California, Los Angeles, White Mountain Research Station:167-174.

_____, 1988b. The occurrence of the desert fan palm, *Washingtonia filifera,* in southern Nevada. Desert Plants 8(4):169-171.

_____, 1989a. Desert Palm Oasis. Palm Springs, Palm Springs Desert Museum.

_____, 1989b. The desert fan palm—not a relict, in Abstracts of Proceedings, 1989 Mojave Desert Quaternary Research Symposium, J. Reynolds, ed. Redlands, San Bernardino County Museum Association Quarterly 36(2):56-58.

_____, 1989c. Another new locality for the desert fan palm in California. Crossosoma 15(2):1-4.

Henderson, R., 1935. Unpublished notes on file at the Western Heritage Center, University of Wyoming, Laramie.

_____, 1946. We camped at Cantu Palms. Desert Magazine 9(10:12-15.

McClenaghan, L.F. and A.C. Beauchamp, 1986. Low genic differentiation among isolated populations of the California fan palm. Evolution 40(2):315-322.

McHargue, L.T., 1969. A floristic and ecological study of the palm oases of Joshua Tree National Monument. Unpublished manuscript submitted to National Park Service.

Munz, P.A., 1959. A California flora. Berkeley, University of California Press.

National Climatic Center, 1980. Local climatological data, 1980, Yuma, Arizona. Asheville, North Carolina, U.S. Department of Commerce.

Owen, O.S., 1980. Natural resource conservation. New York, Macmillan Publishing Company.

New Techniques for Recovery of Vertebrate Fossils from Asphaltic Deposits, with Reference to a New Fossil Deposit from Rancho La Brea

Barbara A. Fischer, Division of Earth Sciences, San Bernardino County Museum, Redlands CA 92374

The Rancho La Brea fossil deposits are located in Hancock Park, Los Angeles, California. In 1986, excavation for the Shin 'en Kan Japanese Art Pavilion at the Los Angeles County Museum of Art in Hancock Park uncovered an asphaltic deposit of terrestrial late Pleistocene (Rancholabrean) vertebrate fossils. These fossils were salvaged, and are currently housed on permanent loan at the San Bernardino County Museum.

Using new techniques developed at the SBCM, one person can process large quantities of fossiliferous matrix without the use of specialized hardware. Blocks of asphaltic sand containing fossils are placed in nested screen "baskets" of varying mesh and submerged in clean 1,1,1 trichloroethane. As the asphalt dissolves, some fossils are exposed and recovered during periodic maintenance. Fossiliferous matrix is passively collected in the screen baskets for later washing, sieving, and laboratory analysis. Once the core of the block is saturated with solvent, it is removed to dry thoroughly, on order to reduce potential fragmentation of the remaining fossils. The block may be excavated using traditional techniques, once dry. The process is conducted outdoors, taking advantage of solar energy to facilitate the breakdown of the asphalt. Chemicals are reclaimed and recycled. This process is useful only in situations where the recovery of taphonomic information from the deposit is not essential.

Criteria for Identification of Small Cricetid Rodents in Late Quaternary Sites of the Mojave Desert

H. Thomas Goodwin and **Karen E. Austin**, Department of Natural Sciences, Loma Linda University, Loma Linda, CA 92350

Seven species of small cricetid rodents today occur in at least portions of the Mojave Desert—*Reithrodontomys megalotis, Peromyscus eremicus, P. maniculatus, P. crinitus, P. boylii, P. truei,* and *Onychomys torridus*. Two other species, *O. leucogaster* and *P. californicus*, occur in adjacent regions and might have colonized the Mojave Desert in the past. Small cricetids are common as fossils in Late Quaternary sites of the Mojave Desert, and some species might be useful paleoenvironmental and paleobiogeographic indicators. To facilitate study of small cricetid fossils, we have attempted to develop methods for discriminating among the above-mentioned species that may be applied to identification of fragmentary fossil material. Our approach utilizes qualitative and simple univariate or bivariate comparisons as well as multivariate discriminant techniques.

The Nature of Line Rock at Hiriart Mountain

Wallace D. Kleck, 1600 W. Struck Ave., #72, Orange, CA 92677.

Line rock is found in many complex pegmatites and is a common feature in the pegmatites at Hiriart Mountain in the Pala District, California. At Hiriart Mountain, line rock occurs in the lower part (below the pocket zone) of the pegmatite dike. This lower part of the pegmatite consists of a medium to coarse grained quartz-feldspar rock with distinct garnet-rich bands parallel to the margins of the dike. The bands are spaced increasingly closer together higher in the dike, and the abundance of garnet in the bands increases upward. Typically, the grains of garnet are euhedral and range between 0.1 and 2 millimeters in diameter.

Certain features found in the line rock at Hiriart Mountain are similar to soft sediment structures in sedimentary rock and to structures described in the layered series of the Skaergaard complex. Found at this locality were small diapirs (due to differential loading), slump structures, and bedding interrupted by gravity induced xenoliths.

It is proposed, for these pegmatites, that: 1) early crystals of garnet sank in the magma, coming to rest on the mushy floor of the pegmatite, 2) gravity created features occurred in the mushy, soft sediment, 3) successive overturns of stratified pegmatite magma mixed and caused sporadic crystallization of garnet (and other minerals), 4) as the pegmatite solidified inward, overturn frequency increased; this was caused by the greater concentration of water and the thinning of the magma body.

Vegetational Changes East of the Range of Light: Evidence for a Pluvial High Stand of Owens Lake during the Wisconsin Glaciation by the Occurrence of Rocky Mountain Juniper

Peter A. Koehler, Quaternary Studies Program, Northern Arizona University, Flagstaff, AZ 86011.

The analysis of plant macrofossils from packrat *(Neotoma)* middens in Owens Valley, California, provides evidence of a warming period and subsequent pluvial high-stand during the Wisconsin glaciation. Midden remains from the Alabama Hills (1460 m) reflect a cold-dry climate prior to ca. 20,000 yr B.P. This is represented by the presence of Utah juniper *(Juniperus osteosperma)* and Joshua tree *(Yucca brevifolia)*. The temporary appearance of Mojavian and Great Basin desert plant species, typified by Ephedra *(Ephedra* spp.), rabbit brush *(Chrysothamnus teretifolius)*, and deer brush *(Purshia glandulosa)* after 19,070 ± 190 yr B.O. suggest a change towards a cool-dry climatic regime at this locality. Reconstructed lake level history from nearby Searles Lake indicates that a high-stand existed during the glacial maxima, ca. 20,000 to 15,000 yr B.P. The increased runoff from Sierra Nevada glacial meltwater would cause Owens Lake to reach a high stand and overflow into the Searles Lake drainage basin. Midden evidence from Owens Lake (1155 m) was found to reflect a Utah juniper *(Juniperus osteosperma)* and piñon pine *(Pinus monophylla)* community before ca. 18,000 yr B.P. However, between 17,680 ± 150 and 16,070 ± 330 yr B.P., the appearance of Rocky Mountain juniper *(Juniperus scopulorum)*, a mesophytic juniper species, in the Owens Lake midden record reflects a potential increase in available soil moisture, perhaps resulting from the pluvial expansion of Owens Lake. This research also documents the first occurrence of Rocky Mountain juniper in California.

An Experimental Design for Assessing Archaeobotanical Site Formation Processes in the Eastern Mojave Desert

Elizabeth J. Lawlor, Department of Anthropology, University of California, Riverside CA 92521

Quaternary vegetation and prehistoric subsistence in the Mojave Desert will be better understood when archaeologists systematically collect and interpret plant remains using advances from other regions. This proposed project lays groundwork for such research by investigating local site-formation processes, establishing vouchered comparative collections, and testing the widely held decay-in-place model of phytolith (plant silica) deposition. Three Chemehuevi seasonal seed-processing sites will be replicated and tested over a two year period for patterns in deposits of plant macrofossils, phytoliths, and phosphates and in rodent and ant activity. Repeated testing after 10 or more years and comparisons with prehistoric sites are also planned.

Among expected results, *Pinus monophylla* (piñon) phytoliths are expected to provide a means of assessing the extent of Pleistocene piñon-juniper woodland away from areas inhabited by packrats. On the replicated sites,

the spatial distribution of plant remains is expected to correspond closely to maps of cultural activities and nearby vegetation on a scale of 3 to 30 m; these patterns are expected to clearly distinguish cultural from noncultural site transformations. Phosphate testing is expected to miss site boundaries detectable with phytoliths. Granivores are expected to prefer the replicated sites to matched microhabitats but to avoid taking carbonized seeds.

Recent Historic and Prehistoric Archaeological Investigations in the Broadwell Valley north of Ludlow, in the Mojave Desert, San Bernardino County, California

Jeanette A. McKenna, McKenna et.al., 6202 So. Friends Avenue, Whittier, CA 90601

Over the past 18 months, McKenna et.al. has been conducting a series of Phase I archaeological investigations within the Broadwell Valley, north of Ludlow, in the Mojave Desert. More recently, the investigations included a Phase II investigation of three of the more prominent historic features in the valley: the Tonopah & Tidewater Railroad right-of-way; historic Crucero Road; and the presence of a reported World War II encampment associated with Patton's training for desert warfare.

Few systematic archaeological sureys have been conducted within the Broadwell Valley. The recent investigations, including the intensive surveying of over nine square miles of the valley floor and secondary investigations of nearby mining claims, has yielded a substantial file (overview) for the area.

As a result of the recent investigations, McKenna et.al. can suggest patterns for the historic use for the area. But more importantly, McKenna et.al. can now make comments on the proposed activities for the area (including the construction of a hazardous waste repository). Construction activities will enable the examination of subsurface deposits not previously exposed, thereby providing an opportunity for specialized studies and data recovery not always available to the various interested parties. In summarizing the recent studies within the Broadwell Valley, McKenna et.al. hopes to increase the data recovery potential associated with the proposed project and increase the overall data base for this portion of the Mojave Desert.

Quaternary Lakes and Geothermal Activity in the Salton Trough

Michael A. McKibben, Department of Earth Sciences and Center for Geothermal Resources Research, I.G.P.P., University of California, Riverside, CA 92521

The Salton Trough of southern California is an active sediment-filled continental rift formed by impingement of the East Pacific Rise spreading system on the North American continent. The northern part of the trough has been isolated from the Gulf of California for the past 4 million years, due to westward progradation of the Colorado River delta across the rift. Waters entering the northern trough therefore must escape mainly by evaporation, and the closed basin has seen multiple cycles of freshwater infilling and desiccation. Within this environment, at least 1700 m (5600 ft) of sediments have been deposited over the last 1-2 million years. Lacustrine evaporites are abundant to depths of at least 1 km and record the frequent formation of saline lakes in the northern trough over the past 2-4 million years. Previous workers have documented at least four stages of modern lake formation between 700 and 1580 A.D. The Salton Sea is actually unique in the long lacustrine history of the northern trough, because it formed from 1905-1907 due to manmade causes.

Modern and Quaternary geothermal activity in the Salton Trough has been significantly affected by the Pliocene and younger lacustrine history of the basin. Within the sediment fill of the central part of the trough, pull-apart basins centered over

spreading ridge fragments are sites of MORB-type dike intrusion at depths as shallow as 3 km. The resulting heat causes buoyant diapiric rise of deep rift basinal brines that accumulated within the last 4 Ma in the closed lacustrine environment of the northern trough.

Within the well-studied Salton Sea system, the domal top of a brine diapir has been mapped out in three dimensions using fluid geochemical and temperature data from commercial and scientific geothermal wells. The rising brine diapir has quantitatively stripped base metals from the volume of metasediments with which it has interacted. The presently-exploited metalliferous brine volume is conservatively estimated at 11 km^3 and contains at least 22 Mt of Fe, 18 Mt of Mn, 5 Mt of Zn, 1 Mt of Pb, 110,000 t of Cu, 353 M oz of Ag, and 176,000 oz each of Au, Pt and Pd. The maximum level of ascent of this ore-forming brine diapir is controlled by its temperature and density as well as the hydrologic head created by the present lake level.

At the margins of the Salton Trough, recently discovered epithermal sinter deposits imply that fossil lake levels may have controlled the efflux of hydrothermal fluids along growth faults and other rift-bounding structures. The Modoc deposit occurs along the intersection between a growth fault and an ancient high stand of Lake Cahuilla, and could be younger than 1000 years in age. Recharge for the gold-bearing hydrothermal system may have come from mixtures of lake waters and meteoric waters derived from the range front. Geological and geochemical studies of this deposit are in progress to assess the paleohydrology of this fossil geothermal system. Because gold deposition can occur when upwelling hot fluids reach shallow depths and undergo boiling, lake levels could have significantly influenced the localization of epithermal gold mineralization along the margins of the evolving rift.

Introduction to the Geomorphic Subprovinces of Southern California and Nevada

Norman Meek, Department of Geography, California State University, San Bernardino, CA 92407

In preparation for the field trip, this presentation focuses on the topographic differences between the three geomorphic subprovinces that will be visited.

The topography of the Mojave Desert subprovince is the product of latest Tertiary and Quaternary strike-slip and thrust faulting in a region that experienced considerable crustal extension during the Miocene. The topography of this region is comparatively subdued because strike-slip faulting only results in relatively minor base-level changes, and the region has been the site of an enormous sediment influx from the adjacent Transverse Ranges during the Quaternary.

East of the Mojave Desert, the topography of easternmost California and southern Nevada reflects Basin-and-Range extension that has been relatively inactive since the latest Tertiary. Comparatively long-term landscape stability is indicated by large basins with very thick pedogenic carbonate accumulations such as the Mormon Mesa calcrete. Latest Tertiary extension of the Colorado River to the Gulf of California and the down-basin growth of tributary drainages into the Colorado River during the Quaternary is leading to the progressive dissection of the region, thus locally increasing the topographic relief.

North of the Garlock Fault in east-central California, a series of large north-south-trending basins and ranges are caused by oblique extension as the Sierra Nevada block moves to the west-northwest. Rapid base-level changes during the Quaternary have resulted in a landscape dominated by linear mountain fronts, enormous relief, and extensive surficial evidence of active faulting.

Stratigraphy and Intra-basin Correlation of the Mojave River Formation, Central Mojave Desert, California

Elizabeth A. Nagy and **Bruce C. Murray**, Division of Geological and Planetary Sciences, California Institute of Technology, MS 170-25, Pasadena, CA 91125

Detailed stratigraphic description of a previously undefined sequence of deposits, in transitional contact with the overlying Pleistocene Manix Formation, has resulted in the definition of an 80+ meter thick section referred to here as the Mojave River Formation. The stratotype is located at the intersection of Manix Wash with the Mojave River. Intra-basin lithologic correlation between three geographically separate exposures of the deposits within the Manix Basin of the Mojave Desert are independently supported by volcanic ash chemistry and geomagnetic reversals.

The deposits of the Mojave River Formation predominantly represent accumulation within a closed basin of a desert depositional system. They record a fairly complete history of changing Plio-Pleistocene depositional environments prior to the formation of Pleistocene Lake Manix. Age assignment based upon stratigraphic relationships, tephrochronology, and magnetic polarity reversals indicate that the Mojave River Formation at the type locality represents about 1.5 Ma of time, spanning from 0.92 Ma to 2.48 Ma.

The deposits yield information concerning the timing and nature of motion along the adjacent Manix Fault, which shows evidence for both left lateral and reverse motion in the type area. Regional implications of the Mojave River strata include the timing of uplift of the Transverse Ranges and change in the flow direction of the "ancestral" Mojave River system from westward to eastward. Both of these developments appear to be post 0.97 Ma.

The Importance of Recording Geologic Information during Paleo Salvage Operations: A Method to the Madness

Alois F. Pajak III, Department of Earth Sciences, San Bernardino County Museum, Redlands CA 92374

One of the primary goals of paleontologic salvage is the recovery of paleontologic data at construction projects. The initial phase of construction, such as grading, brushing, or trenching, reveals a nearly complete stratigraphic column. While monitoring a paleo salvage project, objective descriptions of the stratigraphy can readily be made; yet, these are often neglected and are lost. Methods of description, similar to those found in Compton's (1962) *Manual of Field Geology*, are proposed and include measurement of grain sizes and mineralogy while dry screening, recording obvious discernible sedimentary structures (eg. cross bedding, cut and fill structures, and graded bedding), measuring bedding attitudes, and mapping structure, stratigraphy, and biostratigraphy. These observations are best made with a simple four step procedure:

(1) measure the attitude of the bedding;

(2) measure the attitude of the cut;

(3) make objective observations of the sediments, structure, stratigraphy, and note marker beds and thicknesses;

(4) correct observations to true attitudes.

Since construction offers a perfect view of the stratigraphy, a measured and described column provides essential information with little expense. These observations can easily be accomplished while monitoring for fossils and require only familiarity with basic geologic field procedures and recording methods.

Magnetostratigraphy and Clockwise Rotation of the Plio-Pleistocene Mojave River Formation, Central Mojave Desert, California

Christopher J. Pluhar and **Joseph L. Kirschvink**, Division of Geological & Planetary Sciences, The California Institute of Technology, Pasadena, CA 91125, and **Robert W. Adams**, 7400 Tampa Ave., Reseda, CA 91335

Oriented samples collected for paleomagnetic analysis from sediments of the newly-named Mojave River Formation (Nagy & Murray, 1991) possess stable characteristic components of Natural Remanent Magnetization (NRM). Progressive demagnetization reveals characteristic components of both normal and reversed polarity which are stratigraphically distinct. The oldest sediments exposed within the field area are reversely magnetized and were probably deposited during the early portion of the Matuyama reversed Chron. Stratigraphically higher units contain what appears to be the Olduvai normal Subchron, as well as a shorter normal zone which probably is either the Cobb Mountain or Jaramillo Event. The location of the Brunhes/Matuyama boundary at one site is within an alluvial fanglomerate which grades upward conformably into the lowest unit of the overlying Manix Formation, possibly accounting for the absence of the Bishop ash in the section.

Demagnetization data from 143 samples yielding acceptable least-squares lines suggest a net clockwise rotation of 8 $\pm$ 2.7° over the past two million years, perhaps with some of the rotation during deposition. This rate of rotation could account easily for larger rotations reported elsewhere in the Mojave Desert on units of Miocene age.

The Cadiz Fauna: Possible Irvingtonian Land Mammal Age Sediments in Bristol Basin, San Bernardino County, California

Robert E. Reynolds, Division of Earth Sciences, San Bernardino County Museum, Redlands CA 92374

Recent field work by the San Bernardino County Museum (SBCM) in the vicinity of Cadiz and Chambless was conducted in playa, pond, and lake sediments below the 800' elevation in Bristol Lake Basin. The composite fauna from more than 160 paleontologic localities is given in Table I.

TABLE I
CADIZ COMPOSITE FAUNA

Camelops sp.	extinct large camel
Tetrameryx? sp.	extinct prong horn
cf. *Antilocapra*	prong horn
Equus sp. (lg)	extinct large horse
Equus sp. (sm)	extinct small horse
Felidae (lg)	large cat
Canis sp. (lg)	wolf
Canis latrans	coyote
Taxidea taxus	badger
Lepus sp.	jack rabbit
Sylvilagus audubonii	cottontail rabbit
Leporidae (med)	medium-size rabbit
Spermophilus sp. cf. *S. townsendi*	Townsend's ground squirrel
Thomomys bottae.	Botta's pocket gopher
Dipodomys sp. (lg)	large kangaroo rat
Dipodomys sp. (med)	medium-size kangaroo rat
Dipodomys sp. (sm)	small kangaroo rat
Perognathus sp. (sm)	small pocket mouse
Perognathus sp. (lg)	large pocket mouse
cf. Microtinae (lg)	large microtine rodent
Neotoma sp.	wood rat
Aves sp. (med)	medium-size bird
Aves sp. (sm)	small bird
Lacertilia	lizards
Phrynosoma sp.	horned lizard
Sceloporus sp. (sm)	small spiny lizard
Crotalus sp. (sm)	small rattlesnake
Masticophis sp.	whipsnake or racer
Pituophis melanoleucus	gopher snake
Gopherus sp.	tortoise
Geochelone sp.	extinct giant tortoise
Chelonia (sm)	small tortoise or turtle
Physa sp.	fresh water snail

Eastward, toward the Colorado River, the SBCM recovered a Pleistocene fauna at Archer

at elevation 750', approximately 200 feet above the current 545' elevation of Cadiz playa. The fauna from Archer consists of small vertebrates: rodents, rabbits, birds, lizards and snakes. The fauna contains *Dipodomys ordii*, an extralocal species.

The fauna at Saltmarsh is at approximately 650' elevation, about 40 feet above the playa surface of Danby Lake. The extinct fauna at Saltmarsh includes *Camelops* sp. and a small species of *Equus*. Fossil rodents include *Dipodomys* sp., *D. merriami*, and *Dipodomys* sp. cf. *D. deserti*. The specimen referred to cf. *D. deserti* is notable in that it has unusually thick enamel-walled teeth. The apparent absence of *Mammuthus* and *Mammut* species in the Bristol-Danby basin is conspicuous.

Basalt flows from the youthful-appearing Amboy Crater appear to sit on Bristol Lake sediments at an average elevation of 610'. Flows buried to a depth of 30' by lacustrine sediments corroborate suggested ages of 50,000 to 100,000 years for the flows. This may suggest that the fossiliferous sediments at elevation 720-800' near Cadiz and Chambless were deposited under a different basin configuration, prior to the basalt flows. The presence of *Geochelone* sp., *Tetrameryx?* sp., and the unusual, large *Dipodomys* species may suggest that the higher sediments may date from the early Rancholabrean Land Mammal Age or the Irvingtonian Land Mammal Age.

The Piñon-Juniper Woodlands of Lobo Point and North Wild Horse Mesa in the Mid Hills, San Bernardino County, California

Thomas A. Schweich, 3008 Fairview Avenue, Alameda, CA 94501

The Providence Mountains–Mid Hills–New York Mountains area of California's eastern Mojave Desert is an "island mountain" area containing vegetation not found in the surrounding areas. Most notable are the White Firs of New York Peak and Clark Mountain (Hendrickson and Prigge, 1975) and the Round Valley Sagebrush assemblage. A Pinon–Juniper Woodland containing *Garrya* and Manzanita is found at the north end of Wild Horse Mesa. Lobo Point (Gold Valley) contains a Pinyon–Juniper Woodland at the lowest elevation in the Mid Hills. Lobo Point is also of particular interest to the author because he has camped there many times. What are the plant species found here? How might the vegetation be characterized? What might be the relations between the vegetation of Lobo Point and other nearby areas? Towards an answer to these questions, a literature search and vegetation survey were made.

The vegetation at Lobo Point and North Wild Horse Mesa was surveyed by line-intercept transects. Resulting statistics are discussed and compared to another study of Caruthers Canyon in the New York Mountains and Clark Mountain. The vegetation of the study area is characterized as a Blackbush Scrub containing elements of Creosote Bush Scrub with Pinyons and Junipers where microclimate and edaphic conditions permit. Strong affinity to southern Nevada vegetation is suggested.

The Giant Figure Enigma

Wilson G. Turner, 10433 Lundene Drive, Whittier CA 90601

A recent discovery has located some heretofore unrecorded giant intaglio along the Mojave River. There is a question as to their authenticity.

Giant figure designs made on the surface of the earth throughout the world, much too large to be seen from the ground, have been a mystery to science for a long time. Not only are they found in Europe and South America, but in the late thirties some were located along our own Colorado River.

While working on a new project, giant figures along the Mojave River were discovered. There is at present considerable controversy concerning their authenticity. The main stumbling block seems to be, why weren't they ever noticed before? The answers to this and other questions will be discussed in this paper.

Extinct Megafauna from the Dove Springs Lignites, Northwestern Mojave Desert, California

David P. Whistler[1], **Robert L. Clark**[1], **Shelley M. Cox**[2], **Denny Diveley-White**[1], **Mark R. Faull**[3], **Rob C. Mabie**[1], and **Eric Scott**[4]

A sequence of unnamed stream and pond deposits in Dove Spring Wash, Red Rock Canyon State Park, has previously yielded diverse microfauna containing mollusks and small vertebrates (Whistler and Stewart, 1989; Whistler, 1990). Field work in early summer of 1990 yielded extinct large vertebrates from these deposits including the horse, *Equus* cf. *E. occidentalis* Leidy, 1965; a camel, cf. *Camelops*; the bison, *Bison antiquus* Leidy, 1952; a mastodon, cf. *Mammut* sp.; and the mammoth, *Mammuthus columbi* (Falconer, 1957). The *Bison* is represented by a partial skeleton.

[1] Vertebrate Paleontology Section, Natural History Museum of Los Angeles County, Los Angeles CA 90012
[2] George C. Page Museum, Los Angeles CA 90036
[3] Red Rock Canyon California State Park
[4] Division of Earth Sciences, San Bernardino County Museum, Redlands CA 92374

Pedogenic Carbonate Accumulations, The Rosetta Stone for Deciphering Correlations and Age Relationships in Late Tertiary and Quaternary Deposits of Southeast Nevada

Gustav F. Winterfeld, Dames & Moore, 5330 Office Center Court, Bakersfield CA 93309

Pedogenic carbonates form as part of calcic soil development throughout the arid and semiarid parts of the southwest U.S., northern Great Basin and Range Province, and into the Midwest. They develop on unconsolidated sediments over periods of time ranging from a few thousand to several million years. Because of their widespread occurrence and time dependent development, these carbonates yield important clues to correlation and estimating the ages of late Tertiary and Quaternary deposits in which they are developed.

Such carbonates are generally composed of micritic, low magnesium calcite and have a light calcium isotope composition. Morphological features indicating a pedogenic origin include filaments, coatings, nodules, indurated masses, laminae, pisolites, and breccia. Pedogenic carbonates commonly parallel surface topography, are exposed over lateral distances of several kilometers, and range in thickness from centimeters to several meters.

In southern Nevada, between Glendale and Mesquite, pedogenic carbonate accumulations are associated with four discrete terrace levels. The oldest of these, the Mormon Mesa "caliche", is developed over several hundred square miles and ranges to four meters in thickness. The "caliche" shows all six stages of development for the most advanced pedogenic carbonates recognized in the United States. These include a basal layer of disseminated carbonate nodules and filaments that passes upward into a massive layer of coalesced nodules, and finally into multiple layers of laminated carbonate, pisolites, and breccia.

Estimates on the age of the Mormon Mesa "caliche" based on carbonate dissolution models indicate it is at least 400,000 years old. Geomorphic reasoning related to incision of the Colorado River suggests the "caliche" is at least 2.5 million years old. Fossil vertebrates from the Muddy Creek Formation, on which the Mormon Mesa surface is developed, yield a late Miocene (Hemphillian) age, and thus support a much older age (3 million years plus) for the "caliche".

Ancient Astronomy of the Black Canyon Indians:

The 1991 Mojave Desert Quaternary Research Symposium Evening Lecture

Wilson G. Turner, 10443 Lundene Drive, Whittier, CA 90601

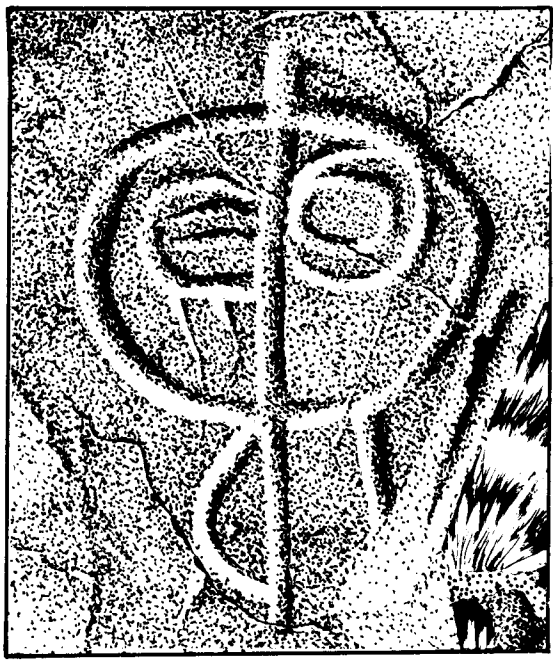

Fig. 1. TMT-31D

Many years ago, Bob Reynolds and I were driving around the desert north of Hinkley and discovered an outcrop at the base of Tortoise Mountain which we hadn't noticed before. Upon investigation, we found that it had over 100 previously-unreported petroglyphs. I immediately dubbed the location Surprise Outcrop. This site would have, in the years to come, a very important part to play in the investigation of the Greater Black Canyon Complex.

The research on the petroglyphs of Black Canyon was started in 1977 (Turner, 1978) with the sole purpose to preserve, for future generations, a record of all the extant glyphs. So much vandalism had gone on, it was feared there wouldn't be any glyphs left to study in the future if and when someone came up with an idea of how to understand them.

In doing the research, it was discovered that the seemingly countless glyphs in the area were of many different ages. Some had possibly been carved over 10,000 years ago while others in all likelihood were no more than 2,000 years old. The dating of these petroglyphs is another story beyond the subject of this paper. It is sufficient to say that there are a number of people working on the subject and many are having very good results (Dorn, 1990).

In this area, as in most of the new world, there is no continuity of culture for such a great period of time. Because of this, there seems to be no way of determining just who made the engravings. For convenience it is said the Indians did them, although when the Europeans first came through here and asked the Indians about the designs, their answer was that they didn't do them, that they had been made by the ancient ones (Mallery, 1893).

This Surprise Outcrop site, (now officially named "Tortoise Mountain site T"), has been ravaged a number of times since its first discovery. There was the instance, in late 1971, when a family of prospectors came to the site. They said they were going to stake a

claim and dig for the gold that the Indians had buried. They pointed out two glyphs somewhat like an M and the figure 8 (Fig. 2, Petroglyphs TMT-24B,C, Turner, 1979) that, to them, indicated the location of a fantastic treasure. Futile attempts were made to talk them out of digging in the area. It was pointed out to them that the Precolumbian California Indians didn't have any gold and didn't know anything about this precious metal. This apparently did not dissuade them, for the next time the site was visited it was discovered a tremendous hole had been made at the base of the cliff, apparently by blasting and bull dozing. The cavity was about fifteen feet deep and some twenty-five feet wide with huge boulders laying all about. It was a place of devastation.

Fig. 2. TMT-24

Approximately two years later, through some good contacts with BLM and the aid of Russ Kaldenberg, the Marine Corp stationed in Yermo came out with heavy equipment and cleaned up the mess. This itself turned out to be almost chaotic. It was late in the summer and the flatbed carrying the backhoe-dozer became trapped in the dry loose sands of the local roads. It took the rest of that day to get themselves out, and they had to return another day to do the backhoe work. The soft, wheel-grabbing road which the big equipment left after driving in and out made a considerable problem for the field personnel who had to drive over it during the balance of the year trying to get through to Black Canyon. Fortunately, the following winter was a wet one and the rain solidified the treacherous sandy roadbed.

By July of 1986, someone had pried the top off one of the huge main boulders leaving its components laying all around on the ground. To this day I do not understand what they must have had in mind, unless, after getting the stone apart, they were unable to lift the pieces into their vehicle because of their tremendous weight. It was decided that the boulder had to be reassembled. In December of that year a crew of students was gathered together along with one of my sons and his wife. They drove to Barstow, rented a hoist (usually used for lifting motors out of automobiles), and pulled it trailer-like out to the site. As they arrived to do the work it began to drizzle—it would have been hard to have picked a worse day for this reconstruction job. The rocks were slippery, the sand was soggy, and the workers were drenched.

This was not an easy job at best. They heaved and hoisted, slung and swung the slippery, large, heavy pieces into place. Keeping them there was another thing. The separate pieces had a tendency to slide out of place with the rain water reacting like a lubricant. When the crew finished the reassembly of the boulder they were jubilant despite their bedraggled condition.

Earlier in the present paper this rock was called one of the main boulders at the site; it may be the most important boulder because of the presence of a particular petroglyph. This centrally located, very visible rock had a Picasso-like portrait of the "Moon Goddess" deeply carved and abraded on one of its surfaces (Figs 1, 3, Turner, 1979, Petroglyph TMT-31D). The design is basically a bifurcated circle. In this paper a circle with a line running through it and extending beyond both sides is referred to as a "phi" design because it resembles the Greek alphabet letter. In the upper right quadrant of the circle, or head, is an eccentric eye that looks happy and on the left there is a narrow-slit eye with tears that looks sad. A breast is carved below the face; this feature helps identifies the portrait as that of a woman.


Fig. 3 TMT-31D

Many ancient groups of Indians felt that the moon was a goddess. They thought of

her much like some oriental cultures feel about the yin-yang design, expressing many opposites: good and evil, dark and light, happy and sad. This design certainly expresses the happy-sad aspects of this idea of the moon goddess.

The phi design and other designs that resemble it (Fig. 4) make up about 16% of all

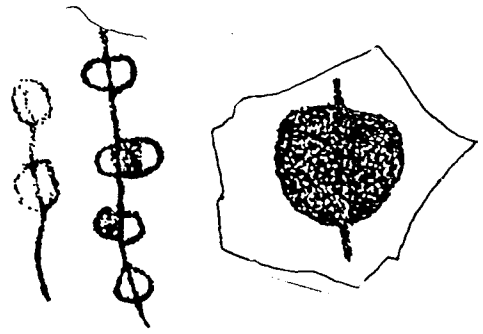

Fig. 4. BBC-3 (left), BCO-7 (right)

of the glyphs in Black Canyon. Frequently it is associated with a snake. The snake was thought of by many groups as a sky being, or god, and was often depicted as sky bands (rainbows), feathered, horned, or occasionally as an undulating body with a head on each end. One of the phi designs in Black Canyon has horns, and the snake symbol is with it (Fig. 5, Turner, 1979, BCQ-1). In general,

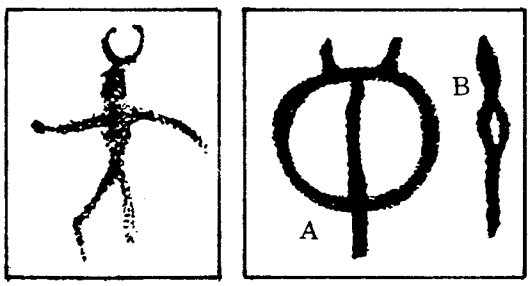

Fig. 5. BCI-17A (left), BCQ-1 (right)

petroglyphs depicting humans with horns on their heads usually represent a moon headdress as worn by a shaman (Fig. 5, Turner, 1978, BCI-17A).

Another aspect of the phi design occurs in connecting chains. At times some of these bisected circles are partially shaded. These could imply phases of the moon (Fig. 4, Turner, 1981, BBC-3V) and the completely filled in phi might suggest the new moon (Turner, 1981, BBL-4).

Other phi designs in the study area associated with snakes—for example, petroglyph illustration SHM-1 (Fig 6). The

Fig. 6. SHM-1 (left), LKB-9 (right)

mark on this phi could be a snake or an undulating projection from the edge of the phi itself. There is a circle design on Lizard Knolls in Black Canyon that has a similar protrusion on its upper right side (Fig. 6, Turner, 1981, LKB-9A).

Further up the canyon at Clay Hill site (Fig. 7, Turner, Summer 1983, CHJ-47A) there is a lone phi design on a large, upright, somewhat pointed boulder. The design faces uphill, away from the canyon. This is unusual because almost all of the designs in our research area face downhill, toward the ravine. If you stand facing the phi design with your back to the hill and look to the west over the design on the pointed boulder, you will notice a large pair of natural sandstone columns near the western horizon. One day in late September 1980 while thus occupied I saw the moon about to set between these two pillars. I became excited about this phenomenon. It was apparent to me that the Indians had been

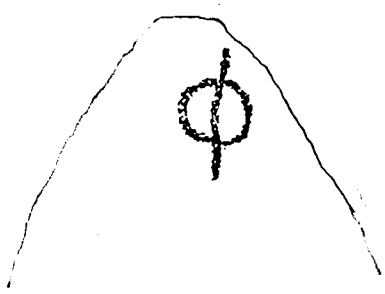

Fig. 7. CHJ-47

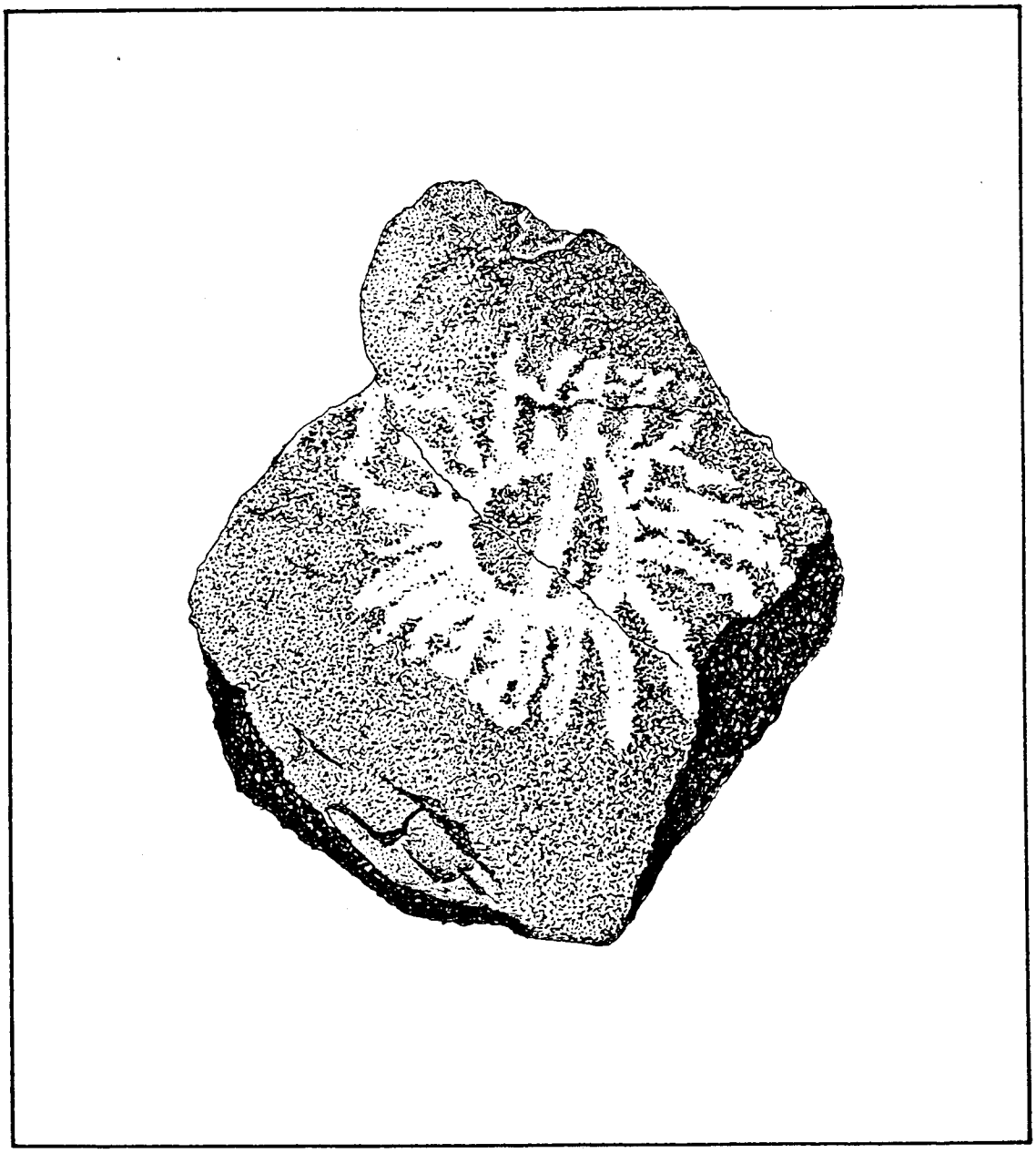

Artist's rendering of petroglyph BCX-3A

Plate 1. This petroglyph design seems to represent an eclipse.

observing the moon from this position, thereby keeping track of time and the seasons.

Dr. Krupp of the Los Angeles Planetarium later explained the complications about the moon and its movements (Krupp, 1978).

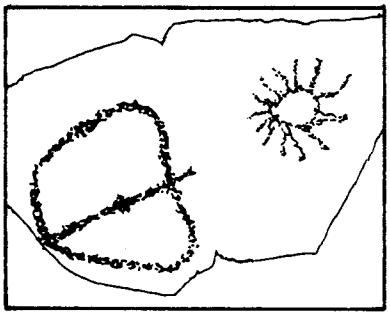

Fig. 8. SHV-58

Unfortunately for my idea, Dr. Krupp said the moon, unlike the sun's yearly movements from its furthest northeast rising at winter solstice to its furthest northwest rising at summer solstice, takes about eighteen and a half years to go from its northernmost position in the sky to its extreme southern position and back again. Beyond this, these periods run in cycles of about a fifty-six years. I doubt that any primitive California Indian would be counting seasons over such extended ranges of time, although the ancient Egyptians and Maya did.

Many other designs have been found that would lead one to believe that the phi design represents the moon. For example, there is a phi juxtaposed to a radiating disk much like a sun (Fig. 8, SHV-58), and there is a petroglyph design that seems to represent an eclipse (Plate 1, BCX-3A Turner, 1981). In many Indian legends the sun and moon are brother and sister and because the moon is so lascivious she, on occasions, has seduced her brother. To me, this obviously refers to a full eclipse of the sun. How better to picture it than to have the phi design overlay a radiating disk and, in this case, to accentuate the display of the sun's corona, seen only on such an occasion. This petroglyph then becomes the moon symbol superimposed on the sun symbol.

In the Black Canyon area there are a number of other motifs that imply sky watching such as star designs with a crescent petroglyph (SHU-67), stars with snakes (SHZ-12) and stars alone (SHX-97) (Fig. 9).

Let's go back to the possibility that the Indians of Black Canyon, on occasions, kept track of daily lunar counts. Although a lunation is usually considered 29.5 days from new moon to new moon, an observer may identify the cycle as between 28 and 30 days. In Black Canyon, we find possible count-inscribed petroglyphs with these many marks on them. For example, one (Fig. 10, Turner, 1983 Summer,WCC-1A) is something like a cartouche with 28 vertical dashes within it. These marks are in four rows: six, seven, eight, and seven. This arrangement could represent the four phases of the moon, or what we now term weeks. Another such design is the boulder I have named the Black Canyon Sky Chart (Fig. 11, Turner, Fall & Winter, 1983 VEA-7). It tallies 30 marks in four rows, two of eight marks and two of seven. Do

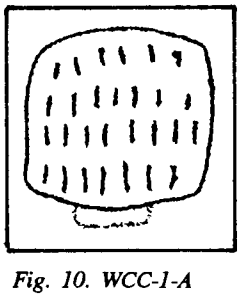

Fig. 10. WCC-1-A

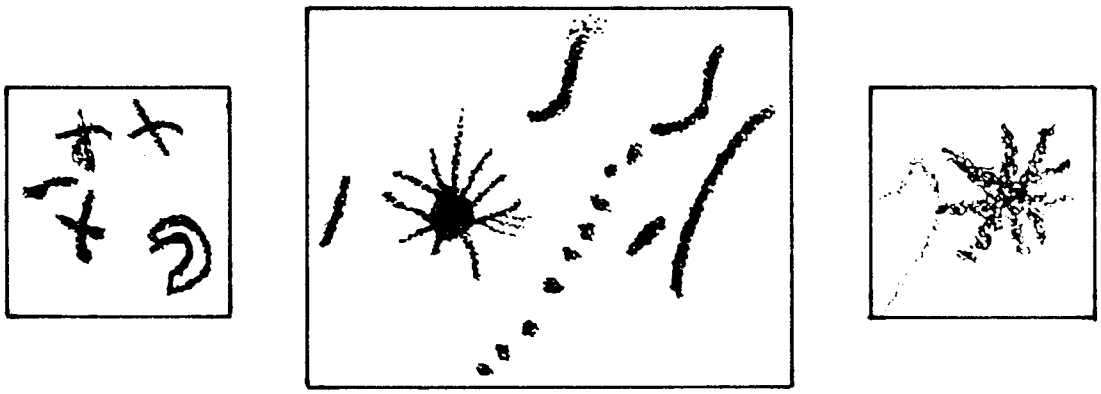

Fig. 9. (left to right) SHU-67, SHZ-12, SHX-97

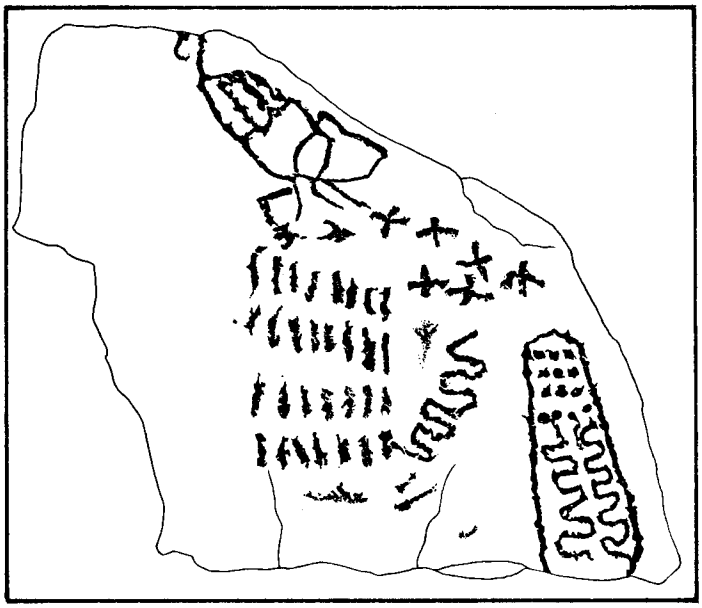

Fig. 11. VEA-7

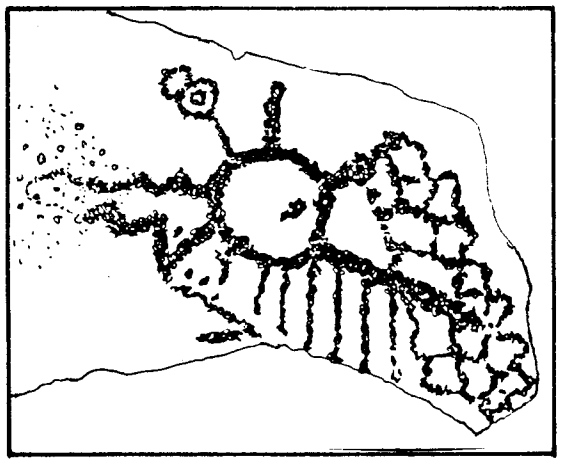

Fig. 12. BCP-32A

these four rows of slashes again represent phases of the moon? Another interesting thing about this group is the snake which seems to attach itself to the thirtieth count mark. The arrangement of the star group above the count marks could represent the Big Dipper, the Little Dipper or even the Pleiades. A giant sky monster or scorpion appears to be grabbing for those stars.

Europeans see a particular group of stars in the night skies as a scorpion, and the Maya and the Aztecs identified this identical group with the same designation. It is therefore possible that the Black Canyon Indians made the same association. Some of the stars in this constellation are so arranged that they do curve back and make an excellent scorpion-like stinger. It is therefore possible that the horrible figure with the recurved tail represents this star cluster.

I checked my sky chart to find that Scorpio was not at all close to the Big Dipper, Little Dipper, or even the Pleiades, but I did discover that Scorpio grabs with its outstretched claws at a part of the constellation Libra which in turn contacts a part of Virgo. These parts of constellations put together form an asterism exactly like that depicted in the Black Canyon nine-star sky chart, even to the curve in the handle and the extra stars beyond the dipper shape to the right and below.

Other petroglyphs in the Black Canyon area seem to relate to astronomy. One appears to be a sun and rain association (Fig. 12, BCP-32A), and another carved boulder with a phi, a chain of filled phi designs, two snakes, and a star, is located so the setting sun at equinox shines on it (Fig. 13, SHV-156). Until these have been studied further, their relationship to the heavenly bodies will not be understood.

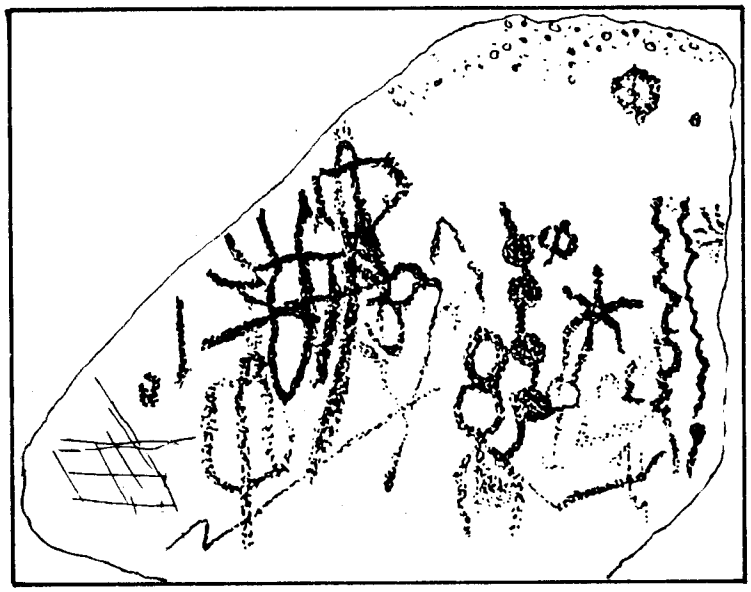

Fig. 13. SHV-156

REFERENCES CITED

Dorn, I. Ronald, 1990. Rock varnish dating of rock art. La Pintura, 17(2).

Hawkins, Gerald S., 1973. Beyond Stonehenge. New York, Harper and Row.

Krupp, Edwin C,Ph.D, 1978. In Search of Ancient Astronomies. Garden City, Doubleday and Co., Inc.

Mallery, Garrick, 1893. Picture-Writing of the American Indian. New York, Dover Publications, Inc.

Menzel, Donald H., 1964. A Field Guide to the Stars and Planets. Boston, Houghton Mifflin Co.

Ottwell, Guy, 1981. The Astronomical Companion. Greenville, SC, Furman University.

Turner, Wilson G., 1977. Dating the Salton Sea petroglyphs. Science News, 3(9):138.

_____, 1978. Recording petroglyphs. Redlands, San Bernardino County Museum Association Quarterly, 15(3).

_____, 1979. Petroglyphs, a further study. Redlands, San Bernardino County Museum Association Quarterly, 27(2).

_____, 1983. Petroglyph field work completed. Redlands, San Bernardino County Museum Association Quarterly, 31(1,2).